UNIVERSITÀ DI PARMA

UNIVERSITA' DEGLI STUDI DI PARMA

DOTTORATO DI RICERCA IN
" *MEDICINA MOLECOLARE* "
CICLO XXXII

An amino acid trade-off between Acute Lymphoblastic Leukemia blasts and bone marrow mesenchymal stromal cells: a possible mechanism for asparaginase resistance

Coordinatore:

Chiar.ma Prof.ssa Stefania Conti

Tutore:

Chiar.mo Prof. Ovidio Bussolati

Dottorando: Giuseppe Taurino

Anni Accademici 2016/2017 – 2018/2019

Abstract

Acute Lymphoblastic Leukemia (ALL) is due to the neoplastic transformation of lymphoid progenitor cells, which start to proliferate in uncontrolled way, to accumulate in bone marrow (BM) and blood, and to invade other organs such as lymph nodes, spleen, liver and brain. The immature neoplastic cells are called blasts. ALL is the most common pediatric cancer and represents 25% of all oncologic diagnoses and 80% of all leukemia cases in children. A peculiar metabolic feature of ALL blasts is the low expression of Asparagine Synthetase (ASNS), the enzyme that synthetizes asparagine (Asn) from aspartate (Asp) and glutamine (Gln). Therefore, ALL blasts are strictly dependent on extracellular Asn. For this reason, L-Asparaginase (ASNase) is used in ALL therapy. providing the first (and, until now, the sole) example of anti-cancer treatment based on a tumor-specific metabolic vulnerability. ASNase hydrolyzes plasma Asn and, with a lower affinity, Gln, thus causing a severe nutritional stress in ALL blasts and, eventually, their death. The ASNases used in clinical medicine derive from *Escherichia coli* and *Erwinia chrysanthemi*. Both produce a severe and long lasting Asn depletion, while the *Erwinia* enzyme has a higher glutaminolytic activity than the *E. coli* counterpart. *E. coli* ASNase and its pegylated form are used in the induction and re-induction phases of ALL therapy, whereas the other is adopted in case of hypersensitivity due to immune reaction.

Although ASNase exploitation led to a substantial improvement of ALL prognosis, leukemic cells may become resistant to the enzyme in a minority of cases. ASNS induction has been invoked as the adaptive mechanism underlying resistance to ASNase, but the expression levels of the enzyme do not correlate with sensitivity to ASNase *in vivo*. For this reason, other mechanisms must support ALL blast survival during ASNase treatment.

Among these, it has been proposed that tumor microenvironment could play an important role in this drug resistance. Several years ago, it has been demonstrated that a line of immortalized human BM-derived Mesenchymal Stromal Cells (MSCs) protects leukemic blasts from ASNase through Asn synthesis and secretion. More recently, it has been also claimed that adipocytes, another component of the BM stroma derived from MSCs, reduce murine ALL blast sensitivity to ASNase through the release of Gln. These data suggest that MSCs could have an important role in the nutritional support of ALL blasts during the treatment with ASNase.

Therefore, the aim of this study is the elucidation of the mechanisms underlying the protection of ALL blasts by MSCs during ASNase treatment. Two original approaches have been adopted: a) evaluating the response of MSCs to ASNase, and b) verifying if

MSCs obtained from ALL patients or healthy donors equally support ASNase-treated ALL cells. Primary MSC, obtained from either ALL patients (ALL-MSCs) or healthy donors (HD-MSCs) were cultured in standard growth medium. In the experiments aimed to evaluate MSC-dependent protection, primary MSCs were cultured in the presence of the BCP-ALL cell line RS4;11 or primary blasts. Gln and Asn depletion was obtained incubating cells with ASNase from *Erwinia chrysanthemi* or in Gln- Asn-free medium.

Both ALL-MSCs and HD-MSCs were poorly sensitive to treatment with ASNase, which caused a drastic fall of intracellular Gln and Asn. Initially, MSCs ceased to proliferate, but rapidly activated an amino acid stress response, indicated by the phosphorylation of the α subunit of the human initiation factor 2 (eIF2α), and induced ASNS and the pro-apoptotic factor CHOP. However, after a few days, they markedly increased the expression of Glutamine Synthetase (GS), which is the enzyme able to synthetize Gln from glutamate and ammonium, stabilized intracellular Gln levels and rescued proliferation. Under these conditions, ASNS protein and Asn levels did not show consistent changes, whereas CHOP expression was lowered at control levels. GS inhibition, mediated by the irreversible inhibitor Methionine-L-sulfoximine (MSO), or GS silencing completely prevented the adaptation of ASNase-treated MSCs, pointing to the essential role of GS expression and/or activity. *Erwinia* ASNase caused a massive cell death in ALL cell cultures. However, when ALL-MSCs were co-cultured with ASNase-treated leukemic cells, the percentage of necrotic leukemia cells was reduced by more than 60%. The presence of MSO in the co-culture markedly hindered, but did not abolish the protective effect. Conversely, GS silencing in MSCs only marginally inhibited the protection on leukemia cells, demonstrating that the MSO inhibitory effect on protection was only partially due to the inhibition of GS activity in the MSCs and suggesting that most of the effect could derive from the suppression of GS activity in ALL cells themselves.

These results are consistent with a working model in which ALL cells provide MSCs with Gln that is then used by the stromal cells to synthetize Asn to be exported. A support to this hypothesis came from the demonstration that MSCs are able to extrude Asn not only in Asn- and Gln-free cell culture medium but also in an advanced plasma-like medium either in the presence of physiological levels of Asn or in the absence of the amino acid, a condition that strictly mimics the BM situation during ASNase treatment. This finding prompted us to identify the transport routes involved in these metabolic exchanges.

To this purpose, we have compared MSCs from healthy donors (HD-MSCs) with ALL-MSCs, demonstrating that the latter protected leukemic cells from ASNase more efficiently

than the former. The expression of genes potentially involved in the protective effect was compared in two panels of primary MSCs from ALL patients and healthy donors, demonstrating that HD-MSCs expressed lower levels of the SNAT5 transporter than ALL-MSCs. SNAT5 is a bidirectional transporter of the System N family, able to mediate a symport of Na^+ with Gln or Asn, either inward- or outward-directed, depending on the substrate gradients. Consistently with gene expression data, ALL-MSCs exhibited faster amino acid efflux. Further experiments demonstrated that ALL blasts induced SNAT5 expression in HD-MSCs but not in ALL-MSCs. These results suggest that the different expression of SNAT5 in MSCs derived from ALL patients is induced by leukemia blasts, and causes a faster efflux of Asn, thus potentially contributing to the enhanced protective effect on ASNase-treated ALL blasts. Further experiments are needed to definitely verify this hypothesis.

While performing the research, we realized that the information available on the metabolism of MSCs themselves is very scarce. For this reason, we have preliminarily characterized MSCs metabolic features in Plasmax™, which is an advanced medium containing the physiological concentrations of an extended list of metabolites found in human plasma, and at low levels of oxygen, thus mimicking, as far as possible, BM conditions *in vivo*. The preliminary results obtained thus far indicate that all the MSC strains tested, from leukemia patients or healthy donors, proliferated at 1%O_2, exhibited an aerobic glycolytic behavior and secreted citrate in the extracellular medium. Further experiments will ascertain if this metabolic behavior is modified by co-culturing MSCs with ALL blasts.

In summary, Glutamine Synthetase and the transporter SNAT5 play key, but distinct, roles in the metabolic exchanges occurring in the ALL BM niche and, therefore, could be proposed as therapeutic targets to counteract ALL resistance to ASNase. These results allow to propose a working model of an amino acid trade-off between ASNS-negative Acute Lymphoblastic Leukemia blasts and mesenchymal stromal cells, in which not only MSCs actively sustain the metabolic needs of ASNS-deficient ALL cells but also ALL cells actively shape the metabolic landscape of the BM niche a) synthetizing and extruding Gln for Asn synthesis in MSCs and b) manipulating MSCs gene expression so as to enhance their capability to extrude Asn. This mechanism would be boosted upon the Gln and Asn depletion induced by the anti-leukemic drug L-Asparaginase, through GS-dependent MSC adaptation, but it may also operate under basal conditions, given the Asn auxotrophy of ALL blasts.

List of abbreviations

α-KG	α-Ketoglutarate
ALL	Acute Lymphoblastic Leukemia
ALL-MSCs	Mesenchymal Stromal Cells derived from Leukemia Patients
Asn	Asparagine
ASNase	L- Asparaginase
ASNS	Asparagine Synthetase
Asp	Aspartic acid
ATF4	activating translation factor 4
BCH	2-aminobicyclo[2.2.1]heptane-2-carboxylic acid
BCP	B Cell Precursor
BM	Bone Marrow
BMN	Bone Marrow Niche
BSA	Bovine Serum Albumin
CAFs	Cancer-Associated Fibroblasts
CRBN	Cereblon
DMEM	Dulbecco's modified Eagle medium
EBSS	Earle's Balanced Salt Solution
eIF2α	α subunit of human initiation factor 2
EVs	Extracellular Vesiscles
FBS	Fetal Bovine Serum
FCCP	Carbonyl cyanide-4-(trifluoromethoxy) phenylhydrazone
GAPDH	Glyceraldehyde 3-phosphate dehydrogenase
GCN2	General Control non Repressible 2
GDH	Glutamate Dehydrogenase
GGT	γ-glutamyltransferase
Gln	Glutamine
GLS	Glutaminase
Glu	Glutamic acid
GPNA	γ-L.glutamyl-p-nitroanilide
GS	Glutamine Synthetase
HD	Healthy Donors
HD-MSCs	Mesenchymal Stromal Cells derived from Healthy Donors

His	Histidine
hTERT	human Telomerase Reverse Transcriptase
LC-MS	Liquid Chromatography tandem Mass Spectrometry
Leu	Leucine
MDR	Minimal Residual Disease
MeAIB	N-methyl,α-methylaminoisobutyric acid
MSCs	Mesenchymal Stromal Cells
MSO	Methionine L-sulfoximine
mTORC	Mammalian Target Of Rapamycin
OCR	Oxygen Consumption Rate
PBS	Phosphate Buffered Saline
PCR	Polymerase Chain Reaction
PI	Protection Index
PNA	p-nitroanilide
RPL-15	Ribosomial Protein L-15
SCT	Stem Cell Transplantation
TCA cycle	tricarboxylic acid cycle
Thr	Threonine
TM	Tumor Microenvironment

Table of contents

1. Introduction

1.1. Acute Lymphoblastic Leukemia (ALL)

Acute Lymphoblastic Leukemia (ALL) is a neoplastic transformation of lymphoid progenitor cells, which start to proliferate in uncontrolled way, to accumulate in bone marrow and blood, and to invade other organs such as lymph nodes, spleen, liver and brain. The immature neoplastic cells are called blasts and can be of two different types:

- Precursors of B lymphocytes, 85% of cases
- Precursors of T-lymphocytes, 15% of cases

The clinical course of acute leukemia is very fast and, if untreated, fatal.

ALL is the second most common acute leukemia in adults and the most common pediatric cancer. Indeed, in children, it represents 25% of all oncologic diagnoses and 80% of all leukemia cases. The incidence is 400 new cases per year in Italy (from Associazione Italiana Ematologica Italiana (AIEOP), https://www.aieop.org/web/famiglie/schede-malattia/leucemia-linfoblastica-acuta/ consulted on October 29, 2019), and follows a bimodal distribution, with a first peak between 2 and 5 years and a second peak after 50 [1]. Incidence is higher in males with a ratio of 2:1; the difference is more evident between 14 and 40, while after 50 incidence is higher in females, suggesting a protective effect of female sexual hormones [2].

ALL causes are unknown, but some risk factors have been identified [3]. For instance, there are genetic syndromes that predispose to ALL, such as Down syndrome, Fanconi anemia, Bloom syndrome, ataxia telangiectasia and Nijmegen breakdown syndrome. Other risk factors are ionizing radiation, pesticides and Epstein-Barr virus and HIV.

The accumulation of blasts causes a reduction of the number of erythrocytes, platelets and mature white blood cells, with anemia, bleeding and susceptibility to infections [3]. ALL symptoms are not specific; the disease presents with very common alterations, such as pallor, weakness, anorexia, fever, bone pain, ecchymosis, dyspnea, lympho-adenomegaly.

In the past, the French-American British (FAB) group identified three different types of ALL on the basis of blast morphologic features [4]:

- L1, small homogeneous blasts with scant cytoplasm and regular nuclei. L1 is the most common subtype in pediatric patients (75%).
- L2, heterogeneous blasts larger than normal lymphocytes, with sizable cytoplasm and irregular nuclei. L2 is very common in adults.

- L3, large homogenous blasts with basophil cytoplasm and aggregated chromatin in nuclei. L3 represents only the 5% of ALL cases.

This classification is not correlated with genetic abnormalities and immunophenotype and does not predict clinical behavior. For this reason, a phenotypic classification is used. It has been revised by World Health Organization (WHO) in 2016, and considers the type of involved lymphocytes (B or T), cell maturation level, and genetic features, in order to define better the prognosis and the therapeutic treatment (see Table 1) [5].

T lymphoblastic leukemia/ lymphoma (pre-T ALL)	B lymphoblastic leukemia/lymphoma (pre-B ALL)
Provisional entity: Early T-cell precursor	non-otherwise specified (NOS)
Provisional entity: Natural killer (NK)	recurrent genetic abnormalities
	t(9;22)(q34.1;q11.2);BCR-ABL1
	t(v;11q23.3);KMT2A rearranged
	t(12;21)(p13.2;q22.1); ETV6-RUNX1
	hyperdiploidy
	hypodiploidy
	t(5;14)(q31.1;q32.3) IL3-IGH
	t(1;19)(q23;p13.3);TCF3-PBX1
	Provisional entity: BCR-ABL1–like
	Provisional entity: iAMP21

Table 1. *WHO classification of pre T and pre B acute leukemias, adapted from Arber et al 2016 [5]*

ALL patients have different clinical outcomes, depending on their age and on the cytogenetic abnormality present (see Table 2) [6]. The most common chromosomal aberrations in ALL are translocations, such as t(9;22) (also known as the Philadelphia chromosome) and t(4;11), which is associated with an adverse clinical outcome. The result of the translocation is the formation of chimeric protein, which alters the transcription of genes involved in cell differentiation and proliferation. For instance, in the case of the translocation (4;11), which is detected in more than 50% of infant leukemias, there are AF4-MLL and MLL-AF4 fusion alleles. The role of AF4-MLL is controversial, although Bursen et al. demonstrated that its presence induce ALL in mice, also in the absence of MLL-AF4 chimeric protein [7]. On the other hand, MLL-AF4 activates the anti-apoptotic factor BCL-2 [8] and the homeobox gene HOXA9, which is usually expressed in hematopoietic stem cells and tends to be down-regulated during cell maturation [9]. Moreover, MLL-AF4 activates the hematopoietic factor RUNX1 that cooperates with AF4-MLL to induce several gene targets [10].

Several subtypes of ALL are characterized by the alteration of epigenetic mechanisms, suggesting that gene silencing through epigenetic methylation during lymphoid development could be involved in leukemic transformation [11].

Chromosome aberration/ genes involved	Children		Adults	
	Frequency	Clinical outcome	Frequency	Clinical outcome
High hyperdiploidy	23–30%	Favorable	7–8%	Favorable Intermediate
Hypodiploidy	6%	Intermediate for patients with 45 chromosomes Adverse for patients with <45 chromosomes Intermediate for patients with <46 chromosomes	7–8%	Adverse
Near-haploidy	0.4–0.7%	Adverse	Rare	Not determined
t(12;21)(p13;q22)/ *ETV6-RUNX1 (TEL-AML1)*	22–26%	Favorable	0–4%	Not determined
t(9;22)(q34;q11.2)/*BCR-ABL1*	1–3%	Adverse	11–29%	Adverse
t(4;11)(q21;q23)/ *MLL-AFF1*(*AF4*)	1–2% 55% of infants	Adverse	4–9%	Adverse
t(1;19)(q23;p13.3)/ der(19)t(1;19)(q23;p13.3)/ *PBX1-TCF3 (E2A)*	1–6%	Favorable Intermediate	1–3%	Favorable Relatively favorable Intermediate Adverse
t(10;14)(q24;q11)/ *TCRA/TCRD-TLX1 (HOX11)*	Rare	Not determined	0.6–3%	Favorable Intermediate
del(6q)	6%–9%	Not prognostic	3–7%	Intermediate
Abnormal 9p	7–11%	Not prognostic Adverse	5–15%	Favorable Relatively favorable Intermediate
Abnormal 12p	3%–9%	Not prognostic	4–5%	Favorable
Normal karyotype (no aberration detected)	31–42%	Relatively favorable	15–34%	Relatively favorable Intermediate

Table 2. *Frequency and clinical outcome of the major chromosome aberrations in pediatric and adult Acute Lymphoblastic Leukemia, adapted from Mrózek et al 2009 [6].*

The diagnosis of ALL is based on a multistep strategy, which includes analysis of morphology, cytochemical, immunophenotype, classic cytogenetic, molecular features and gene rearrangement of Ig and T-cell receptor [12]. The first step is a bone marrow aspiration and blood cell count, which allows to evaluate the number of cells and their morphologic and cytochemical features through the May Grunwald Giemsa stain. The percentage of ALL blasts in bone marrow cells is higher than 30%. The subtype of ALL (pre B or pre-T) is then determined through an immunophenotype analysis. Fluorescence in situ hybridization (FISH) and Polymerase Chain Reaction (PCR) are used for cytogenetic and molecular studies and allow to evaluate the karyotype. In some cases a lumbar puncture is needed to collect cerebrospinal fluid in order to evaluate the involvement of central nervous system [3]. All these approaches allow to obtain a correct patient stratification and, thereafter, to choose the best therapeutic treatment.

1.2. ALL treatment

In the last decades, the 5-year disease-free survival of pediatric ALL patients has been improved from 5% to more than 85%, thanks to the intensification of treatments, even if the prognosis is still poor in adults [13].

The main treatment is chemotherapy, which is divided into three phases (see Table 3):

1. Induction, to restore normal hematopoiesis
2. Consolidation, to remove the residual leukemia blasts, which consists in an early phase of treatment intensification and a late one of re-induction. The latter improves clinical outcome in patients with standard or higher risk [14].
3. Maintenance, to prevent a relapse

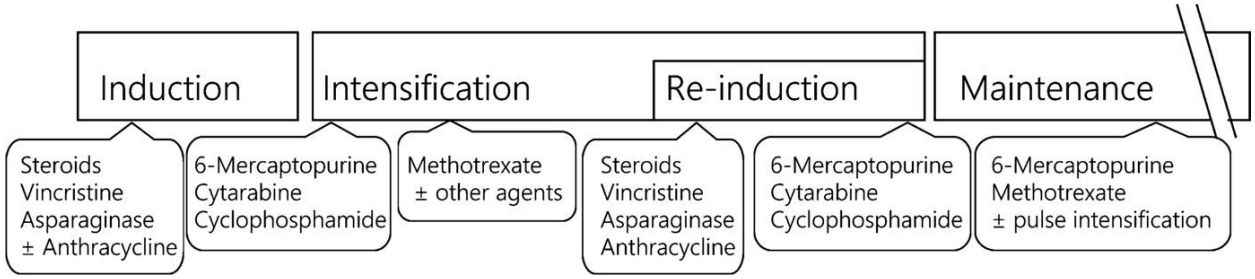

Table 3. *Treatments in Acute Lymphoblastic Leukemia therapy, from Kato et al 2018 [13].*

Cranial irradiations are adopted to prevent the spread of leukemia cells to central nervous system, although this approach increases the risk of second neoplasm and neurocognitive deficits. Therefore, Pui et al proposed to replace it with an effective risk-adjusted chemotherapy [15].

In the case of BCR-ABL1-like (Ph-like) ALL patients, the fusion protein is a tyrosine kinase that stimulates cell proliferation and, for this reason, a targeted therapy is possible. Indeed, the use of tyrosine-kinase inhibitors (TKI), such as Imatinib, improves the overall survival of these patients, which usually had a very poor clinical outcome [3].

Nevertheless, with all these therapeutic options, 10-15% of ALL patients still relapse. Therefore, in the future, novel treatments have been proposed, such as the use of monoclonal antibodies against several antigens of leukemia cells membrane, proteasome inhibitors like Bortezomib (already approved for multiple myeloma treatment), JAK inhibitor, PI3/mTOR inhibitor and hypomethylating agent [3].

The most recent approach is adoptive immunotherapy, where T cells are genetically engineered and express chimeric antigen receptor (CAR), which are able to bind specific antigens of leukemia blasts [16].

Finally, in the presence of relapses or high-risk patients, an option of treatment is a stem cell transplantation (SCT) to replace leukemia blasts with normal cells. However, SCT reduces the possibility of relapses, but is associated with increased treatment-associated mortality [17]. Allogeneic transplantation with bone marrow derived from matched-donor is recommended and is associated with a significant increase of the 5-year disease-free survival of the patient than unmatched donor SCT [18].

After the therapeutic treatment, depending on the outcome, ALL patients can be divided into three groups:

1. Complete remission: there are no signs or symptoms and the number of leukemia blasts in bone marrow is less than 5%
2. Active Disease: the number of ALL blasts is more than 5% in bone marrow and there are signs of disease relapse.
3. Minimal Residual Disease (MRD): there are still blasts in bone marrow, but they can be seen only using flow cytometry or PCR.

Recently, a metabolomics study shows that in bone marrow plasma of MDR patient glucose decreases and metabolites of the pentose phosphate pathway and the TCA cycle increase compared with the bone marrow in complete remission, suggesting a glycolytic activity of ALL cells [19]. Indeed, treating several ALL cell lines with inhibitors of nicotinamide phosphoribosyltransferase (NAMPT), which is the enzyme able to generate NAD^+ needed for glyceraldehyde 3-phosphate in glycolysis, cell viability is reduced. The authors propose metabolomics as method for risk stratification of ALL patients, especially in the case of MRD, which is the strongest risk for relapse.

This is not the only therapeutic approach based on the metabolic features of ALL blasts. Indeed, L-Asparaginase (ASNase), a bacterial enzyme able to hydrolyze plasma Asparagine (Asn) and, with a lower affinity, Glutamine (Gln), is a mainstay of therapy in the induction and re-induction treatments. Indeed, ALL cells express very low levels of Asparagine Synthetase (ASNS), the enzyme able to synthetize Asn from aspartate (Asp) and Gln, and, thus, they are dependent on extracellular Asn (Asn auxotroph). For this reason, the treatment with ASNase reduces Asn levels in plasma and causes a severe nutritional stress in ALL blasts and, eventually, their death[20].

1.3. L-Asparaginase: the first metabolic drug

The enzyme L-asparaginase was discovered in 1953 by Kidd, who observed that guinea pig serum inhibited the growth of lymphosarcoma xenografts in mice [21, 22]. Then, Broome demonstrated that the presence of an asparaginase activity in guinea pig serum was the responsible of this tumor regression [23, 24]

The anti-neoplastic effects of ASNase are associated to its ability to catalyze the hydrolysis of Asn (see Graph 1), and the rationale for its use in ALL therapy is based on the lack of ASNS expression in most of ALL blasts [25].

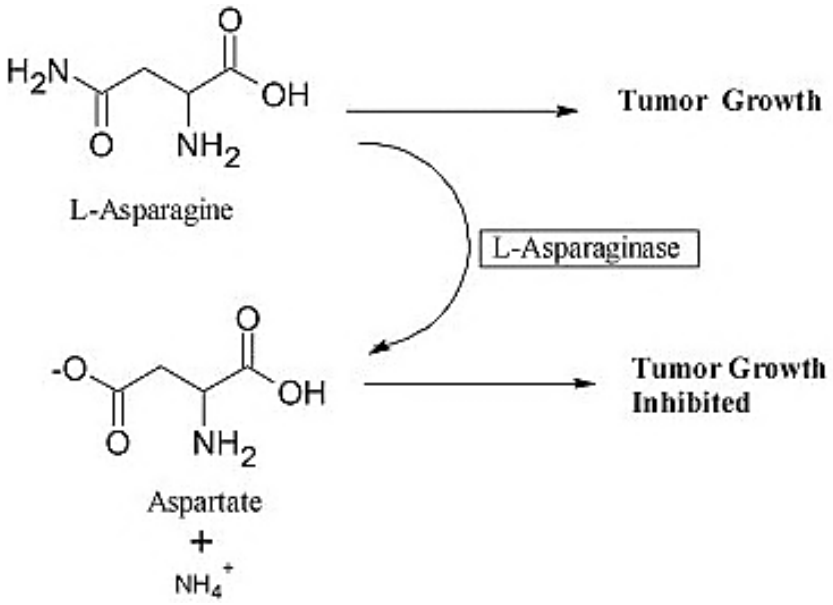

Graph 1. *Mechanism of action of L-Asparaginase, from Narta et al 2007 [25].*

A sizable ASNase activity does not exist in most mammalian cells (and in particular in human cells). This seems to be an adaptive process that allows cells to better adapt to variations of extracellular glutamine. Indeed, upon glutamine depletion, when mammalian cells are transfected with ASNase derived from zebrafish, Asn levels cannot be maintained, because it is converted into Asp by ASNase, and cells growth is blocked [26].

On the other hand, sources of ASNase are bacteria, yeasts, fungi, actinomycetes and algae [27]. In particular the most known forms, exploited for clinical treatments, derived from different bacteria like *Escherichia coli* and *Erwinia chrysanthemi* (now Dickeya dadantii [28]).

Both forms are tetramers, with an active site for each subunit, and the molecular weight is of 133-141 kDa for *E. coli* and 138 kDa for *E. chrysantemi.* Although the major enzymatic

activity of ASNase is asparaginolytic, the drug is also able to hydrolyze glutamine into glutamate and ammonium. Therefore, this drug causes both an intracellular and an extracellular Gln depletion *in vivo* [29] and *in vitro* [30]. Since Gln is the obliged substrate of ASNS, Asn synthesis is impaired. This explains why ASNase efficacy versus those ALL blasts which are endowed with sizable ASNS expression depends on its glutaminolytic, rather than asparaginolytic activity [31]. Moreover ASNase glutaminase activity is needed for durable anticancer activity *in vivo*, also against ASNS-negative ALL blasts [32]. Until now, ASNase is used to the treatment of hematologic malignancies (ALL, NK lymphomas, other selected cases of T-cell lymphoma), but, in theory, its clinical use may be extended also to Gln auxotroph or Gln addicted tumors [33].

At the moment, three different ASNase preparations are used for ALL treatment: the native *E. coli* (Colaspase), the pegylated *E. coli* (Pegaspargase) and the native *E. chrysanthemi* (Crisantaspase or Erwinase). The asparaginolytic activity is comparable in all of ASNase forms, whereas the glutaminolytic capacity is higher in Erwinase (see Table 4).

	E. coli		*Erwinia* (Native)
	Native	PEGylated	
Activity (IU/mg protein)	280–400	280–400	650–700
K_m (μM)-L-asparaginase	12	12	12
K_m (μM)-L-glutaminase	3000	3000	1400
L-Glu/L-Asp (maximal activity)	0.03	0.03	0.10
Molecular weight	141000	–	138000
PI	5.0	5.0	8.7

Table 4. *Features of different preparations of L-Asparaginase (ASNase), from Narta et al 2007 [25].*

Colaspase and Pegaspargase are used in the first line therapy. The pegylated form is the native enzyme conjugated with monomethoxypolyethylene glycol and thus shows a prolonged half-life and reduced immunogenicity. In the case of hypersensitivity, treatment is switched to Erwinase, even if the disadvantage is a shorted half-life [34].

ASNases are administered either by intramuscular or intravenous injection and are mainly confined in the vascular space, as well as in the pleural and ascitic fluids, but do not reach the cerebrospinal fluid. The clearance of the drug is mediated by reticuloendothelial system (RES) cells, which cleave ASNase by proteolytic enzymes (i.e cathepsin) [25]. Therefore, since a severe depletion of blood Asn is caused by ASNase blood levels of 0.4-

0.7 IU/ml, the activity of the drug should be measured in ALL patients during the treatment. In the case of pegylated ASNase, if the activity is lower than 0.1 IU/ml it is necessary to switch the therapy to Erwinase [34]. Studies, aimed at the development of novel ASNase preparations to improve pharmacokinetics and tolerance, are ongoing [35].

In optimally treated patients, blood Asn is depleted from 50 μM to 3 μM or lower for 2-3 days, whereas glutamine concentration is reduced from 600 μM to 80 μM for several hours [20]. Therefore, while Asn levels remain low during the treatment, Gln levels are restored to values higher than 400 μM already after one day [36].

Side effects are associated with ASNase use in ALL therapy [37]. Some patients develop pancreatitis, thrombosis and nervous system disorders, such as encephalopathies somnolence, confusion, lethargy.

These effects are mainly attributed to ASNase activities on tissues with high rate of protein synthesis, such as the liver and pancreas, which are particularly sensitive to the amino acid shortage caused by the drug. Indeed, hepatic toxicity leads to steatosis, increase of transaminase and bilirubin, decrease in serum albumin, fibrinogen and lipoprotein levels, endocrine disorders, and coagulation dysfunction [38].

Given that ASNase is an exogenous and ,hence, an immunogenic protein, it can cause hypersensitivity reactions and the development of antibodies [39].

In spite of the side effects, the introduction of ASNase in therapeutic protocols dramatically improved ALL clinical outcome and was strongly correlated with higher overall survival of the patients [40]. Several studies demonstrated that patients receiving ASNase in the induction therapy survive more than those treated without the enzyme [41-43].

1.4. L-Asparaginase resistance: role of the stromal microenvironment

Although ASNase had led to a substantial improvement of ALL therapy, leukemic cells may become resistant to the enzyme [31]. The adaptive induction of ASNS, triggered by the amino acid deprivation caused by ASNase, has been proposed as a resistance mechanism [44] but the correlation between ASNS expression level and patient sensitivity to ASNase is very poor [45, 46]. These results suggest that additional mechanisms could be involved. Nevertheless, Nakamura et al demonstrated that the inhibition of GCN2 sensitizes cancer cells with very low levels of ASNS, like ALL blasts, to the treatment with ASNase [47]. GCN2 (general control non repressible 2) is one of the activator kinases of an integrated stress response [48], activated by uncharged tRNA in response to an amino acid depletion. GCN2 phosphorylates the alpha subunit of eukaryotic translation initiation factor 2 (eIF2a) on serine 51. This factor is the main sensor of nutritional stress and, when phosphorylated, attenuates protein synthesis and promotes the translation of selected mRNAs like that for the activating translation factor ATF4, which induce the expression of several genes, such as *ASNS* itself, to recover homeostatic conditions, or *DDIT3* (encoding for the pro-apoptotic factor CHOP) to drive the cell towards an apoptotic death.

In fact, it is now accepted that ALL blasts become ASNase resistant through a complex process, which involves multiple metabolic adaptations [49] and the overexpression [50] or down regulation [51] of several genes.

Most of these studies have concerned the ALL cell itself. However, also tumor microenvironment (TM) could actively contribute to ASNase resistance of ALL blasts *in vivo*. Indeed, TM plays a key role in supporting neoplastic cells: it is metabolically flexible, rich of paracrine signals, endowed with aberrant vessels and stromal cells, which may assume a tumor-promoting role [52, 53]. Peculiar metabolic relationships between neoplastic and stromal cells have been characterized in a variety of human tumors [54]. For instance, in several kinds of tumors under hypoxic conditions, lactate is exchanged between glycolytic cancer cells and stromal cells, which rely more on oxidative metabolism [55, 56]. Moreover, in both non-haematological [57, 58] and haematological cancers [59, 60], stromal cells can release nutrients to support neoplastic cells.

In haematological malignancies a rich cross-talk, mediated by both physical contact and extracellular vesicles (EVs), exists between stromal cells of the Bone Marrow Niche (BMN) and cancer cells leading to the organization of a cancer-specific pro-tumorigenic environment. BMN is a highly dynamic structure and includes, besides hematopoietic progenitors, fibroblasts, Mesenchymal Stromal Cells (MSCs), immune cells and

endothelial cells, all of which can modulate the exchange of metabolites with the microenvironment in response to stress conditions, inflammatory mediators, endocrine factors or paracrine signals [61].

BMN features is profoundly modified by the presence of leukemia blasts, which create an abnormal “malignant” microenvironment, secreting anti-apoptotic factors, hindering normal hematopoiesis, and promoting the neoplastic progression [62].

For instance, the production of inflammatory cytokines, such as IL1β, TNF-α and chemokines like CXCL10, CXCL8, CXCL1, CCL2, increases in ALL BMN [63]. It has been also shown that CCL2 synthesis and production by ALL cells is induced by MSCs through the release of the multifunctional extracellular factor Periostin (POSTN) [64]. Conversely, POSTN expression is up-regulated in MSCs by a signaling pathway activated by CCL2 itself. On the other hand, CXCL12 levels in BMN are lowered, suggesting that bone marrow self-reinforcing is independent of the axis CXCR4/CXCL12 [65].

Thus, not only neoplastic cells, but also TM may be a target for anti-cancer drugs. This is already the case of Trabectedin (Yondelis®), which is a DNA binder used in sarcoma and ovarian cancer treatment. It is cytotoxic for human monocytes *in vitro* and inhibits the production of some cytokines such as CLC2, thus showing also a potential effect on stromal cells [66].

Some reports proposed the involvement of BMN in the resistance of ALL blasts to ASNase. For instance, Van den Meer et al. evaluated the biodistribution of radiolabeled ASNase in C57BL/6 mice and showed that the drug was accumulated in tissues rich in macrophages, such as liver, spleen and bone marrow. These cells promote a rapid clearance of the drug, which is phagocyted and degraded by the lysosomal protease cathepsin B. Authors propose that BM-resident macrophages may thus provide protection to ALL blasts during the treatment with ASNase [67].

Another evidence of the BMN importance was provided by Iwamoto et al.[68], who demonstrated that a line of immortalized human BM-derived MSCs protected leukemic blasts from ASNase through Asn synthesis and secretion. Interestingly, MSCs with an higher expression of ASNS protected more efficiently ALL cells than ASNS negative MSCs, suggesting that metabolic properties of stromal cells can significantly modulate their relationship with the tumor. Consistently, aspartate concentration increases in the BM blood during ASNase treatment *in vivo* [69], a finding attributable to increased Asn synthesis and subsequent hydrolysis by ASNase [70]. The protection from ASNase effects

is hampered by vincristine but not by imanitib, implying that Asn secretion, the mechanism of which has not been elucidated yet, requires functional microtubules [71].

More recently, using murine ALL models and adipocyte-differentiated 3T3-L1 cells, it has been also claimed that adipocytes, another component of the BM stroma derived from MSCs, reduce ALL blast sensitivity to ASNase through the release of Gln [72]. The process is hampered by methionine-L-sulfoximine (MSO), an irreversible inhibitor of Glutamine Synthetase (GS), which is the enzyme able to synthetize Gln from Glu and ammonium.

All these data suggest that MSCs could have an important role in the nutritional support of ALL blasts during the treatment with ASNase although the involved mechanisms have not been investigated yet.

1.5. Mesenchymal stromal cells (MSCs)

MSCs were isolated from human bone marrow by Friedenstein in 1976 [73]. They are multipotent stem cells, which can differentiate into several types of cells such as adipocytes, chondrocytes and osteoblasts (see Graph 2).

The self-renewal and differentiation of MSCs are regulated by intrinsic (genetic) and extrinsic (microenvironment features) factors

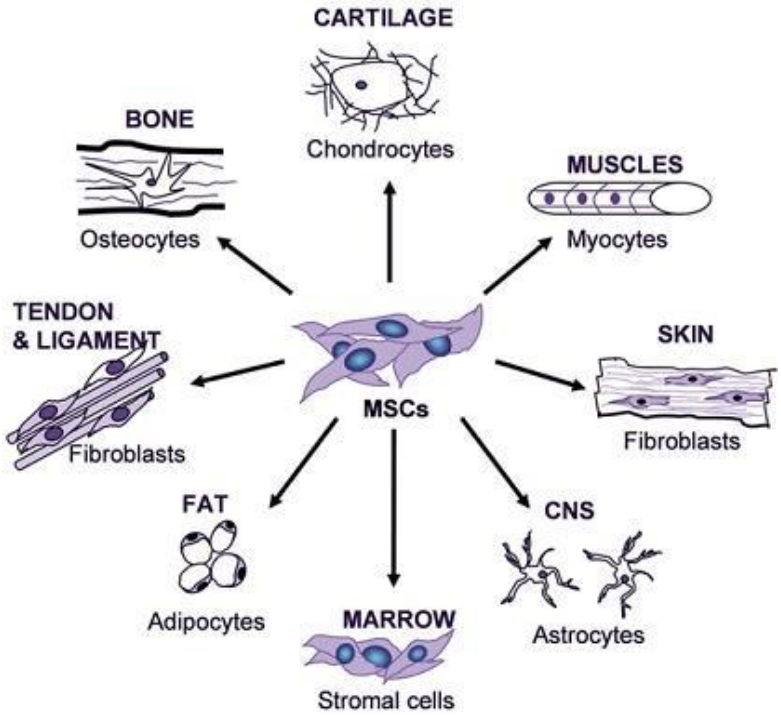

Graph 2. *Potential differentiation pathways of bone marrow Mesenchymal Stromal Cells (MSCs), from Chicago Biomedical Consortium (https://www.chicagobiomedicalconsortium.org/mesenchymal-stem-cells/ Accessed on October 26, 2019).*

In 2016 the international Society for Cellular Therapy proposed the minimal criteria to define MSCs, which must: [74]

1. adhere at the plastic when they are cultured *in vitro*
2. express markers such as CD105, CD73, CD90 but not typical hematopoietic markers such as CD45, CD34, CD14, CD19, CD11b
3. have the ability to differentiate into chondrocytes, osteoblasts and adipocytes.

MSCs can be isolated from several tissues such as bone marrow and adipose tissue. They grow at low density, modify their features reaching senescence and their proliferative rate progressively slow down with passages *in vitro*. All these data suggest that in experiments *in vitro* should use cells for few passages [75].

MSCs show several features that could be used in therapy. Indeed, they regulate hematopoiesis, have an elevated plasticity and a pluripotent differentiation capacity. In addition, they are endowed with an immunomodulatory activity and are able to migrate to sites of injury to support tissue repair. All these properties prompt clinical applications of MSCs in different conditions such as bone or cartilage lesions, cancer, cardiovascular or immune-mediated diseases [76].

In several contexts it has been demonstrated that MSCs, promoting tissue repair and angiogenesis, and are able to support cancer cell growth [77]. Besides these indirect activities, they may also directly interact with tumor cells and help them to create a pro-tumorigenic environment. The cross-talk between the two cell populations is direct or indirect. Direct interaction needs physical contact between stromal and cancer cells; examples are the activation of Notch signaling, or the exploitation of gap junctions (or nanotubes for longer distances) to transfer small molecules or, in the case of nanotubes, even whole organelles. Further possible mechanisms are trogocytosis, which consists in an exchange of plasma membrane, and, in rare cases, the formation of a fusion cell.

Indirect interactions are characterized by the transfer of molecules without physical contact between cells. Thus, cells (either stromal or cancer) can release signaling molecules such as cytokines, chemokines, growth factors or metabolites and all of them can be secreted directly into the extracellular environment or internalized into exosomes or microvesicles. In this way, MSCs could, for example, contribute to the resistance of cancer cells to chemotherapy. In particular, there are several studies demonstrating the protection of ALL blasts by MSCs through both nutritional and nutritional-independent mechanisms (see below).

In addition to the already cited reports, in which authors propose that MSCs support ALL blasts from ASNase through Gln or Asn synthesis and release, another example of nutritional mechanism has been provided by Boutter et al. These authors have shown that MSCs secrete cystine through the xCT transporter, which mediates an exchange of cystine and glutamate, and provide it to ALL blasts, which internalized and metabolized the amino acid to cysteine [78]. In this way cancer cells have a large availability of the limiting substrate to generate and maintain glutathione in order to reduce oxidative stress. Indeed, cysteine depletion, using cysteine dioxygenase, resulted in leukemia cell death.

As far as nutritional-independent mechanisms are concerned, Naderi et al showed that MSCs protect ALL cells from P53 accumulation and, thus, apoptotic death, through the production of PGE_2 [79]. Moreover, the inhibition of PGE_2 synthesis reduces stromal cell protection. Other studies propose an involvement of the Notch pathway, the inhibition of which decreases the survival of B-ALL cells, either cultured alone or co-cultured with stromal cells derived from normal donors or B-ALL patients [80].

ALL BMN presents peculiar features, including striking modifications in BM plasma amino acids, in particular aspartate and glutamine, which are key substrates for anabolic reactions [81].

1.6. Glutamine metabolism

Glutamine (Gln), the most abundant amino acid in human blood (0.5-0.7 mM), is essential for nitrogen trafficking among tissues. Indeed, the liver eliminates the excess of ammonia as urea from Gln via the urea cycle, a process first identified by Krebs. Moreover, kidney metabolism of Gln is a major factor for the maintenance of the acid–base homeostasis. Some tissues, as skeletal muscle, are able to synthetize Gln through Glutamine Synthetase (GS), which catalyzes the ATP-synthesis of Gln from glutamate (Glu) and ammonium. Gln availability is crucial for the kidney, the gastrointestinal tract, keratinocytes and several types of immune cells, especially under catabolic stress conditions [82]. Moreover, it is a compatible osmolyte for the regulation of cell volume under hypertonic conditions. Rapidly dividing cells such as activated lymphocytes, enterocytes and cancer cells, avidly consume Gln for both energy production and biomass accumulation [83].

In the last years several studies have investigated the mechanisms through which Gln is needed in several cancer cells to support tumor growth and proliferation. The amino acid is involved in several metabolic processes (see Graph 3 [84]).

Gln is the obliged nitrogen donor for the biosynthesis of purines and pyrimidines [85]. Regarding the first, the γ nitrogens of two molecules of Gln are added to the growing purine ring, and a third is used in the conversion of xanthine monophosphate to guanosine monophosphate, whereas for pyrimidines production the conversion of uridine triphosphate into cytidine triphosphate requires one nitrogen derived from Gln.

Gln is also the precursor of different biologically important molecules, such as glucosamine, other non-essential amino acids (i.e. asparagine, glutamate and, through Glu, several transaminase substrates and proline), glutathione, which is the most abundant intracellular antioxidant, and GABA [84]. The biosynthesis of glucosamine is catalyzed by glutamine-fructose-6-phosphate aminotransferase 1 (GFPT1), using Gln and fructose-6-phosphate [86]. The product of this reaction, N-acetylglucosamine (GlcNAc), is a substrate for heparin sulfate and hyaluronic acid biosynthesis.

The synthesis of asparagine and glutamate are mediated by Asparagine Synthetase (ASNS) and Glutaminase (GLS), respectively. ASNS synthetizes Asn from Gln and Asp, whereas GLS mediates a deamidation of Gln to produce Glu and ammonium [84].

Glu, in turn, is required for the biosynthesis of other non-essential amino acids, such as alanine, serine and glycine, and is a constituent of the tripeptide glutathione (γ-glutamyl-cysteinil-glycine, GSH). Moreover, Glu favors the influx of cystine, the dimer of cysteine, through the xCT exchanger (encoded by *SLC7A11*), thus promoting indirectly the

biosynthesis of GSH [87]. Lastly, Glu is deaminated to α-ketoglutarate (α-KG, 2-OG) by either glutamate dehydrogenase (GDH) or transaminases, thus providing a Krebs cycle intermediate. For this reason, Gln can be considered an anaplerotic substrate [84].

Finally, Gln is an activator of the mammalian target of rapamycin (mTORC1), a serine/threonine kinase that stimulates protein synthesis and inhibits autophagy. mTORC1 is the master regulator of protein synthesis, cell size and growth by integrating different signals from nutrients, energy status and the presence of stress conditions. Nicklin et al. [88] have proposed that Gln indirectly activates mTOR by promoting leucine (Leu) uptake through a secondary active transport; however there are also evidences that Gln activates mTORC1 independently of Leu [89, 90].

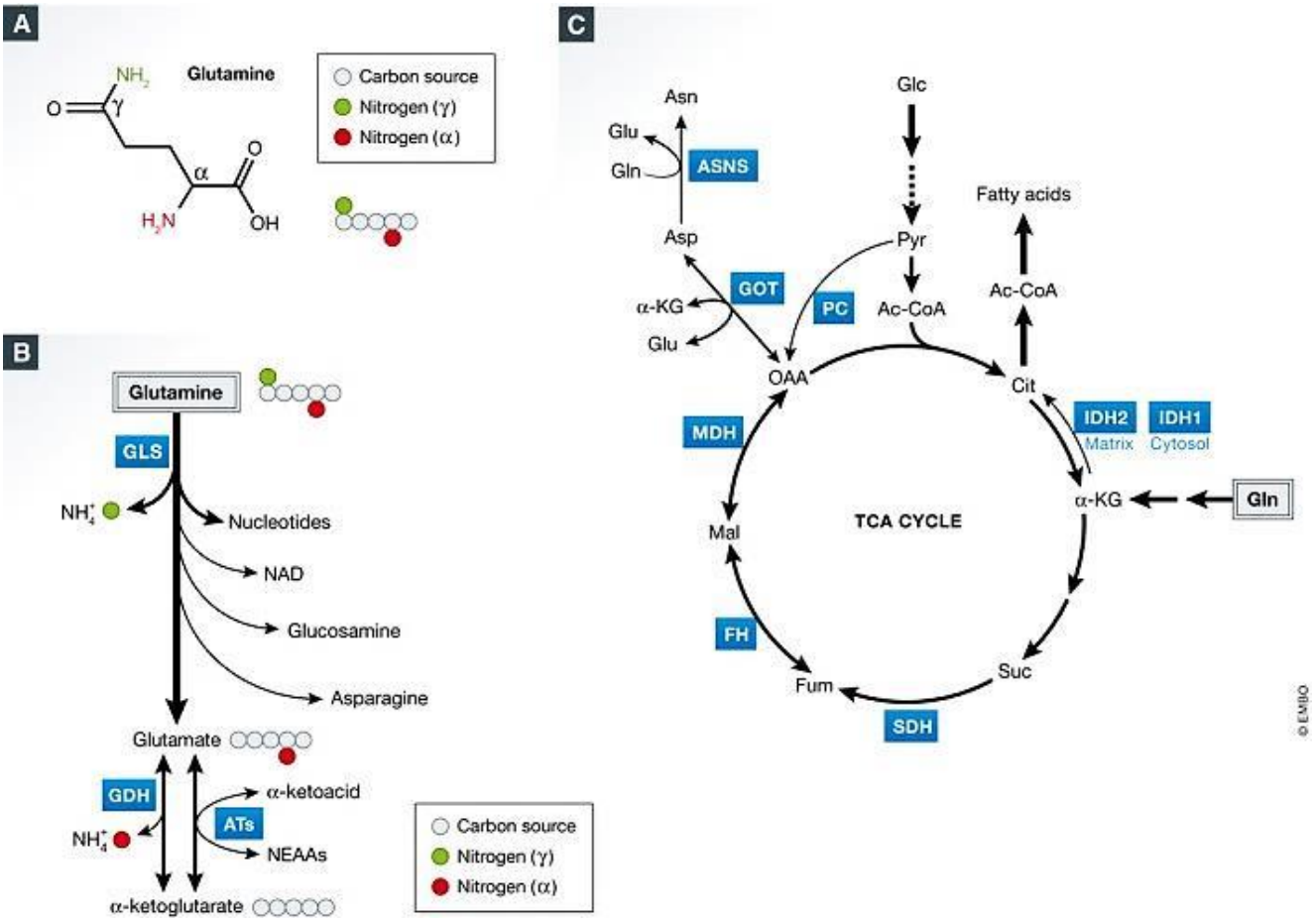

Graph 3. *Glutamine (Gln) involvement in several biosynthetic reactions. (A) Chemical structure of Gln, (B) Gln as nitrogen source, GLS: glutaminase; GDH: glutamate dehydrogenase; ATs: aminotransferases (transaminases), (C) Gln as carbon source for the TCA cycle, α-KG: α-ketoglutarate; Suc: succinate; Fum: fumarate; Mal: malate; OAA: oxaloacetate; Cit: citrate; Glu: glutamate; Asp: aspartate; Asn: asparagine; Glc: glucose; Pyr: pyruvate; Ac-CoA: acetyl-CoA; SDH: succinate dehydrogenase; FH: fumarase; MDH: malate dehydrogenase; GOT: aspartate aminotransferase; ASNS: asparagine synthetase; PC: pyruvate carboxylase; IDH1/2: isocitratedehydrogenase 1/2. From Zhang Ji 2017 [84]*

Certain tumors preferentially use Gln to fulfill their anaplerotic demands, even in the presence of glucose, and, therefore, require huge amounts of the amino acid. This behavior was defined “Glutamine Addiction” by Wise et al. [85]. Examples of glutamine-addicted tumors are multiple myeloma [91], β-catenin mutated hepatocellular carcinoma [30, 92], some types of acute myeloid leukemia [93]. The treatment of cells from these tumors with ASNase caused nutritional stress and cell death. These results suggest that drugs like ASNase could be used to target glutamine-dependent cancers [94]. Moreover, ^{18}F-labeled Gln can be used as a PET probe for localization of these tumors, given their craving for the aminoacid, and there are studies ongoing about this diagnostic approach.

On the other hand, Gln also plays an important role in metabolism of normal cells. Indeed, even if Schop et al showed that Gln is not important as energy source for human MSCs [95], metabolomics analysis indicated that glutamine is the most consumed amino acid by these cells [96].

At low levels of oxygen, the normal BM condition *in vivo*, the expression of Glutamine Synthetase decreases in MSCs and, consistently, glutamate is not used for Gln synthesis, but it is rather metabolized and used as anaplerotic substrate [97].

Gln metabolism is also affected by MSC aging. Indeed, aged MSCs reduce autophagy, preferentially use glucose as energy source and show a lowered capacity to use glutamine and fatty acids as alternative fuels [98].

Importantly, Gln metabolism plays a pivotal role in MSC differentiation into osteoblasts, chondrocytes and adipocytes and, consequently, in potential bone disease [99]. Moreover, during osteoblastogenesis, MSCs up-regulate GLS, suggesting an anaplerotic use of the amino acid [100].

1.7. Glutamine synthesis

Several types of mammalian cells are able to synthetize Gln through ATP-dependent condensation of Glu with ammonium, a reaction mediated by the enzyme GS, encoded by the gene *GLUL* localized on the long arm of chromosome 1. GS is mainly expressed in brain, skeletal muscle [101] and perivenous hepatocytes [102], while it is poorly expressed in smooth muscle, spleen and periportal hepatocytes. Astrocytes convert Glu (the excitatory neurotransmitter taken up from the synaptic cleft) into Gln, through GS, to allow its safe recycling to neurons [103], while perivenous hepatocytes express GS to detoxify the residual ammonium, which has not been fixed in urea by periportal hepatocytes. In the liver the expression of *GLUL* is under the control of the Wnt/β-catenin pathway [104]. β-catenin is a cytoskeletal protein that connects cadherin with actin, promoting intercellular interactions, but, once in the nucleus, it can also activate transcription factors to promote the transcription of several genes such as *GLUL* and *MYC*. Moreover, MYC increases GS expression through DNA demethylation, thus promoting Gln anabolism [105], and GLS, thus boosting Gln catabolism [106]. However, GS expression is peculiarly regulated at post-transcriptional levels, since the half-life of the protein is modulated by the intracellular Gln concentration [107]. Indeed, in the presence of Gln, GS is acetylated at lysine 11 and 14, conditions needed for the ubiquitinylation by $CRL4^{CRBN}$ and the degradation by proteasome. Cereblon (CRBN) is a substrate receptor of the cullin-RING ubiquitin ligase 4 (CRL4) complex. The expression of GS in cancer is a very complex issue [108]. Indeed, there are tumors with high levels of GS such as glioblastoma multiforme, which use the enzyme to synthetize Gln to support nucleotide production [58]. On the other hand, low expression of GS is considered a typical marker of glutamine addiction, since these cancer cells, such as multiple myeloma plasma cells, depend on extracellular Gln [91]. In glutamine-addicted tumors, low GS cancer cells internalize extracellular Gln, thus modifying metabolic features of TM, and eventually inducing GS in cancer-associated fibroblasts (CAFs), adipocytes and immune cells [108].

However, cancer cells can be Gln-auxotrophic but not addicted. An example of this situation is provided by human oligodendroglioma cells, which are GS negative and need Gln to survival, but do not used the amino acid as an anaplerotic substrate [109].

GS activity can be inhibited using the irreversible inhibitor methionine-L-sulfoximine (MSO), which is an analogue of the amino acid. The inhibition of Gln *de novo* biosynthesis has anti-tumor effects in hepatocellular carcinoma (HCC). Indeed, GS inhibition has clear cut anti-cancer effects on murine models of β-catenin-mutated HCC [92].

1.8. Asparagine synthesis

The synthesis of Asn, which is about 40μM in plasma, is mediated by the enzyme Asparagine Synthetase (ASNS), which catalyzes its ATP-dependent biosynthesis from aspartate and the amido-N of Gln [110].

The human ASNS gene is located at chromosome 7q21.3 and is 35 kb with 13 exons [111]. The ASNS protein (561 aa) has two primary domains, and is expressed in many tissues, with high levels in the pancreas, brain, thyroid and testes, while the liver has a low expression of the enzyme.

ASNS expression is regulated at transcriptional level and it is a target of two signalling pathways aimed to ensure cell survival under conditions of unbalanced amino acid availability, the Amino Acid Response (AAR) [112], and of Endoplasmic Reticulum stress, the Unfolded Protein Response (UPR) [113]. Both pathways lead to the phosphorylation of eIF2α, the activation of ATF4 and the induction of ASNS (see above 1.4.)

The expression of ASNS can be high or low, depending on the type of cancer. A typical example of low-ASNS tumor is ALL [13]. Until now ASNase therapy of ALL is the only successful example of a therapeutic approach targeting a metabolic vulnerability of a specific form of cancer. Other low ASNS cancers, potentially sensitive to ASNase, are the M5 subgroup of acute myeloid leukemias (AML) [114] and more than 50% of sporadic pancreatic ductal adenocarcinomas (PDAC) [115].

On the other hand, in several models of human solid cancers, ASNS expression has been found to be positively correlated with tumor growth. For instance, in breast cancer cells, ASNS is a target of the IGF1/IGF2-dependent anabolic signaling [116] and, consistently, ASNS silencing depressed cell proliferation in two distinct cell lines, one of which derives from a triple negative tumor [117]. Moreover, ASNS expression and Asn availability have been found to be strongly correlated with the metastatic behavior of breast cancer [118].

Other examples of high-ASNS tumors are prostate cancer [119] and colorectal cancer, where ASNS has been found up-regulated in several human cell lines and clinical specimens derived from colon carcinoma with mutated KRAS [120].

In theory, either low or high ASNS expression can confer some advantages to cancer cells. Low ASNS allows cells to preserve the intracellular pool of Asp. Indeed, human cells cannot use Asn as a source of Asp, due to lack of sizable expression of enzymes with asparaginase activity; therefore the metabolic relationship between the two amino acids is a one-way pathway, where Asp can be used as an Asn source, while the reverse is not possible. Interestingly, if the expression of guinea pig ASNase is forced in human cancer

cells, Asn uptake can fuel the intracellular pool of Asp, and cell growth is stimulated [121], providing a proof-of-principle demonstration of the importance of an adequate Asp availability for fast cell proliferation.

On the other hand, high levels of ASNS allow to increase Asn availability for protein synthesis. Moreover, other additional roles are attributed to Asn, beyond being a proteinogenic amino acid. For instance Krall et al. have proposed that Asn can be used as an exchange factor to promote entry and consumption of other amino acids, such as serine, arginine, leucine and histidine, although the transport routes involved were not identified [122]. Due to this activity, Asn enters indirectly into the restricted group of amino acids that can regulate mTORC1 activity and thus, global protein synthesis.

All these Asn activities and potential roles prompt to envisage possible therapeutic treatments against both low and high ASNS cancers. For the first group, a classic approach is the use of ASNase, whereas for the second one many classes of ASNS inhibitors have been proposed [123], in some cases with high potency [124] and promising results *in vitro* [125, 126], but none has been yet tested in clinical experimentation.

1.9. Glutamine and Asparagine transport

Since Gln and Asn are highly hydrophilic molecules, their uptake needs the mediation of membrane transporters. Several transporters of the two amino acids were identified at the molecular level in mammalian cell plasma, and some of them have been found overexpressed in different cancer types [127].

ASCT2 ("ASCT" stands for system ASC (Alanine-Serine-Cysteine) Transporters), encoded by *SLC1A5*, is a Na^+- coupled exchanger for neutral polar amino acids. The transport process is prevalently electroneutral, involving the influx of Na^+ /amino acid coupled with the efflux of Na^+ /amino acid. It is expressed in the intestine, kidney, lung, testis, skeletal muscle, and adipose tissue, and overexpressed in many solid tumors [128], such as hematological cancers like multiple myeloma [91]. Moreover, its expression is under the control of MYC in glutamine-addicted cancers. The natural substrate threonine (Thr), which has a fairly high affinity for ASCT2, could block the transporter. However, the ASCT2 inhibitor most commonly exploited in experimental studies is GPNA (γ-L.glutamyl-p-nitroanilide), which, for example, is able to reduce multiple myeloma cell proliferation in murine xenografts [91]. However, GPNA specificity for ASCT2 is questionable since it has been recently shown that GPNA may interact with SNAT transporters [129] and inhibits also the influx of essential amino acids through LAT1/2 transporters [130]. Moreover, it has been recently demonstrated by our group that GPNA cytotoxic effects do not only depend on the inhibition of amino acid uptake, but also derive from GPNA conversion into the cytotoxic compound PNA (p-nitroanilide) by the enzyme γ-glutamyltransferase (GGT) [131].

LAT1 ("LAT" refers to system L amino acid transporters), encoded by *SLC7A5*, is a Na^+-independent exchanger, which mediates the influx of aliphatic or aromatic amino acids (most essential amino acids belong to this category), like leucine, coupled to the efflux of an another amino acid (i.e. Gln/Asn). LAT1 have 12 transmembrane domains and is incorporated into the plasma membrane through a covalently bound 4F2hc chaperone (*SLC3A2*). It is expressed at the highest levels in the endothelial cells of the blood-brain barrier and in the placenta, and it is overexpressed in several tumors [132]. An inhibitor of LAT1 transporter is BCH (2-aminobicyclo[2.2.1]heptane-2-carboxylic acid); however, it is unspecific and blocks all the transporters of system L. Therefore, Oda et al. proposed a novel compound (KYT-0353 or JPH203) as selective LAT1 inhibitor [133].

The family of *SLC38* transporters, which are present in all human cell types, mediate the influx and efflux of small neutral amino acids, regulating their extra and intracellular

concentrations. All *SLC38* transporters are Na^+ dependent and each of them is regulated in a specific way by nutritional stimuli (eg amino acid depletion), physical stress (eg hypertonicity) or hormonal signals (eg insulin) [134].

The *SLC38* transporters are divided into two groups, the system A transporters ("A" stands for alanine-preferring) and the system N transporters ("N" stands for amido, see Table 5 [135]). Transporters of System A are concentrative, mediate an unidirectional flux of substrates, regulated by depletion or excess of amino acids, and can be inhibited by the specific analogue MeAIB (N-methyl-aminoisobutyric acid). On the other hand, carriers of System N are bi-directional and resistant to MeAIB, while no specific inhibitor is known.

Table 1 Members and properties of the SLC38 family

Gene Name	Protein Name	Alias	Mechanism	Substrate specificity	Function	Expression profile	Length
SLC38A1	SNAT1	GlnT, SAT1, ATA1, SA2, NAT2	S:1Na^+	(G),A,S,C,N,Q,H,(M)	System A	Ubiquitous	486
SLC38A2	SNAT2	SAT2, ATA2, SA1	S:1Na^+	G,P,A,S,C,N,Q,H,M	System A	Ubiquitous	505
SLC38A3	SNAT3	SN1, NAT	S:1Na^+/A:1H^+	Q,N,H	System N	Eye, liver, brain, pancreas	503
SLC38A4	SNAT4	ATA3, NAT3, SAT3, PAAT	S:1Na^+	G,(P),A,S,C,N,(M), R, K	System A	Liver, bladder	546
SLC38A5	SNAT5	SN2	S:1Na^+/A:1H^+	Q,N,H,A,S	System N	Mouth, cervix, bladder, bone, intestine, kidney, oesophagus, lung, eye	471
SLC38A6	SNAT6			Unknown		Oesophagus, cervix, mouth, lung, kidney, muscle	520
SLC38A7	SNAT7		Na^+ dependent	Q,N,A,H,S	System N	Ubiquitous	461
SLC38A8	SNAT8			Unknown		Testis	434
SLC38A9	SNAT9			Unknown		Parathyroid, testis, adrenal gland, thyroid	560
SLC38A10	SNAT10			Unknown		Ubiquitous	1118
SLC38A11	SNAT11			Unknown		Spleen, eye, bone marrow, pharynx	405

Table 5. *Features of several members of SLC38 family. Mechanism: A, antiport; S, symport. Substrate specificity: G, glycine, A, alanine, S, serine, C, cysteine, N, asparagine, Q, glutamine, H, histidine, M, methionine, P, proline, R, arginine, K, lysine, from Bröer et al 2014 [135].*

The most common transporters of System A are SNAT1/2, encoded by *SLC38A1* and *SLC38A2,* respectively. They use the transmembrane electrochemical gradient of Na^+ as the driving force and can transport several amino acids at low affinity, among which Gln and Asn. They are expressed in many tissue such as brain, liver, muscle, pancreas and placenta. SNAT2 is up-regulated in response to amino acid depletion, in parallel with the enzyme ASNS. Another system A transporter is SNAT4 (*SLC38A4*), which is liver-specific, may transport amino acids independently of Na^+ [135]. Recently, it has been identified SNAT8 (*SLC38A8*) which is able to mediate the Na^+- dependent transport of Gln, Alanine, Arginine, Histidine (His) and Aspartate and is neuron-specific [136].

On the other hand, the transporters of System N are bidirectional, indicating that they can mediate either net influx or net efflux of substrates. They have a relatively limited substrate

specificity with preference for the transport of Gln, Asn and His [135]. The transport stoichiometry is characterized by a symport of 1 Na^+:1 amino acid in exchange for 1 H^+, thus the process is electroneutral and not concentrative [134]. The most studied isoforms of N transporters are SNAT3 (named also SN1) and SNAT5 (called also SN2), encoded by *SLC38A3* and *SLC38A5*, respectively, and predominantly expressed in the liver and brain. Given their bio-energetics, the increase of intracellular Na^+ stimulates the efflux of Gln, suggesting that the availability of Na^+ may be an important factor that regulates the flow through SNAT3 and SNAT5. Similarly, an increase in the intracellular concentration of Gln stimulates its efflux through N transporters [137]. Moreover, all the transporters of the system N show a marked sensitivity to pH, with efflux increased when the external pH is lowered below in the physiological range (pH 7.0-7.8) [138].

These transporters are relatively poorly studied, but they are involved in various physiological mechanisms [135]. For example in the central nervous system SNAT3/5 are present on the membrane of astrocytes and promote the release of Gln in the extracellular space [139], so that it can be used by neurons as a substrate to synthesize neurotransmitters such as glutamate and GABA (see graph 4). At hepatic level, in periportal hepatocytes SNAT3/5 allow the uptake of Gln, which is subsequently converted into glutamate and ammonium, detoxified via the urea cycle. On the contrary, in perivenous hepatocytes SNAT3 mediates the efflux of Gln, which is synthetized by GS to detoxify the residual ammonium (see graph 5). Interestingly, in rat liver, SNAT5 is more expressed than SNAT3 in the periportal hepatocytes, suggesting a role of SNAT5 in the modulation of Gln flux in liver [138].

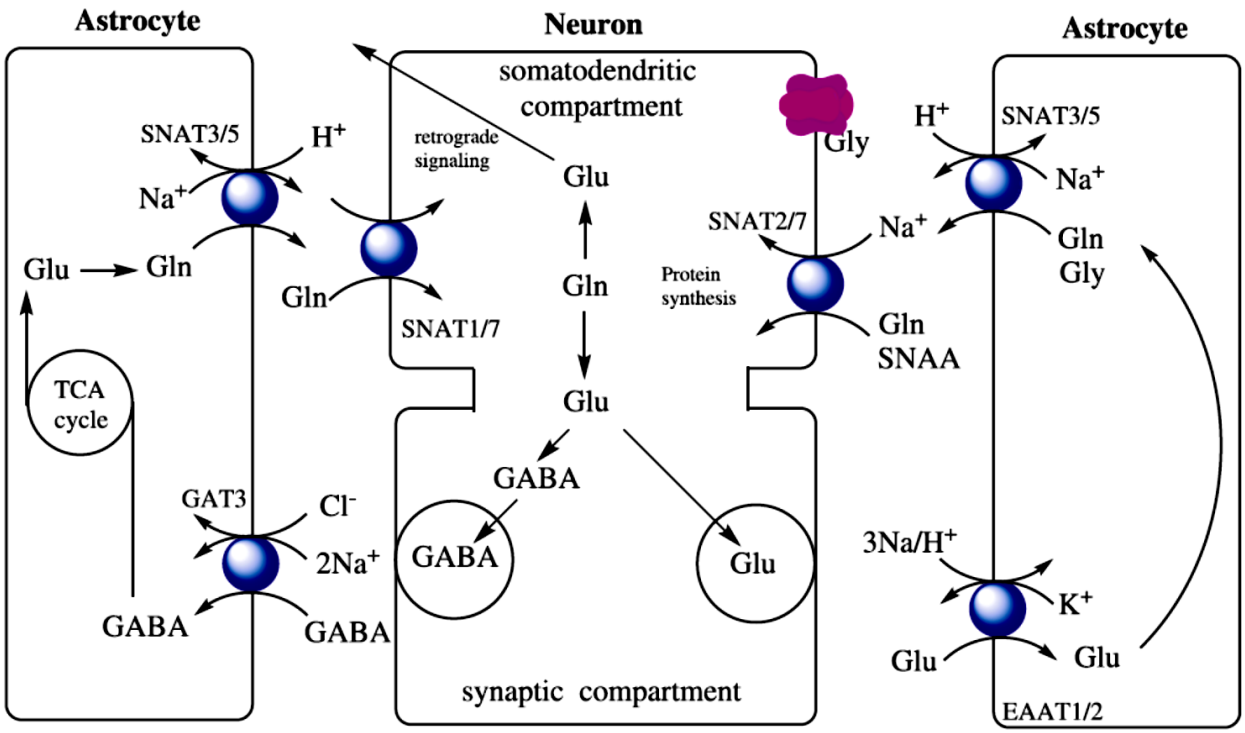

Graph 4. *Role of System N in Glutamine-Glutamate cycle in brain, from Bröer et al 2014 [135].*

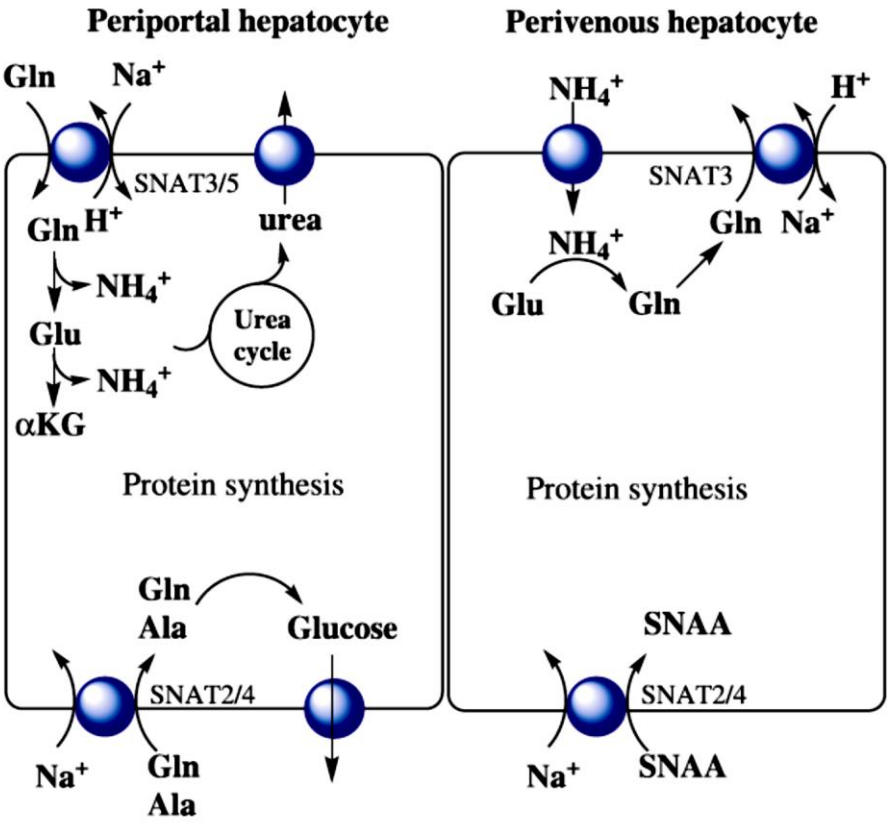

Graph 5. *Role of System N in Ammonium detoxification in liver, from Bröer et al 2014 [135].*

SNAT5 was cloned for the first time almost 20 years ago [140]. It is formed by 472 amino acids, and expressed predominantly in the stomach, brain, liver, lung, and intestinal tract, showing several alternative splicing transcripts. The human *SLC38A5* gene is localized on chromosome Xp11.23. Moreover, SNAT5 has a higher affinity for His than for Gln and Asn. Interestingly, it has been demonstrated that SNAT5 plays an important role in a feedback mechanism between glucagon-receptor signalling in liver and in the increase of pancreatic α cell mass [141]. Indeed, when glucose levels are low in blood, glucagon (synthetized by pancreatic cells) stimulate gluconeogenesis in liver. Thus, hepatic cells use blood amino acids as gluconeogenesis substrates. The inhibition of hepatic glucagon receptor causes an increase of plasmatic amino acids, which promote a mTOR-mediated hyperplasia of α cells in pancreas, in order to produce further glucagon. Under this condition, SNAT5 is upregulated in pancreatic cells and, consistently, *SLC38A5*-deficient mice exhibit a reduction of α pancreatic cells hyperplasia.

Recently, another N transporter, called SNAT7 (encoded by *SLC38A7)* has been identified [142]. It shows the same features of carriers belonging to System N. Indeed, it is a Na^+ dependent amino acid transporter, expressed in the brain, in glutamatergic and GABAergic neurons, but not in astrocytes. Its preferred substrate is Gln, but it is also able to transport other amino acids such as His, serine, alanine, Asn and Asp.

2. Aim of the study

Aim of this study is the elucidation of the mechanisms underlying the protection of ALL blasts by MSCs during the treatment with ASNase. Two original approaches have been adopted:

a) to evaluate the response of primary MSCs, obtained from bone marrow of ALL patients (ALL-MSCs) or healthy donors (HD-MSCs), to ASNase from *Erwinia chrysanthemi*

b) to verify if the two types of MSCs equally support ASNase-treated ALL cells. This aspect was evaluated in co-cultures of MSCs with the BCP-ALL cell line RS4;11 or with primary ALL blasts.

In addition, we have preliminarily characterized the metabolic features of primary MSCs in conditions mimicking, as far as possible, the bone marrow niche *in vivo*.

3. Materials and Methods

3.1. Patients and donors

Informed consent to participate to the study was obtained for all BCP-ALL patients and healthy donors (HD) in accordance with the Declaration of Helsinki. All BCP-ALL patients were enrolled in the AIEOP-BFM ALL 2009 protocol (EudraCT-2007-004270-43) and their samples collected at the Pediatric Department of Fondazione MBBM/San Gerardo Hospital (Monza, Italy). Enrolled HDs were stem cell donors whose BM was collected at the Pediatric Department of Fondazione MBBM/San Gerardo Hospital (Monza, Italy) for transplant purposes. The characteristics of patients are detailed in Table 6. Primary blasts obtained from the BM of UPN#1-7 were used for co-culture experiments, while ALL-MSCs were isolated from the BM of UPN#5-16. HD-MSCs were isolated from the BM of 17 different healthy donors (HD; median:10; range:3-24 years-old).

UPN	Diagnosis	Cell type	Age at diagnosis (yrs)	Sex	% of BM blast infiltrate at diagnosis	Traslocations
1	BII-ALL	Blasts	4	F	93	t(1;19)
2	BII-ALL	Blasts	12	M	98	NEG*
3	BII-ALL	Blasts	4	F	95	NEG*
4	BII-ALL	Blasts	4	F	88	NEG*
5	BII-ALL	Blasts+MSCs	5	M	90	NEG*
6	BII-ALL	Blasts+MSCs	3	F	90	NEG*
7	BII-ALL	Blasts+MSCs	3	M	85	NEG*
8	BII-ALL	MSCs	5	M	80	NEG*
9	BII-ALL	MSCs	3	M	90	NEG*
10	BII-ALL	MSCs	17	M	86	NEG*
11	BIII-ALL	MSCs	8	M	78	NEG*
12	BII-ALL	MSCs	4	F	77	NEG*
13	BII-ALL	MSCs	8	F	94	NEG*
14	BII-ALL	MSCs	8	M	80	NEG*
15	BII-ALL	MSCs	10	M	80	t(9;22)
16	BII-ALL	MSCs	6	F	95	NEG*

Table 6. Characteristics of patients: **Negative for t(4;11), t(9;22), t(12;21), t(1;19)*

3.2. Cells culture and treatments

Bone-marrow mesenchymal stromal cells (MSCs) were isolated as described in previous report [143] from ALL patients (ALL-MSCs) and healthy donors (HD-MSCs) and provided by Prof. Giovanna D'Amico (Centro di Ricerca M. Tettamanti, Pediatric Department, S. Gerardo Hospital, Monza). A line of human telomerase reverse transcriptase -immortalized MSC (hTERT-MSC) was provided by Prof. Dario Campana, S.Jude Children's Research Hospital, Memphis (TN), USA [144]. MSCs, seeded at 3,000 cells/cm^2, were grown in low-glucose Dulbecco's modified eagle medium (DMEM, EuroClone) supplemented with 2 mM Gln, 10% fetal bovine serum (FBS) and antibiotics (100 U/ml penicillin, 100 µg/ml streptomycin). At passage 3, cells were screened for the expression of CD73, CD90, CD105 CD14, CD34 by flow cytometry and for their ability to differentiate into osteoblasts and adipocytes. For the experiments, MSCs were not used for more than 7 passages.

Primary BCP-ALL cells were isolated at diagnosis from BM aspirates by Ficoll (GE Healthcare, Uppsala, Sweden) gradient separation and cryopreserved in liquid phase nitrogen until usage. The pre-B acute lymphoblastic leukemia cell lines RS4;11(ATCC® CRL-1873™), Reh (ATCC® CRL-8286), NALM-6 (DSMZ ACC 128) were cultured in low-glucose DMEM supplemented with 2 mM Gln, 400 µM Asn, 10% FBS and antibiotics, at a cell density of $5 \cdot 10^5$ cells/ml.

Cells were maintained at 37°C in an atmosphere of 5% CO_2 in air, pH 7.4.

For the experiments of metabolic characterization, MSCs were grown in Plasmax™, an advanced medium containing the physiological concentrations of metabolites found in human plasma (provided by dr. Saverio Tardito, Beatson institute, Cancer Research UK, Glasgow (UK) [145, 146]), supplemented with 10% FBS, and antibiotics. To evaluate preliminarily the effects of different media on cell growth and proliferation, MSCs were seeded at the density of 3,000 cells/cm^2 in DMEM or Plasmax™ and counted every 3 days. In the experiments in which hypoxic conditions were adopted, MSCs were incubated at 1% O_2, 5% CO_2, 95% N_2 at 37°C in water-saturated air.

Erwinia chrysantemi asparaginase (ASNase, a generous gift of Jazz Pharmaceutics) was used at 1 U/ml, except for the dose-response curves, where a dose range from 0.003 to 10 U/ml was adopted.

The Glutamine Synthetase (GS) inhibitor methionine-L-sulfoximine (MSO, Sigma-Aldrich, Milan, Italy) was used at 1 mM.

3.3. Viability assay

MSCs were seeded at a density of $3 \cdot 10^3$ cells/cm^2 in standard growth medium, which was replaced after 24h with fresh medium containing the drugs to be tested. At the experimental times, cell viability was assessed with the resazurin method [147], incubating cells in a solution of resazurin (44 μM) in serum-free medium. Resazurin is a blue, non-fluorescent dye, that is reduced by NADH-dependent enzymes to resorufin, a pink fluorescent dye, which is released into the extracellular medium. After 3h, fluorescence was measured at λ_{ex} 515 nm and λ_{em} 586 nm with a fluorimeter (EnSpire® Multimode Plate Readers, Perkin Elmer). Cell viability was expressed as percentage of control calculated through the following formula:

$$CV(\%) = \frac{Fluorescence\ (treated\ well)}{Fluorescence\ (untreated\ well)} \times 100 \qquad \text{Eq. 1}$$

3.4. Determination of Protection Index

To evaluate the protective capacity of MSCs, RS4;11 cells (5 x 10^5/ml) were added on a confluent layer of MSCs, which had been seeded the day before at a density of 25,000 cells/cm^2 and medium was supplemented with ASNase (1 U/ml) in the absence or presence of MSO (1 mM). After 48h, cells were harvested, RS4;11 were labeled with a monoclonal antibody anti-human CD45-FITC (Beckman Coulter, Fullerton, CA) for 45 min at RT in the dark, and the necrotic fraction was assessed. Cells were washed with phosphate buffered saline (PBS) and suspended in Propidium Iodide staining buffer (Sigma Aldrich, final concentration, 2.5 μg/ml). After 15 min at RT in the dark, cells were analyzed using an Epics XL flow cytometer and with the Expo ADC software (Beckman Coulter), quantifying cell death as propidium positivity. Flow cytometry experiments were performed in the Laboratory of Anatomy and Histology of Prof. Mirandola (Dept. of Medicine and Surgery, University of Parma).

To estimate the protective effect of MSCs on ASNase-treated ALL cells, we used a Protection Index, calculated through the following formula:

$$PI = \mathrm{Log}_2 \frac{\%\ ALL\ necrosis\ without\ MSCs}{\%\ ALL\ necrosis\ with\ MSCs} \qquad \text{Eq. 2}$$

where PI=0 indicates absence of protection.

Experiments with MSCs/blasts co-cultures were performed in the Laboratory of Prof. Giovanna D'Amico, following the same protocol described above.

3.5. Modulation of gene expression in co-culture systems

To identify the effects of co-culturing on gene expression of ALL cells/blasts and MSCs, RS4;11 ($1x10^6$/ml) cells or primary ALL blasts ($6x10^6$/ml) were directly added on a MSC confluent layer or suspended in the apical compartment of a transwell insert (Costar Transwell® Permeable Supports, Corning Inc., MA, USA, pore size 0.4 μm) in asparagine-free DMEM, supplemented with 2 mM Gln and 2% FBS. After 72h, ALL cells were collected after extensive washing with PBS, in the case of direct contact co-culture, or from the apical chamber of the transwell insert, while MSCs were collected using trypsin; total RNA was isolated following manufacturer's instructions. Cells were extracted and RNA processed for RT-PCR analysis (see below).

Experiments with MSCs/blasts co-cultures were performed in the Laboratory of Prof. Giovanna D'Amico, following the same protocol described above.

3.6. Gene silencing

MSCs were seeded at the density of 25,000 cells/cm^2 in standard growth medium and *GLUL* and *SLC38A5* were silenced after 24h following the DharmaFECT™ protocol. In brief, after a washing in PBS, MSCs were incubated in serum- and antibiotics-free DMEM, supplemented with 2 mM Gln, 6 μl/ml DharmaFECT transfection reagent and scramble RNA (ON-TARGETplus Non-targeting Pool) or siRNAs targeting *GLUL* (ON-TARGETplus Human *GLUL* siRNA-SMARTpool) or *SLC38A5* (ON-TARGETplus Human *SLC38A5* siRNA-SMARTpool) at 25nM. After 18h, cells were washed with PBS, and medium replaced with fresh standard growth medium.

a) In *GLUL*-silencing experiments, cells were used after further 24h for protection experiments (see above) or treated with ASNase in the presence or absence of MSO for viability assay (see above).

b) In *SLC38A5*-silencing experiments, cells were used after 72h for the evaluation of amino acid efflux (see below) and protection experiments (see above)

3.7. RT-PCR

Total RNA, isolated with GenElute™ Mammalian mRNA Miniprep Kit (Sigma, Italy) or with GeneJET RNA Purification Thermoscientific™, was quantified (Nanodrop 2000TM,Thermo Scientific), and 1μgr was reverse transcribed as described [91]. For real time qPCR, cDNA was amplified in a StepOne^{TM} Real-Time PCR System (Applied Biosystems, Foster City, CA, USA) employing a GoTaq® qPCR Master Mix (Promega, USA) along with the primers (5 pmol each). The primers used and the conditions adopted are summarized in Table 7. The reaction consisted of 35 cycles including a denaturation step at 95°C for 30s, followed by separate annealing (30s) and extension (30s, 72°C) steps. Fluorescence was monitored at the end of each extension step. A no-template, no-reverse-transcriptase control was included in each experiment. At the end of the amplification cycles a melting curve analysis was added. Data analysis was made according to the Relative Standard Curve Method [148]. Gene expression was normalized for the expression of the housekeeping gene *RPL-15*.

Gene	Forward	Reverse	T (°C)
Asparagine Synthetase *(ASNS)*	5’ GATTGCCTTCTGTTCAGTGTCT 3’	5’ GGGTCAACTACCGCCAACC 3’	57
Glutamine Synthetase *(GLUL)*	5’ TCATCTTGCATCGTGTGTGTG 3’	5’ CTTCAGACCATTCTCCTCCGG 3’	57
Solute carrier family 38 member A1 *(SLC38A1)*	5'CACCACAGGGAAGTTCGTAATC 3'	5' CGTACCAGGCTGAAAATGTCTC 3'	57°
Solute carrier family 38 member A2 *(SLC38A2)*	5’ ATGAAGAAGGCCGAAATGGGA 3’	5' TGCTTGGTGGGGTAGGAGTAG 3'	57°
Solute carrier family 38 member A5 *(SLC38A5)*	5’ GCTACAGGCAAGAACGTGAGG 3’	5’ ATTCCAAACGATGTCTTCCCC 3’	59°
Solute carrier family 38 member A3 *(SLC38A3)*	5' CGGGCATTATCCTTTTCCTGT 3'	5' GGACTTGAGTAGCAGGTGGATG 3'	59°
Solute carrier family 1 member A5 *(SLC1A5)*	5’ TGGTCTCCTGGATCATGTGG 3’	5’ TTTGCGGGTGAAGAGGAAGT 3’	57°
DNA-damage-inducible transcript 3 *(DDIT3)*	5’ CTTCTCTGGCTTGGCTGACT 3’	5’ TCCCTTGGTCTTCCTCCTCT 3’	57°
Ribosomal protein L15 (*RPL-15*)	5’ GCAGCCATCAGGTAAGCCAAG 3’	5’ AGCGGACCCTCAGAAGAAAGC 3’	55°

Table 7. Primers and temperatures of annealing

3.8. Protein lysis and Western Blot

Cells were washed in PBS with Ca^{2+} and Mg^{2+} and lysed in a Tris-HCl buffer (20 mM Tris-HCl, pH 7.5, 150 mM NaCl, 1 mM EDTA, 1 mM EGTA, 1% Triton, 2.5 mM sodium pyrophosphate, 1 mM β-glycerophosphate, 1 mM Na_3VO_4, 1 mM NaF, 2 mM imidazole) supplemented with a cocktail of protease inhibitors (Complete, Mini, EDTA-free, Roche). Lysates were transferred in Eppendorf tubes, sonicated for 5s, and centrifuged at 12,000*g* for 10 min at 4°C. After quantification with the Bio-Rad protein assay (Bio-Rad, Hercules, CA, USA), 40 µg of proteins were mixed with Laemmli buffer 4x (250 mM Tris-HCl, pH 6.8, 8% SDS, 40% glycerol, 0.4 M DTT), warmed at 95°C for 5 min, and loaded on a 10% of sodium dodecyl sulphate-polyacrylamide gel electrophoresis (SDS-PAGE) together with known-molecular-weight proteins (Rainbow Markers, Biorad). After electrophoresis, proteins were transferred to PVDF membranes (Millipore-Immobilon-P). Non-specific binding sites were blocked with a 1h-incubation at RT in blocking solution (Roche Diagnostic Spa, Milano, Italia), diluted in TBS-Tween. Blots were then incubated at 4°C overnight with the primary antibodies (see Table 8) diluted in a 5% BSA TBS-Tween solution. After washing, blots were exposed for 1h at room temperature to HRP-conjugated anti mouse or anti-rabbit IgG antibody (Cell Signaling Technology), diluted 1:10,000 in the blocking solution. Immunoreactivity was visualized with Immobilon Western Chemiluminescent HRP Substrate (Millipore).

Protein expression was normalized for Actin or GAPDH and quantified through densitometric analysis using the software ImageQuant® (Molecular Dynamics).

3.9. Immunofluorescence and confocal microscopy

MSCs, seeded on four-chamber slides (Falcon) at a density of 3,000 cells/cm^2, were washed twice in ice-cold PBS and incubated for 15 min in paraformaldehyde 3.7%, for further 7 min in Triton 0.1% in PBS and, lastly, for 1h in a solution of 5% BSA and 10% Normal Goat Serum (DAKO SpA, Milan, Italy) in 0.3 M glycine. Cell monolayers were then incubated overnight in the presence of anti-SNAT5 (1:200, polyclonal, rabbit, Abcam) and anti-β-tubulin (1:2,000, monoclonal, mouse, Sigma-Aldrich) antibodies, in 5 % BSA in PBS. The day after, cells were rinsed three times with PBS and exposed to the secondary antibodies Alexa Fluor 488 goat anti-mouse and Alexa Fluor 543 goat anti-rabbit IgG (both at 1:300, 1h). In the last 5 min of incubation, the antibody solution was supplemented with DRAQ5 (5µM, Thermo Fisher Scientific, Monza, Italy) for nuclei counterstaining. At the end

of the incubation, filters were mounted on glass slides, covered with anti-fade mounting medium to preserve fluorescence and sealed with coverslides. Immunostained cells were observed with an inverted LSM 510 Meta confocal system (Carl Zeiss, Jena, Germany) using a 40x. Single-plane confocal images were taken with excitation at 633 nm and emission recorded through a 670 long pass filter for visualization of nuclei stained with DRAQ5; excitation at 543 nm and emission recorded through a 580-630-nm band pass barrier filter for Alexa Fluor 543 to visualize SNAT5; excitation at 488 nm and emission through a 515-540-nm band pass filter for Alexa Fluor 488 to visualize tubulin.

Antibody	Host	Clonality	Dilution	Company	Code
Anti-Asparagine Synthetase (ASNS)	Mouse	Monoclonal	1:1000	Santa-Cruz Biotechnology	Sc365809
anti-eIF2α phospho-S51	Rabbit	Monoclonal	1:1000	Abcam	Ab32157
Anti-Glutamine Synthetase (GS)	Mouse	Monoclonal	1:1500	BD Transduction Laboratories	610518
Anti-Actin	Rabbit	Polyclonal	1:1000	Sigma	A2066
Anti-SNAT5	Rabbit	Polyclonal	1:1000 (WB) 1:200 (IF)	Abcam	ab72717
Anti-Glyceraldehyde 3-phosphate dehydrogenase (GAPDH)	Rabbit	Polyclonal	1:4000	Sigma	G9545
Anti-Tubulin	Mouse	Polyclonal	1:2000	Sigma	T5168

Table 8. Antibodies

3.10. Intracellular amino acids

For the study of ASNase effects on MSCs, cells were seeded at 8,000 cells/ cm^2 in standard growth medium and, after 24h, treated with ASNase in the presence of absence of MSO. For studying the effects of Gln-free incubation, MSCs were seeded at 25,000 cells/cm^2 in standard growth medium, which was substituted with serum- and Gln-free DMEM, supplemented with antibiotics, after 24h. At the indicated experimental times, cells were washed twice with ice-cold PBS and incubated for 10 min with absolute ethanol, in order to extract intracellular metabolites. Cell extracts were used for intracellular amino acids determination. Specifically, the content of Gln and Asn was measured with liquid chromatography tandem mass spectrometry (LC-MS/MS), using an Agilent HP 1100 apparatus coupled with a API4000 triple-quadrupole mass spectrometer (AB SCIEX, Framingham, MA, USA) by Prof. Roberta Andreoli (Laboratory of Industrial Toxicology, Dept. of Medicine and Surgery, University of Parma), as previously described [91]. Intracellular amino acid content (nmoles of amino acids) was normalized for cell proteins, determined with the Lowry assay, and data were expressed as percentage of control (cultures maintained in standard growth medium).

3.11. Amino acid efflux

For Gln and Asn efflux, 20 x 10^3/cm^2 MSC were seeded in 96-well dishes. After 24h amino acid efflux was measured in Earle's Balanced Salt Solution (EBSS, composition in mM: NaCl 117, $NaHCO_3$ 26; KCl 5.3, $CaCl_2$ 1.8, $MgSO_4 \cdot 7H_2O$ 0.81, choline phosphate 0.9, glucose 5.5, supplemented with 0.02 % Phenol Red, kept at pH 7.4 under CO_2 5%). For the experiments, cells were washed in EBSS and incubated in the same solution for 30 min at 37 °C so as to deplete the intracellular amino acid pool. Cells were then incubated for 5 min in EBSS supplemented with [^{3}H]Gln (Perkin-Elmer Italia, Milan, Italy), at a concentration of 500 μM and an activity of 10 μCi/ml, or Asn (1mM) and, after one washing, incubated in 40 μl of fresh EBSS. After 3 min, extracellular fluid was recovered, transmembrane fluxes were blocked with ice-cold, isotonic urea (300 mM), and cell monolayers were extracted with 50 μl of cold absolute ethanol. Gln radioactivity, contained either in the extracellular fluids or in the cells extracts, was measured in a liquid scintillation spectrometer Wallac Trilux (Perkin-Elmer). Similarly, Asn was measured with LC-MS/MS. In either case, amino acids were normalized for protein content in the well, quantified with the Lowry assay.

Fractional efflux was calculated through the following formulas:

$$(\text{Gln or Asn})_{extra}/[(\text{Gln or Asn})_{extra} + (\text{Gln or Asn})_{intra})] \times 100 \quad \text{Eq. 3}$$

3.12. Oxygen consumption rate measurement

The oxygen consumption rate (OCR) by MSCs was measured through a Seahorse XF96 analyzer (Seahorse Bioscience, Billerica, MD). MSCs were seeded at the density of 45,000 cells/cm^2 in XF96 Seahorse® microplate in Plasmax^{TM}. After 24h, medium was substituted with fresh Plasmax^{TM}, supplemented with 10% dialyzed FBS and antibiotics. In parallel, the sensor cartridge was hydrated with XF Seahorse Calibrant Buffer and incubated overnight at 37°C. After further 24h, OCR was measured using the Agilent Seahorse XF Cell Mito Stress Test Kit, which allows to estimate cell basal respiration, mitochondrial ATP production, maximal respiration as well as the cell capability to respond to a maximal energetic demand. This is performed by a sequential injection of the ATP synthase inhibitor oligomycin (1µM), the mitochondrial oxidative phosphorylation uncoupler Carbonyl cyanide-4-(trifluoromethoxy) phenylhydrazone (FCCP, 8µM) and a mix of rotenone/antinomycin A (1µM), which inhibits the complexes I and III. OCR values were normalized for the amount of proteins, quantified using bicinchoninic acid protein assay kit (Pierce™ BCA Protein Assay Kit, Thermo Scientific), and data were expressed as pmoles/min/µg protein.

3.13. Targeted metabolic analysis

The intracellular levels and exchange rates of metabolites were determined in MSCs at the Beatson Institute (Cancer Research UK, Glasgow, UK). Cells were seeded at the density of 10,000 cells/cm^2 in six-well plates in 2ml of DMEM (+ 2 mM Gln) or Plasmax^{TM}. After 24h (day 0), media were renewed with 8ml (a) or 2ml (b) of fresh medium, supplemented with 10% dialyzed FBS and antibiotics, for the determination of intracellular levels (a) or exchange rates (b) of metabolites, respectively.

After 48h (day 2), samples were prepared for LC-MS analysis, as previously described [146]:

a) cells were washed three times with ice-cold PBS and the intracellular metabolites were extracted after 5 min of incubation in 500 µl of methanol, acetonitrile, water (5:3:2) at 4°C;

b) medium was harvested and diluted 1:50 in the solution of methanol, acetonitrile, water. Cell-free medium was also collected after an incubation of 48h, performed in parallel.

Media and cell extracts were centrifuged at 16,000 g, 4°C, for 10 min; the supernatants were collected, and the metabolites were measured using LC-MS in the Metabolomics facility of the Beatson Institute.

Data were normalized for the protein content, which was quantified using Lowry assay. Moreover, for the evaluation of exchange rates of metabolites, proteins were also determined at the day 0. Data were expressed as peak area/µg protein for the intracellular content (a) and as nmoles/ µgr protein/day for the exchange rates (b), which were calculated using the following formula for each metabolite:

$$X = \left(\frac{(nmol\ in\ cell\ medium - nmol\ in\ cell{-}free\ medium)}{(\mu gr\ prot\ day\ 2 - \mu gr\ prot\ day\ 0)/2} \right) /2 \qquad \text{Eq. 4}$$

3.14. $^{13}C_5$ Glutamine tracing

^{13}C labeled Glutamine (Cambridge Isotopes Laboratories, MA, USA) was used to measure peak areas of each isotopologue of metabolites.

MSCs were seeded at 10,000 cells/cm^2 in twelve-well plates in 0,8ml of Plasmax™. After 24h, media were substituted with:

a) 3.2 ml of fresh Plasmax™, supplemented with 10% dialyzed FBS and antibiotics, containing 0.6mM of $^{13}C_5$ Glutamine, for the evaluation of intracellular metabolites;

b) 0.8ml of fresh Plasmax™, supplemented with 10% dialyzed FBS and antibiotics, containing 0.6mM of $^{13}C_5$ Glutamine, for the determination of exchange rates of metabolites. The experiment was performed either at the physiological concentration of Asn (41µM) or in a modified. Asn-free Plasmax™.

For both experiments, MSCs were incubated in normoxia (21% O_2, 5% CO_2) or in hypoxia (1% O_2, 5% CO_2, 95% N_2) at 37°C in water-saturated air and, after 48h, processed as described above.

3.15. Statistics

Data were expressed as means ± SD. For statistical analysis, two-tail or one-tail Student's t test for paired or unpaired samples, Mann-Whitney test or one sample t test were used, as specified for each experiment. GraphPad Prism 6.0™ was used for the statistical analyses, and p values < 0.05 were considered statistically significant. TraceFinder 4.0 was used for the analysis of mass spectrometry data.

4. Results

4.1. MSCs from ALL patients protect ALL cells from ASNase toxicity

In a preliminary experiment, shown in Figure 1A, we have determined the expression of Asparagine Synthetase (ASNS) in three ALL cell lines (RS4;11, Reh and NALM-6), incubated in normal growth medium in the absence or in the presence of *Erwinia* L-asparaginase (ASNase). Both Reh and NALM-6 cells had lower ASNS levels than the myeloma cell line OPM2 and induced it upon ASNase treatment. Conversely, RS4;11 cells, which had the lowest ASNS expression, did not appreciably induce the enzyme upon incubation with ASNase. RS4;11 cells were thereafter used as an ALL cell model in this study. Using a line of immortalized Mesenchymal Stromal Cells (MSCs), Iwamoto et al. demonstrated a protective effect on ALL cells [68]. We show here that also MSCs from ALL patients (ALL-MSCs) efficiently protect ASNase-treated RS4;11 cells (Figure 1B)

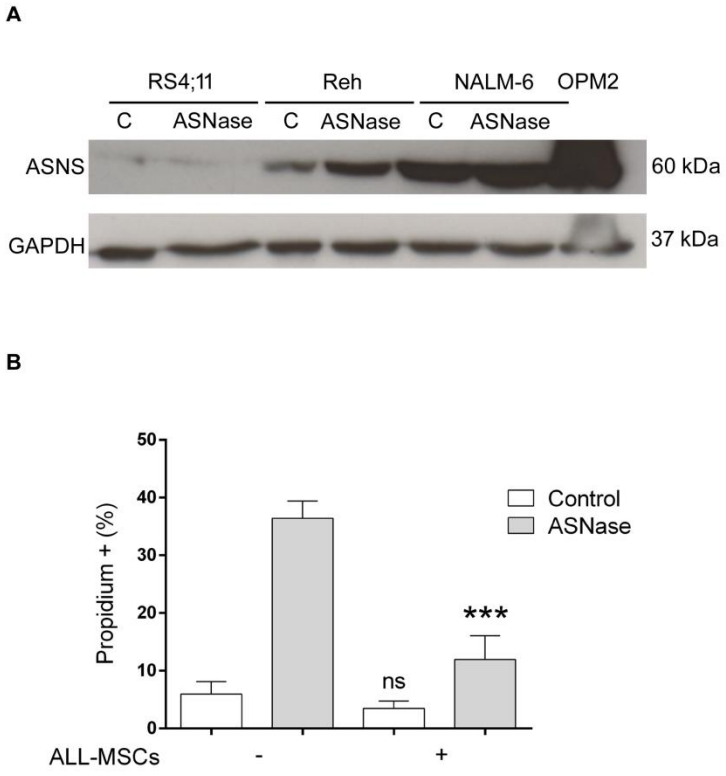

Figure 1. ASNase effects on ALL cells: protection by MSCs from ALL patients. *Panel A. The expression of Asparagine Synthetase (ASNS) was determined in the indicated ALL cell lines incubated for 48h in the absence or in the presence of L-Asparaginase from E. chrysanthemi (ASNase, 0.05 U/ml). The human myeloma cell line OPM2 was used as a positive control for ASNS expression. A representative Western Blot is shown. Panel B. RS4;11 cells were treated for 48h with ASNase (1 U/ml) in the absence or in the presence of bone marrow MSCs from different ALL patients (n = 4). After the treatment, cell death was estimated in cytofluorimetry from propidium positivity. *** p< 0.001 vs. ALL cells treated with ASNase in the absence of MSCs (two-tail t-test for unpaired data).*

4.2. MSC adaptation to ASNase requires Glutamine Synthetase activity

In order to investigate the mechanism underlying the protective effect sustained by MSCs, we studied their response to ASNase. ALL-MSCs were poorly sensitive to ASNase with an IC_{50} >10 U/ml (Figure 2A). MSO, an irreversible inhibitor of Glutamine Synthetase (GS), increased ASNase toxicity in MSCs. When treated with 1 U/ml of ASNase, the growth of MSCs, initially blocked, was partially rescued from the third day of treatment (Figure 2B), so that after 6d of treatment viability was doubled compared with the initial control. Conversely, in the presence of both MSO and ASNase, cell growth was not rescued and, after 6d of treatment, viability was markedly lower than the initial control. In the absence of ASNase, MSO alone had no effect on cell viability. We next investigated the effect of ASNase on the expression of genes associated with apoptosis or adaptation to nutritional stress. The mRNA of *DDIT3*, which encodes for the pro-apoptotic protein CHOP, was significantly induced after 6h of treatment with ASNase or ASNase + MSO (Figure 2C). However, in cells treated with ASNase alone *DDIT3* expression had returned at control values after 24h, while it was still markedly induced in cells treated with ASNase and MSO. A clear cut transient induction of *ASNS* was also observed at 6h of treatment with either ASNase or ASNase + MSO, while *GLUL*, which encodes for Glutamine Synthetase (GS), exhibited a modest increase only at 24h. Both *DDIT3* and *ASNS* are ATF4-dependent genes readily induced upon the phosphorylation of the α subunit of the human initiation factor 2 (eIF2α), a marker of nutritional stress [91, 110] Consistently, both in the absence and in the presence of MSO, ASNase treatment promoted eIF2α phosphorylation (Figure 2D). The effect was already evident after 6h of incubation and persisted at later time points in the absence but not in the presence of MSO. At variance with the clear induction observed at mRNA level, ASNS protein, which was already well detectable under control conditions, did not increase upon ASNase treatment. In contrast, at 24h and, more evidently, at 48h of ASNase treatment a clear-cut expression of GS was evident in the absence of MSO, while it was only barely detectable in the presence of the inhibitor. The intracellular content of Asn and Gln, measured in parallel (Figure 2E), . was dramatically decreased after 6h with ASNase. Asn content continued to decline either in the presence or the absence of MSO, while cell Gln remained stable in the absence of MSO and further decreased in the presence of the GS inhibitor.

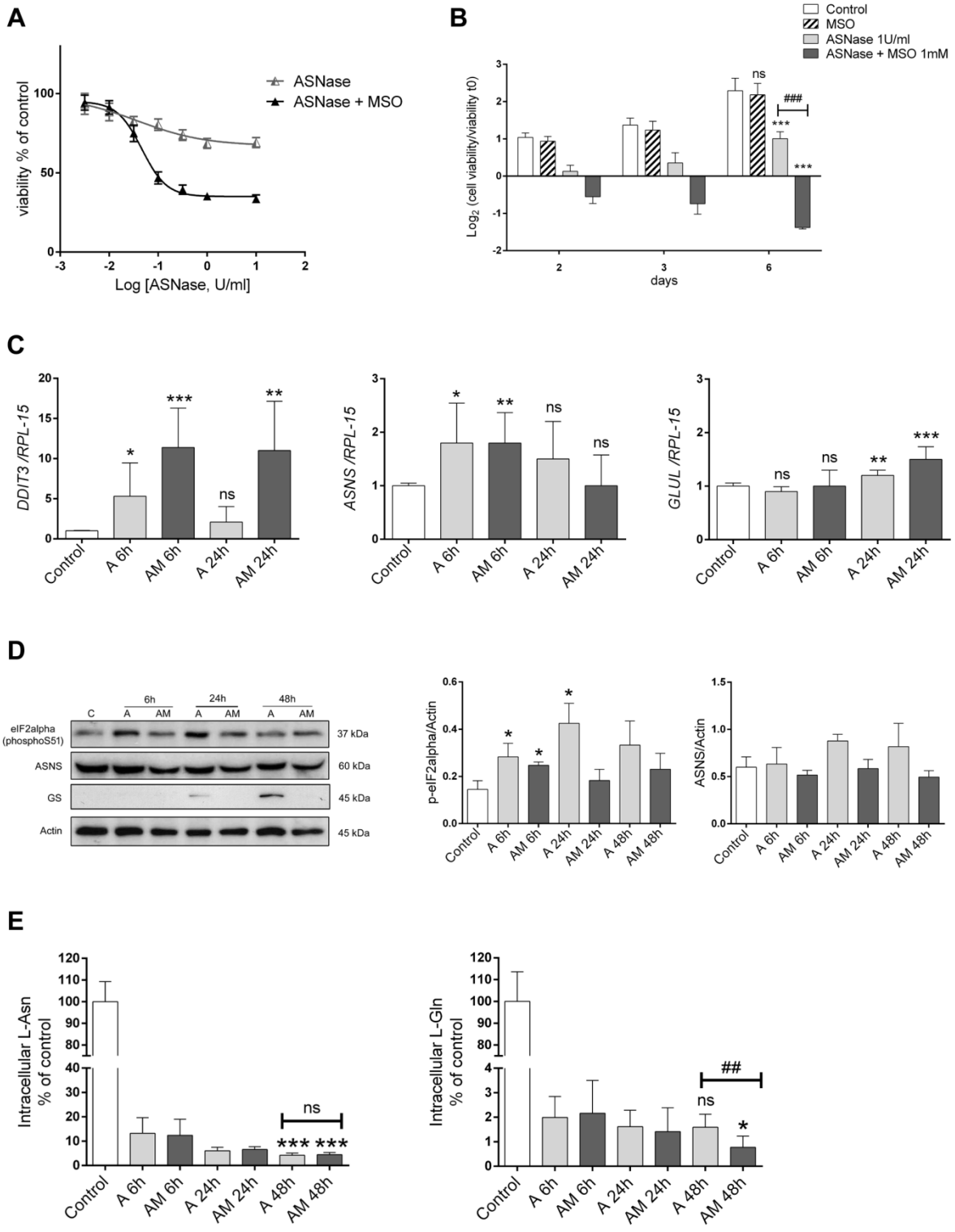
A
viability % of control
ASNase
ASNase + MSO
Log [ASNase, U/ml]
B
Control
MSO
ASNase 1U/ml
ASNase + MSO 1mM
Log2 (cell viability/viability t0)
ns
###
***
***
days
C
DDIT3 /RPL-15
ASNS /RPL-15
GLUL /RPL-15
Control
A 6h
AM 6h
A 24h
AM 24h
D
6h
24h
48h
C
A
AM
eIF2alpha (phosphoS51)
ASNS
GS
Actin
37 kDa
60 kDa
45 kDa
45 kDa
p-eIF2alpha/Actin
ASNS/Actin
A 48h
AM 48h
E
Intracellular L-Asn % of control
Intracellular L-Gln % of control
##

Figure 2. Effects of ASNase and MSO on MSCs from ALL patients. *Panel A. MSCs from three ALL patients were incubated for 48h with ASNase in the absence or in the presence of MSO (1 mM), and viability was assessed with the resazurin method (see Materials and Methods). Data are means ± SD of nine independent determinations. Non-linear regression analysis was used to obtain dose response curves. Panel B. Growth of MSCs incubated in the absence (Control) or in the presence of ASNase (1 U/ml), MSO (1 mM) or ASNase + MSO. Data are expressed as Log_2 of the ratio between viability at the experimental time and viability at time 0, and are means ± SD of 6 independent determinations obtained with cells from two patients. *** p< 0.001 vs. control cells at 6d; ### p< 0.001 ASNase vs. ASNase + MSO (two-tail t test for unpaired data). Panels C-D-E. ALL-MSCs were maintained in normal growth medium (C, Control) or treated for the indicated times with ASNase (A) or ASNase + MSO (AM). Cells were then extracted for mRNA (Panel C), protein (Panel D) or amino acid (Panel E) analysis. Panel C. The relative expression of DDIT3, ASNS and GLUL was determined, expressing the results as fold increase of the value obtained in MSCs under control conditions, kept at 1. Data are means ± SD of expression data obtained with MSCs from three different patients, performed in duplicate. * p< 0.05, ** p< 0.01, *** p< 0.001 vs. control cells (two-tail t test for unpaired data). Panel D. A representative Western blot of eIF2α (phospho-S51), ASNS and GS (left). Actin was used for loading control. The experiment was performed with ALL-MSCs from four different patients, and the mean relative expression of ASNS and p-eIF2α is reported (right). * p < 0.05 vs. control cells (one-tail t test for unpaired data). Panel E. The intracellular content of Asn (left) and Gln (right) was determined at the indicated times. Data are expressed as % of control and are means ± SD of nine independent determinations. * p< 0.05, *** p< 0.001 vs. cells undergoing the same treatment for 6h ## p< 0.01 ASNase vs. ASNase + MSO (two-tail t test for unpaired data).*

4.3. Mesenchymal stromal cells secrete Gln and Asn

Intracellular amino acids were also measured in cells incubated in Gln- and Asn-free medium (Figure 3A, top), both in the presence and in the absence of MSO. Under this condition, less stringent than the incubation with ASNase, intracellular Asn was substantially spared, while Gln, after the initial decrease, was partially, but significantly, rescued in the absence, but not in the presence, of the GS inhibitor. In the same experiment, the extracellular concentration of the two amino acids was also measured (Figure 3A, bottom). After 6h, both amino acids were detectable in the extracellular medium. Extracellular Asn exhibited a positive trend, although the increase did not reach the statistical significance, and was comparable in the absence and in the presence of MSO. On the contrary, extracellular Gln progressively increased in the absence but not in the presence of MSO.

To assess if MSCs secrete Asn and Gln under physiological conditions, we have cultured cells in Plasmax™ (see Materials and Methods), an advanced medium that closely mimics human plasma, supplemented with $^{13}C_5$-Glutamine at 0.6 mM (the average Gln plasma concentration). After 48h of incubation at physiological levels of Asn, there was a net uptake of both Asn and Gln, although a small extrusion of both amino acids was also detected (Figure 3B). The efflux of ^{13}C-labelled Gln-derived Asn was evident also in the absence of Asn, a condition that reproduces the bone marrow situation after the treatment with ASNase [36, 70].

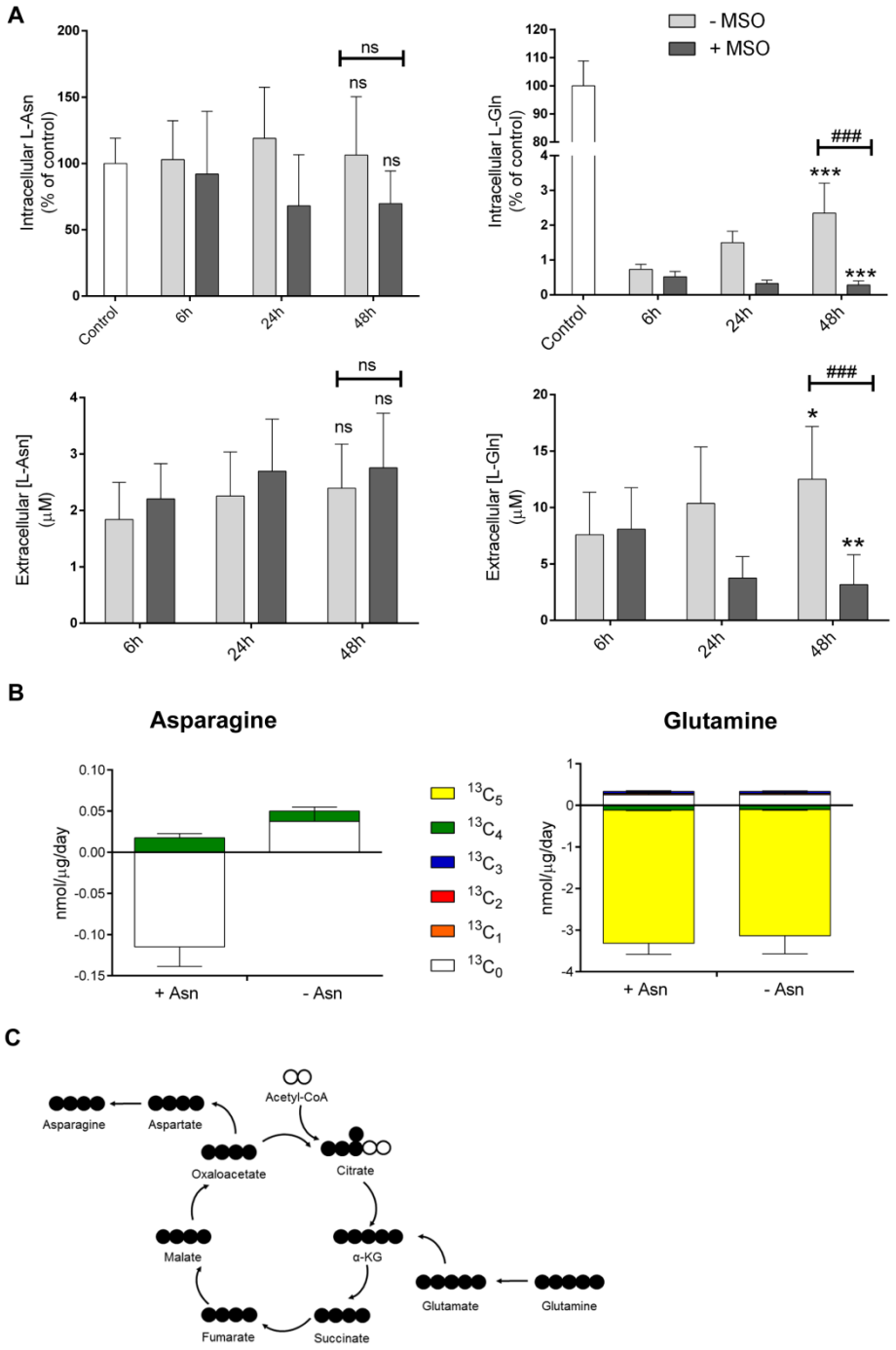

Figure 3. Intracellular glutamine and asparagine and amino acid secretion in ALL-MSCs under Gln- and Asn- free conditions. *Panel A. MSCs from four ALL patients were incubated for 48h in a Gln- and Asn-free medium in the absence or in the presence of ASNase (1 U/ml), ASNase + MSO (1 mM) or maintained in normal growth medium (Control). At the indicated times, the intracellular (upper panels) and extracellular (lower panels) Gln and Asn were determined. Data are expressed as % of control (upper panels) or μM (lower panels) and are means ± SD of eleven independent determinations. * p< 0.05, ** p< 0.01, *** p< 0.001 vs. cells undergoing the same treatment for 6h; ### p< 0.001, cells incubated in the absence vs. cells incubated in the presence of MSO, (two-tail t test for unpaired data). Panel B. Exchange rates of Gln and Asn in $^{13}C_5$-Gln-labelled ALL-MSCs incubated in Plasmax™ medium (Gln = 0.6 mM) in the absence or presence of Asn (41 μM) for 48h. Data represent means ± SD of MSCs from four different patients, each used in triplicate. Exchange rates are expressed as nmol/μg protein/day and are calculated according to Eq. 4 (Materials and Methods). Panel C. A schematic representation of labelling of intracellular metabolites upon incubation with ^{13}C-Gln.*

4.4. The silencing of Glutamine Synthetase in ALL-MSCs suppresses MSC adaptation to ASNase and lowers the protective effect on ALL cells.

To verify if the effects of MSO were only attributable to GS inhibition, *GLUL* was silenced in ALL-MSCs (Figure 4). After 2d of transfection, *GLUL* mRNA was markedly lowered, and no induction of the enzyme protein was observed after further 3d in the presence of ASNase (Figure 4A-B). Viability of *GLUL*-silenced cells was comparable to that of scramble-transfected cells under control conditions and in cultures treated with ASNase + MSO, but much lower when cultures were treated with ASNase alone (Figure 4C). Images of the MSC populations (Figure 4D), obtained in parallel, indicated that the density of scramble-transfected MSCs treated with ASNase was comparable with that of control, whereas ASNase-treated *GLUL*-silenced MSCs and cells simultaneously incubated with ASNase and MSO were much sparser.

To evaluate the role of GS in the protective effect of ALL-MSCs on ASNase-treated ALL cells, we incubated RS4;11 cells and MSCs, either scramble or *GLUL*-silenced, with or without ASNase and MSO. MSO markedly lowered the protective effect produced by control cells, scramble-transfected or *GLUL*-silenced MSCs (Figure 4E). In the absence of the GS inhibitor, scramble-transfected MSCs cells protected ALL cells less than untransfected cells but significantly more than *GLUL*-silenced MSCs.

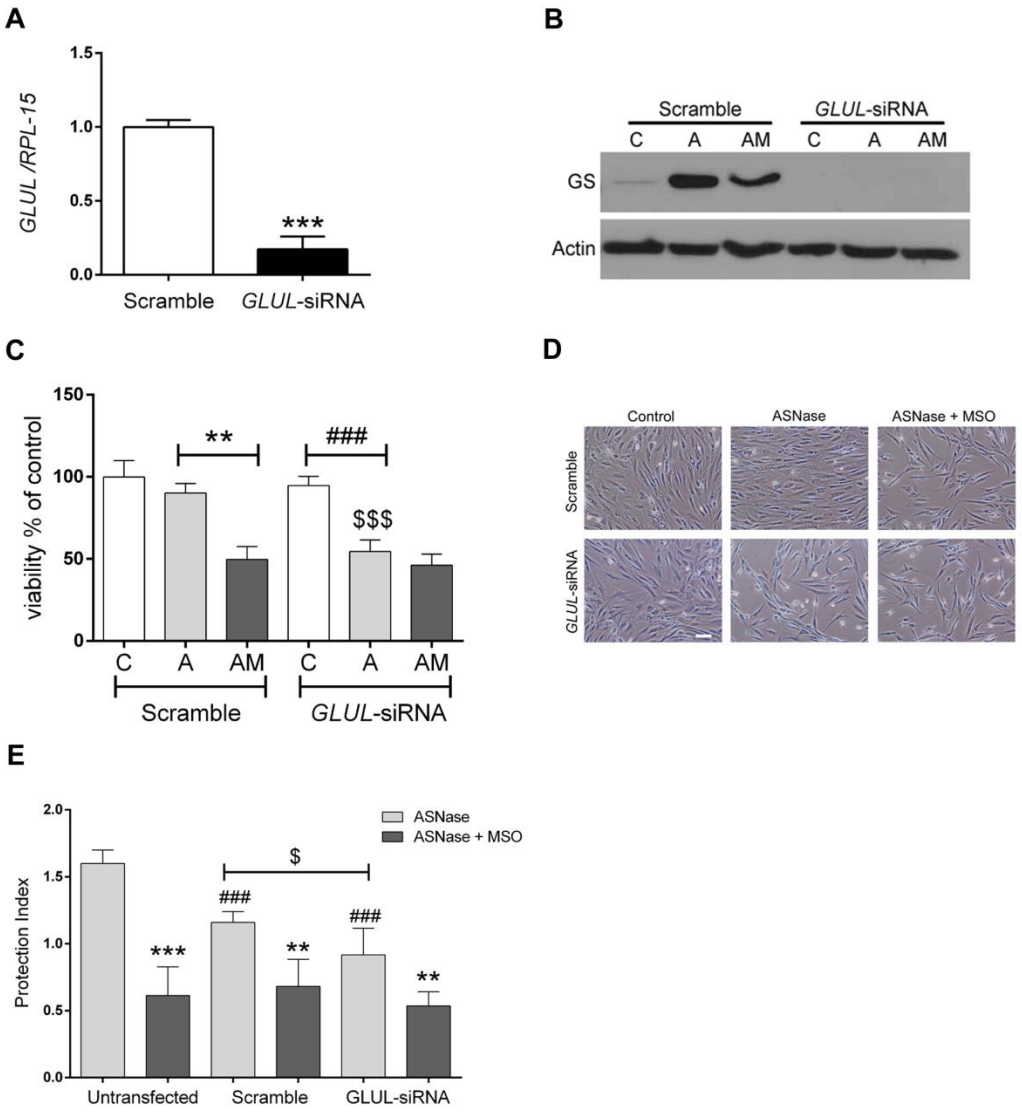

Figure 4. Effects of GS silencing on MSC adaptation to ASNase. *Panel A. ALL-MSCs from four different patients were transfected with scramble or GLUL-siRNA (see Materials and Methods) and the expression GLUL mRNA was evaluated after 2d. The relative expression of GLUL was determined, expressing the results as fold increase of the value obtained in scramble-transfected MSCs, kept at 1. *** p< 0.001 (two-tail t test for unpaired data). Panels B-C. Expression of GS protein (B, a representative experiment) and viability (C) of scramble-transfected or GLUL-silenced MSCs from two different patients was evaluated after 3d of treatment with ASNase (A) or ASNase + MSO (AM). In panel B, Actin was used for loading control. In panel C, data are expressed as % of the viability of scramble-transfected cells not treated with ASNase or ASNase + MSO. Data are means ± SD of twelve independent determinations. ** p< 0.01 scramble-transfected cells treated with ASNase vs. scramble-transfected cells treated with ASNase + MSO; $^{###}$ p< 0.001 ASNase-treated GLUL-silenced cells vs. control GLUL-silenced transfected cells; $^{\$\$\$}$ p< 0.001 ASNase-treated GLUL-silenced cells vs. ASNase-treated scramble transfected cells (two-tail t test for unpaired data). Panel D. Scramble-transfected or GLUL-silenced cells were treated for 3d with ASNase or with ASNase + MSO, as indicated. Representative fields are shown. Bar = 100 µm. Panel E. The Protection Index (Eq. 2,Materials and Methods) for ASNase-treated RS4;11 cells, maintained in mono-culture or co-cultured with scramble-transfected or GLUL-silenced ALL-MSCs, in the absence or in the presence of MSO. Data are means ± SD of four independent determinations from MSCs of two different patients. ** p< 0.01, *** p< 0.001 vs. corresponding cultures treated with ASNase alone; $^{###}$ p< 0.001 vs. untransfected cells treated with ASNase alone; $^{\$}$ p< 0.05 ASNase-treated scramble-transfected cells vs. ASNase-treated GLUL-silenced cells (one-tail t-test for unpaired data).*

4.5. MSCs from ALL patients protect leukemia cells better than MSCs from healthy donors.

At variance with the results presented here with ALL-MSCs cells, mesenchymal cell lines do not efficiently protect ALL cells from *E. chrysantemi* ASNase toxicity although they clearly induce GS [72]. To assess if MSCs from leukemic bone marrow have a peculiar ability to shield ALL cells from ASNase effects, we performed ASNase treatment in co-cultures of RS4;11 cells with either ALL-MSCs or MSCs from healthy donors (HD-MSCs). The representative experiment, shown in Figure 5A, indicated that the protective effect was evident with both MSC types but much larger with ALL-MSCs, which lowered cell death by over 60%, compared with the 30% observed with HD-MSCs. The results were confirmed in a panel of MSCs derived from ALL patients or healthy donors (Figure 5B), indicating that with the latter cell group the Protection Index was significantly smaller. Interestingly, MSO lowered the protection due to either cell panel, although the inhibition did not reach the statistical significance with HD-MSCs. The boosted protective efficiency of ALL-MSCs was also confirmed with primary ALL blasts. In the two representative experiments shown in Figure 5C, ALL blasts from two different patients (UPN#4, #5, see Table 6) were treated with ASNase or ASNase + MSO in monoculture or in co-culture with MSCs derived from an healthy donor or an ALL patient (UPN #8). In both cases, ALL-MSCs protected ALL blasts better than HD-MSCs, either in untreated cultures or in cultures treated with ASNase, and, in both cases, MSO lowered (Blasts of Patient 5) or suppressed (Blasts of Patient 4) the protective effect.

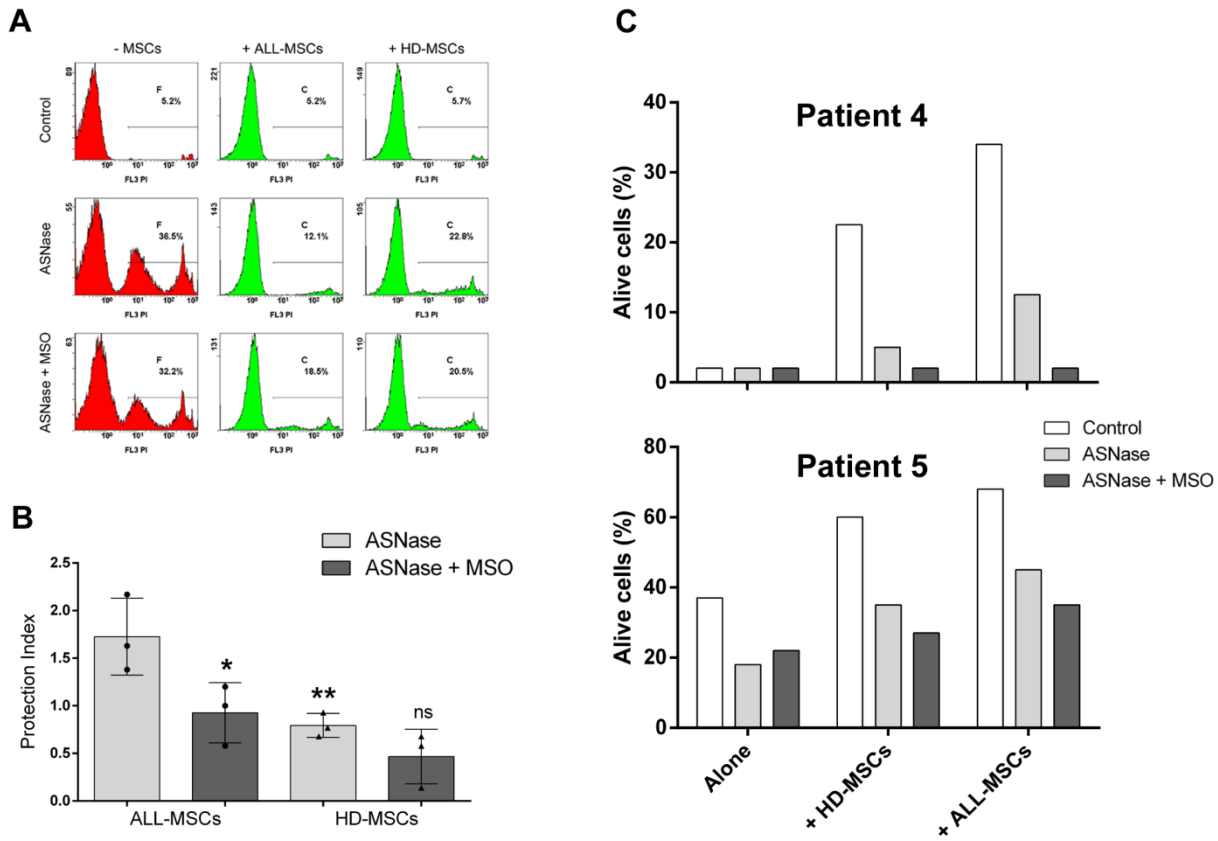

Figure 5. The protective effect on ASNase-treated ALL cells is GS-dependent and larger with MSCs from leukemic patients. *Panel A. MSCs from an ALL patient or from a healthy donor were co-cultured with RS4;11 ALL cells in the presence of ASNase or ASNase + MSO. After 48h, the percentage of necrotic RS4;11 cells was determined with cytofluorimetry. A representative experiment, performed three times with MSCs from different donors with comparable results, is shown. Panel B. The protection index (Eq. 2, Materials and Methods) is showed in the four conditions. * p< 0.05, ** p< 0.01 vs. the protection index obtained with ALL-MSCs in the absence of MSO (one-tail t test for unpaired data). Panel C. Blasts from two different ALL patients (Patient UPN #4, upper; Patient UPN #5, lower) were treated with ASNase or with ASNase + MSO, either in monoculture or in co-culture with MSCs from the same healthy donor or the same, unrelated ALL patient (UPN #8). Blast viability was determined after 48h as described in Materials and Methods.*

4.6. MSCs from healthy honors adapt to ASNase treatment through an overexpression of Glutamine Synthetase.

To elucidate the mechanisms underlying the limited capability of HD-MSCs to protect ALL-cells, we assessed their response to ASNase treatment (Figure 6). Analogies with the behavior of ALL-MSCs, as reported in Figure 2, were evident. Importantly, as in ALL-MSCs, cell proliferation was rescued at later times of treatment (Figure 6A), GS was induced at later times of treatment with ASNase (Figure 6B), and adaptation was hindered by MSO (Figure 6C), indicating the essential role of GS also in the adaptation of HD-MSCs. However, the pattern of changes in the intracellular amino acids during ASNase treatment (Figure 6D) was different. Indeed, at variance with what observed in ALL-MSCs, in HD-MSCs cell Gln exhibited a clear cut increase at 48h compared with 6h of treatment. This partial rescue was observed in the absence, but not in the presence of MSO, which instead cause a further decrease of the amino acid. A comparable behavior was seen using the immortalized human cell line hTERT-MSCs (data not shown).

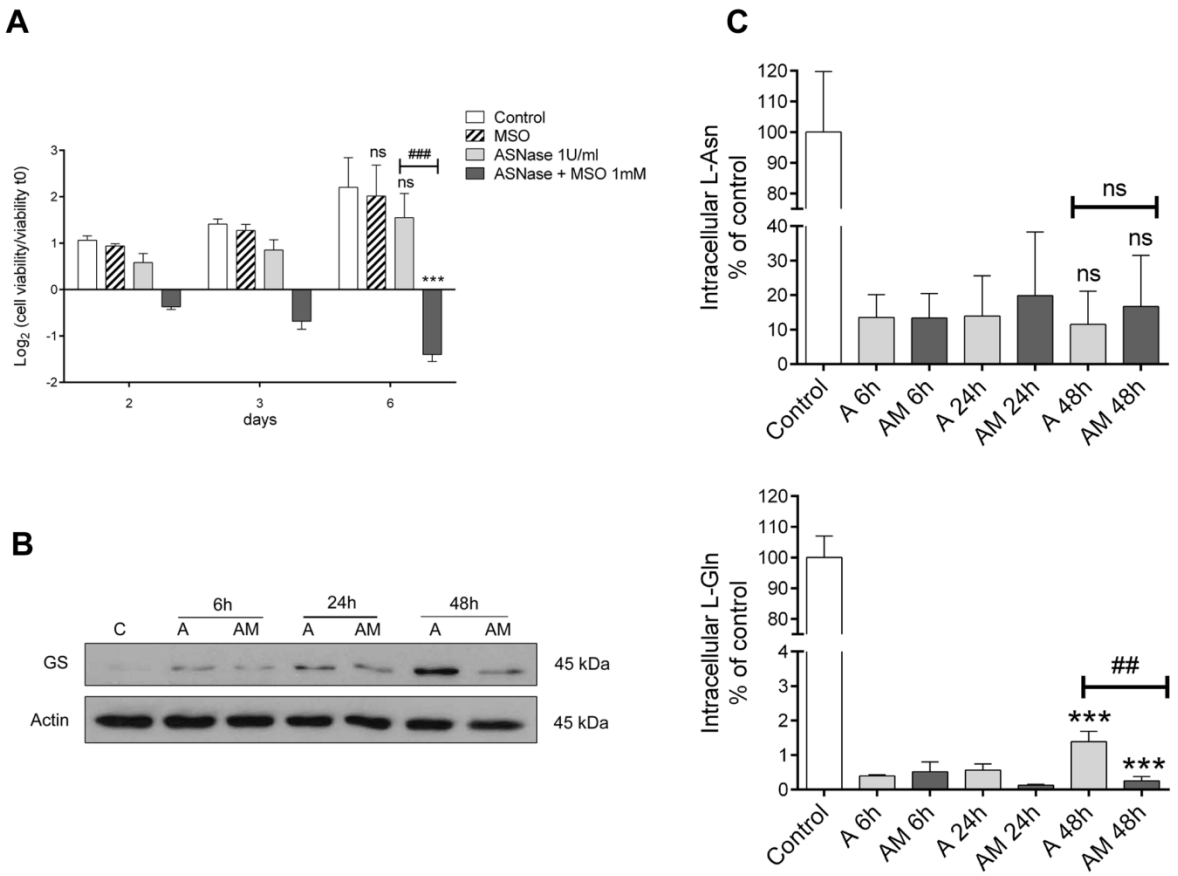

Figure 6. Effects of ASNase and MSO on bone marrow MSCs from healthy donors (HD-MSCs). *Panel A. MSCs were incubated for the indicated times in the absence (Control) or in the presence of ASNase (1 U/ml), MSO (1 mM) or ASNase + MSO. Data are expressed as Log_2 of the ratio between viability at the experimental time and viability at time 0, and are means ± SD of 6 independent determinations obtained with cells from two different donors. *** p< 0.001 compared with control cells at 6d; $^{###}$ p< 0.001, cells treated with ASNase vs. cells treated with ASNase + MSO (two-tail t test for unpaired data). Panel B. HD-MSCs were treated for the indicated times in the presence of ASNase (A) or ASNase + MSO (AM). Control cells were maintained in normal growth medium. Western blot of GS was performed at the indicated times of treatment. Actin was used for loading control. The experiment was performed with HD-MSCs from three different donors with comparable results. Panel C. MSCs from three healthy donors were treated as described in Panel B. After cell extraction, the intracellular content of Gln and Asn was determined at the indicated times. Data are means ± SD of nine independent determinations. *** p< 0.001 vs. cells undergoing the same treatment for 6h; $^{##}$ p< 0.01(two-tail t test for unpaired data).*

4.7. MSCs from ALL patients express higher levels of the SLC38A5/SNAT5 transporter.

In the past, the protective effect of MSCs on ASNase-treated cells was attributed to the synthesis and efflux of Asn and/or Gln from stromal cells [68, 72]. However, while the role of ASNS and GS has been repeatedly investigated, little interest has been thus far given to the mechanisms that account for Asn and Gln efflux. To address this issue, we have evaluated the expression of several transporters, as well as that of *ASNS* and *GLUL,* in a panel of ALL- and HD-MSCs (Figure 7A). The results indicated that the most significant difference concerned *SLC38A5*, a gene that encodes for SNAT5, a transporter that mediates net influx or net efflux of either Gln or Asn, depending on the transmembrane gradients of its substrates [135]. *SLC38A5* expression was almost three-fold higher in ALL-MSCs compared with HD-MSCs. Also *SLC38A1*, which encodes for the active, inward transporter SNAT1, was significantly increased in ALL-MSCs compared with HD-MSCs. On the contrary, *SLC38A2* and *SLC1A5,* encoding for the transporters SNAT2 and ASCT2, respectively, were not significantly different between the two experimental groups. Importantly, also the expression of *ASNS* and *GLUL* did not show significant changes between the two cell panels. The Western Blot analysis showed that the SNAT5 protein was more than two-fold expressed in ALL-MSCs than in HD-MSCs (Figure 7B). This result is consistent with the images of MSCs obtained by confocal microscopy (Figure 7C), where SNAT5 expression on the cell membrane was more evidently detectable in ALL-MSCs. To verify the functional consequences of the different SNAT5 expression, we measured the fractional efflux of pre-accumulated Gln and Asn (Figure 7D) in MSCs from ALL patients or healthy donors. Consistently with the higher expression of the transporter detected in ALL-MSCs, Gln and Asn efflux was significantly faster from MSCs derived from leukemia patients.

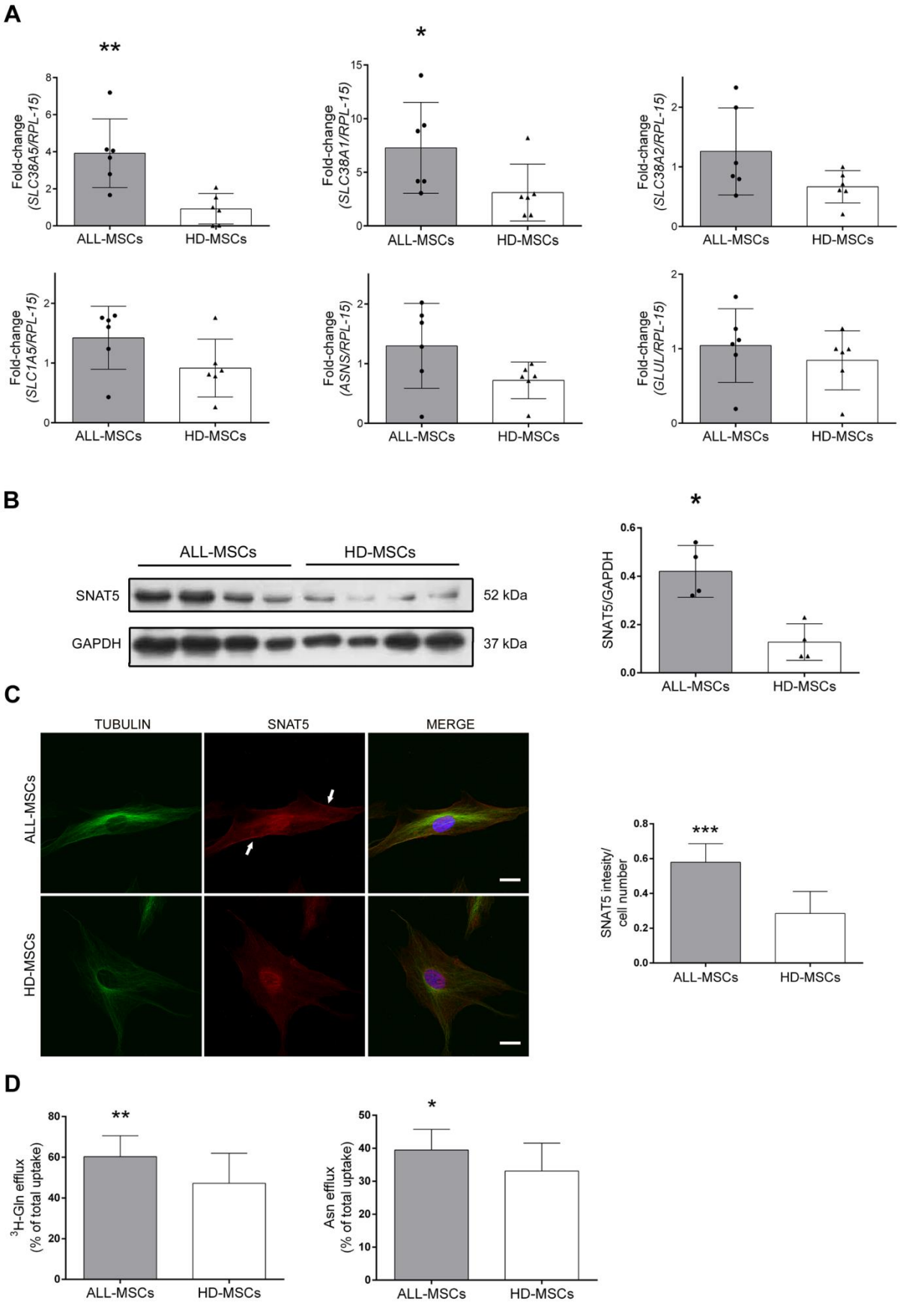
A
**
*
Fold-change (SLC38A5/RPL-15)
Fold-change (SLC38A1/RPL-15)
Fold-change (SLC38A2/RPL-15)
Fold-change (SLC1A5/RPL-15)
Fold-change (ASNS/RPL-15)
Fold-change (GLUL/RPL-15)
ALL-MSCs
HD-MSCs
B
ALL-MSCs
HD-MSCs
SNAT5
GAPDH
52 kDa
37 kDa
*
SNAT5/GAPDH
C
TUBULIN
SNAT5
MERGE
ALL-MSCs
HD-MSCs
***
SNAT5 intesity/ cell number
D
**
*
3H-Gln efflux (% of total uptake)
Asn efflux (% of total uptake)

Figure 7. Differential expression of SLC38A5 in MSCs from healthy donors and leukemic patients. *Panel A. The expression of the indicated genes was determined in a panel of MSCs from six healthy donors (HD) and six ALL patients (ALL). The relative expression of indicated genes was determined. Data are expressed as fold-change, keeping at 1 the expression in MSCs from a single, arbitrarily chosen, healthy donor. Panel B. Left, Western blot of SNAT5 expression in two panels of MSCs obtained from ALL patients or healthy donors. GAPDH was used for loading control. Right, densitometric analysis of SNAT5 expression, normalized for GAPDH (n = 4). For Panels A and B, lines and bars represent median values for Mann-Whitney test. * p< 0.05; ** p< 0.01. Panel C. Left, representative confocal images of MSCs derived from an ALL patient (upper) or a healthy donor (lower). Single confocal sections are shown. Comparable images have been obtained from MSCs of four ALL patients and three healthy donors. Bar = 20 µm. Green, tubulin; red, SNAT5; blue, nuclei. right, the mean intensity of SNAT5 signal was detected in 10 whole fields of ALL-MSCs and 19 whole fields of HD-MSCs. Data are expressed as the ratio between mean intensity and the number of cells in the same fields (81 for ALL-MSCs and 93 for HD-MSCs) *** p< 0.001 (two tail t test for unpaired data). Panel D. Fractional Gln efflux (Eq. 3, Materials and Methods) was determined in MSCs from three ALL patients and three healthy donors. Data are means of 15 independent determinations with SD. * p< 0.05, ** p< 0.01 (two-tail t test for unpaired data).*

4.8. Co-culture with primary ALL blasts induces SLC38A5 expression in HD-MSCs

The results presented above indicate that *SLC38A5* and *SLC38A1* are differentially expressed in MSCs from HD or ALL patients. In the ALL bone marrow environment, MSCs establish strict relationships with the leukemic blasts. It is, therefore, possible that this interaction modifies gene expression in MSCs. To assess this hypothesis, we have measured the expression of the two transporters, as well as of other genes potentially involved in the protective effect on ALL blasts, in co-cultures of MSCs from healthy donors and blasts from ALL patients or in the corresponding monocultures.

Figure 8A shows the expression of *ASNS, GLUL, SLC38A5*, and *SLC38A1* in MSCs from four different healthy donors and in blasts from three different ALL patients. Cells were maintained for 72h either in monoculture or in co-cultures, established in double chamber systems, with MSCs in the lower compartment, or keeping the two cell types in direct contact. With either co-culture modality, *SLC38A5* and *ASNS* expression significantly increased in MSCs. The largest increase in expression was detected for *SLC38A5*, which was induced above the level determined in the monoculture in all the eight independent co-cultures tested, although at a variable extent. As far as gene expression in ALL blasts was concerned, a clear cut, highly significant decrease in *ASNS* expression was detected upon co-culture with MSCs. An increase in *SLC38A5* expression was also detected, although below the level of statistical significance. A significant induction of *SLC38A5* was also observed upon co-culturing of HD-MSCs with RS4;11 ALL cells (Figure 8B). On the contrary, when ALL blasts were co-cultured with ALL-MSCs (Figure 8C) derived from the same ALL patient, no significant induction of the transporter gene was detected in the MSCs or in blasts compared with the expression measured in the monoculture.

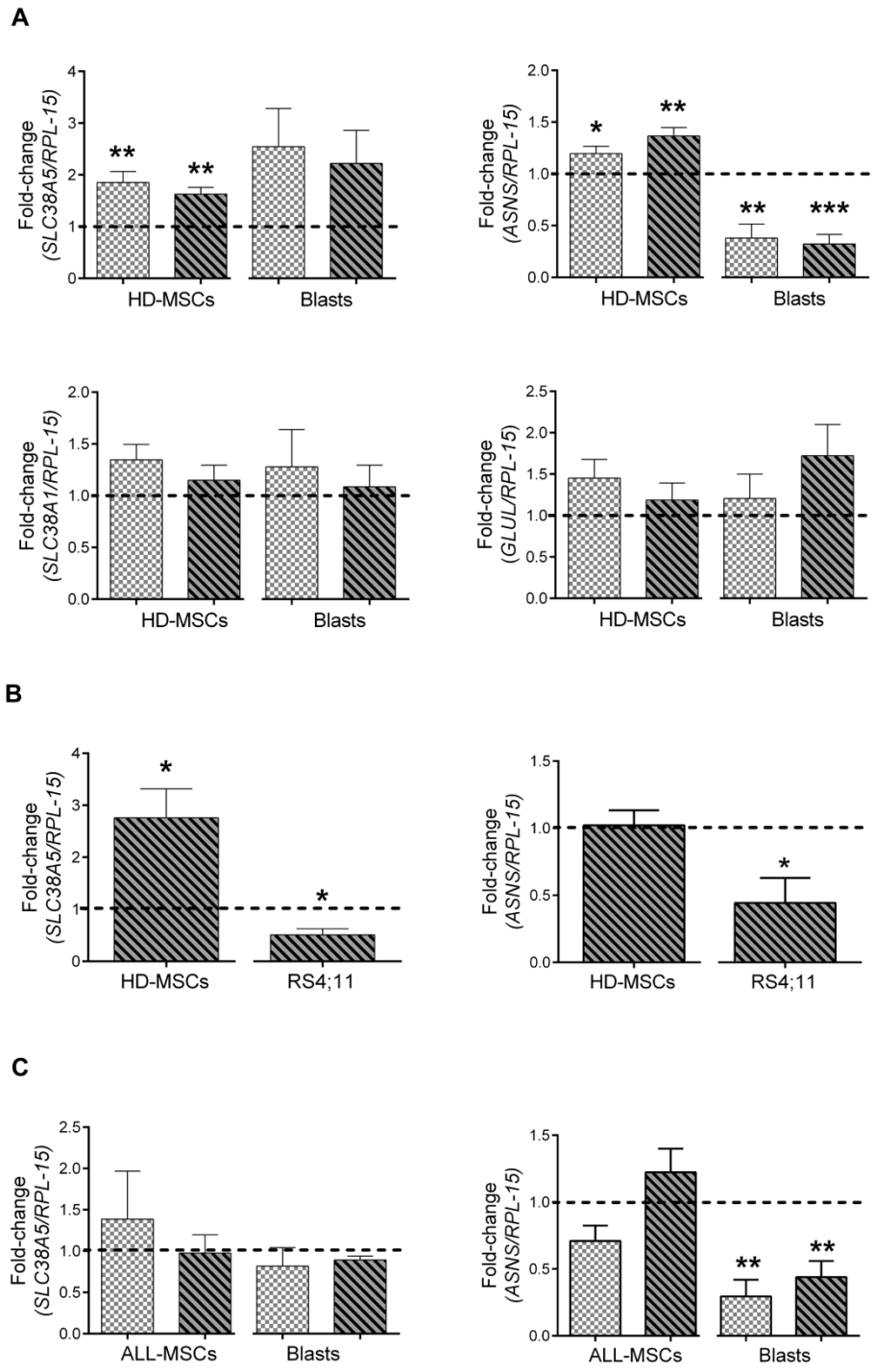

Figure 8. Changes in gene expression induced by co-culture of MSCs with ALL blasts or cells. *Panel A. MSCs from four distinct healthy donors were cultured for 72h in DMEM + 2% FBS, without asparagine, in the absence or in the presence of ALL blasts obtained from three different ALL patients. At the end of the experiments, the expression of ASNS, GLUL, SLC38A5 and SLC38A1 was analyzed by RT-PCR in the two cell types. Panels B, C. SLC38A5 expression was evaluated after co-culture of MSCs from two healthy donors and RS4;11 cells (Panel B) or after the co-culture of ALL-MSCs and ALL blasts from two distinct ALL patients (each blast population was co-cultured with MSCs derived from the same patient) (Panel C). For all panels, data were reported as fold change of the mean value obtained in each cell type in monoculture, considered 1 (line). Data are means of eight (panel A), four (panel B), or three (panel C) determinations performed in duplicate ± SD. * p< 0.05, ** p< 0.01, *** p< 0.001, as assessed with one-sample t test.*

The results presented above demonstrate that (1) differences exist between ALL-MSCs and HD-MSCs in terms of gene expression and protective capacity towards ALL cells, and that (2) leukemic blasts are able to induce gene expression, and in particular the expression of SLC38A5/SNAT5, in stromal cells.

At present, these data are the bases for further developments aimed at:

1) Ascertaining the role of SLC38A5 in the protection
2) Evaluating the possibility that ALL- and HD-MSC exhibit different metabolic features.

4.9. Appendix 1 – Effects of SLC38A5 silencing in MSCs

4.9.1. Transfection procedure causes SNAT3 induction in MSCs

The first approach to elucidate the role of SNAT5 in the protective effect by MSCs and verify if SNAT5 suppression decreases MSC protective capacity was to evaluate the effect of *SLC38A5* silencing in ALL-MSCs.

After 4d of transfection, *SLC38A5* mRNA was markedly lowered (Figure 9A) and, consistently, SNAT5 protein was found reduced after further 2d (Figure 9B). However, measuring the fractional efflux of pre-accumulated Gln, both scramble-transfected and *SLC38A5*-silenced cells secrete more Gln than untransfected MSCs, with only a very slight reduction of Gln efflux by silenced cells (Figure 9C). Consistently, when *SLC38A5*-silenced and scramble transfected MSCs were co-cultured with ASNase-treated RS4;11 cells, the difference in the protective effect did not reach the statistical significance (Figure 9D). To understand why *SLC38A5*-silencing did not affect either amino acid efflux or the protective capacity of MSCs, we evaluated the expression of another transporter of System N, SNAT3, which was expressed at very low levels in MSCs derived from either leukemia patients or healthy donors (data not shown). After 4d of transfection, SNAT5 expression was markedly lowered in silenced cells compared with scramble-transfected and untransfected MSCs, whereas *SLC38A3* expression was significantly induced, either in scramble-transfected or in *SLC38A5*-silenced cells (Figure 9E).

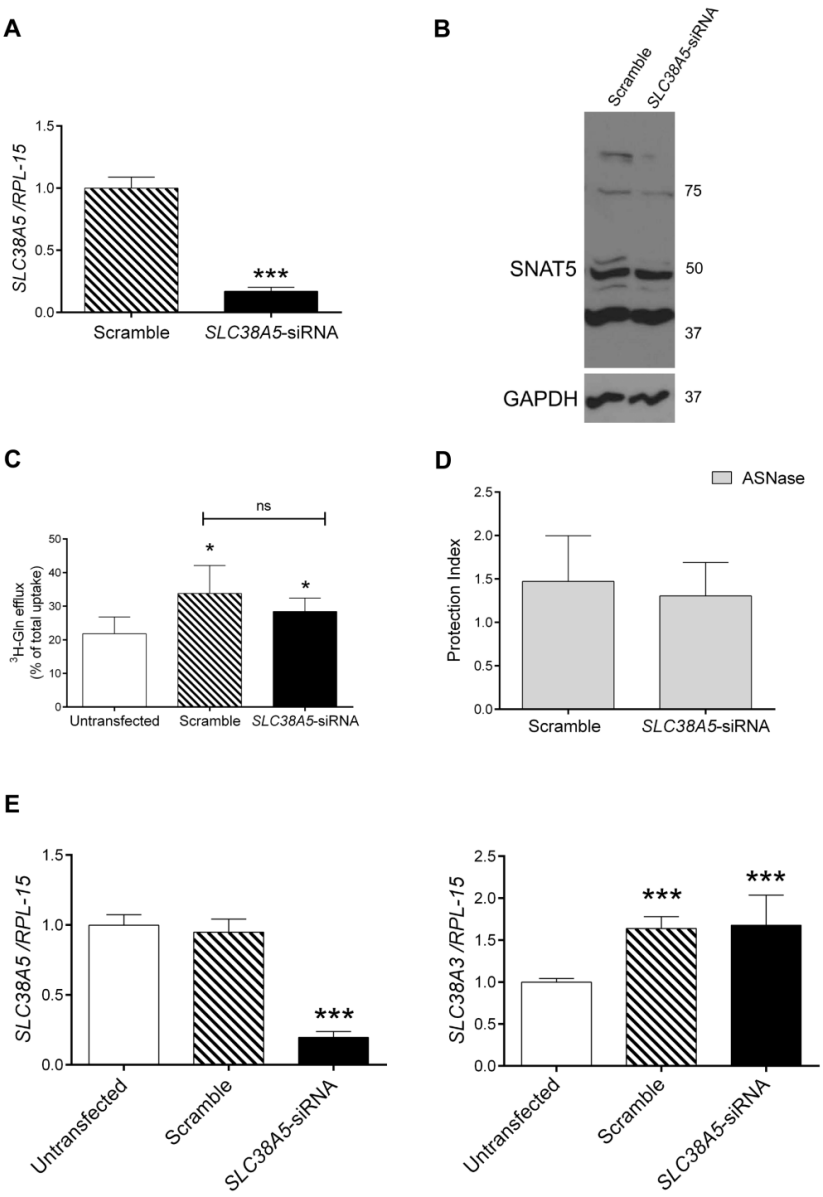

Figure 9. Effects of SLC38A5 silencing in MSCs. *Panel A-B. ALL-MSCs from two different patients were transfected with scramble or SLC38A5-siRNA (see Materials and Methods), and the expression of SLC38A5 mRNA (A) and SNAT5 protein (B, representative experiment) was evaluated, respectively, after 4d and 6d. In panel A, the relative expression of SLC38A3 was determined expressing the results as folds of the mean value obtained in scramble-transfected MSCs, kept at 1. Data are means ± SD of nine independent determinations *** p< 0.001 (two-tail t test for unpaired data). In panel B, GAPDH was used for loading control. Panel C. Fractional Gln efflux (Eq. 3, Materials and Methods) was determined in MSCs from an ALL patient, untransfected or transfected with scramble or SLC38A5-siRNA. Data are means of 5 independent determinations with SD. * p< 0.05 (two-tail t test for unpaired data). Panel D. The Protection Index (Eq. 2 Materials and Methods), was determined for ASNase-treated RS4;11 cells, maintained in mono-culture or co-cultured with scramble-transfected or SLC38A5-silenced ALL-MSCs. Data are means ± SD of eight independent determinations from MSCs of two different patients. Panel E. The expression of SLC38A5 and SLC38A3 mRNA were evaluated in untransfected, scramble- and SLC38A5- transfected MSCs after 4d of transfection. The relative expression of SLC38A5 and SLC38A3 were determined expressing the results as fold increase of the value obtained in untransfected MSCs, kept at 1. Data are means ± SD of five independent determinations from MSCs of two different patients, *** p< 0.001 (two-tail t test for unpaired data)*

4.10. Appendix 2 – Different metabolic features of ALL- and HD-MSCs: Towards a metabolic characterization of human MSCs

4.10.1. MSCs accelerate proliferation in a physiological culture medium

We have preliminary ascertained that very scarce information is available on the metabolism of bone marrow mesenchymal stromal cells. For this reason, we decided to preliminarily characterize the metabolic features of MSCs under conditions mimicking as far as possible the bone marrow environment. To this purpose, we cultured ALL- and HD-MSCs at physiological concentrations of nutrients and metabolites in Plasmax™ medium (see Materials and Methods).

First, we evaluated cell growth, so as to determine cell proliferative rate in this condition. As shown in Figure 10, cell number of both MSC groups increased by more than 3-fold after 3d and by more than 5-fold after 6d of incubation in Plasmax™. Moreover, cell number was significantly higher when cells are cultured in Plasmax™ than in the standard growth medium DMEM.

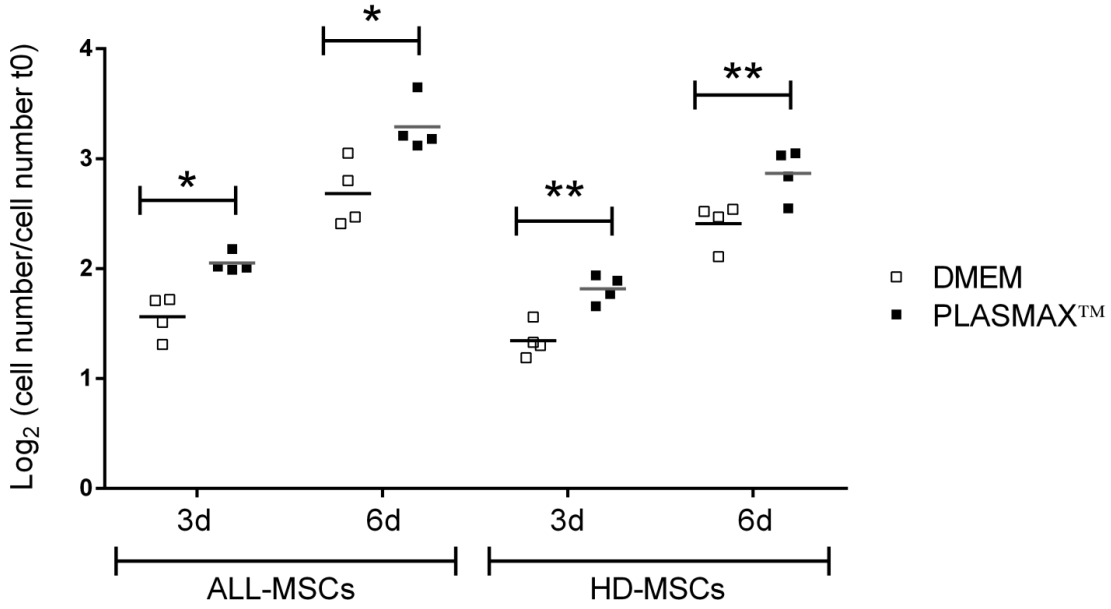

Figure 10. Growth of MSCs in Plasmax™ and DMEM. *MSCs from four ALL patients and four healthy donors were cultured in PLASMAX™ or in DMEM, supplemented with 10% FBS for 3d and 6d. Cell growth was evaluated from cell counts. Data are expressed as Log_2 of the ratio between cell number at the experimental time and cell number at time 0, and are means ± SD of cells from four ALL patients and four healthy donors, each used in triplicate. * p< 0.05, ** p< 0.01 cells cultured in Plasmax™ vs. cells cultured in DMEM (two-tail t test for paired data).*

4.10.2. MSCs exhibit aerobic glycolysis

To study the metabolic features of MSCs, we evaluated the exchange rates of metabolites between medium and cells (see Materials and Methods) at 21% O_2 or under hypoxic conditions (1% O_2), thus mimicking more closely bone marrow environment. At 21% O_2, more than 20 nmol/µg prot/day of glucose were consumed, with this value doubled in hypoxia; consistently, more than 30 nmol/µg prot/day of lactate were secreted at 21% O_2 and more than 60 nmol/µg prot/day at 1% O_2 (Figure 11A). Thus, the percentage of glucose converted into lactate was more than 60% in both MSCs groups independently from O_2 levels, suggesting that these cells are glycolytic even under aerobic conditions (Figure 11B). To further validate this conclusion, we evaluated the oxygen consumption rate (OCR) in MSCs in the presence of 21% O_2 with a Seahorse analyzer (Figure 11C). OCR was very low at baseline but already represented the maximal levels that MSCs were able to reach. Consistently with their prevalent glycolytic behavior, MSCs proliferate also in hypoxia and, after 3d, cell growth was not significantly different at 21% or 1% O_2 (Figure 11D). However, at later times of incubation, the proliferative rate of cells cultured in hypoxia was significantly lower compared with cells maintained at 21%O_2.

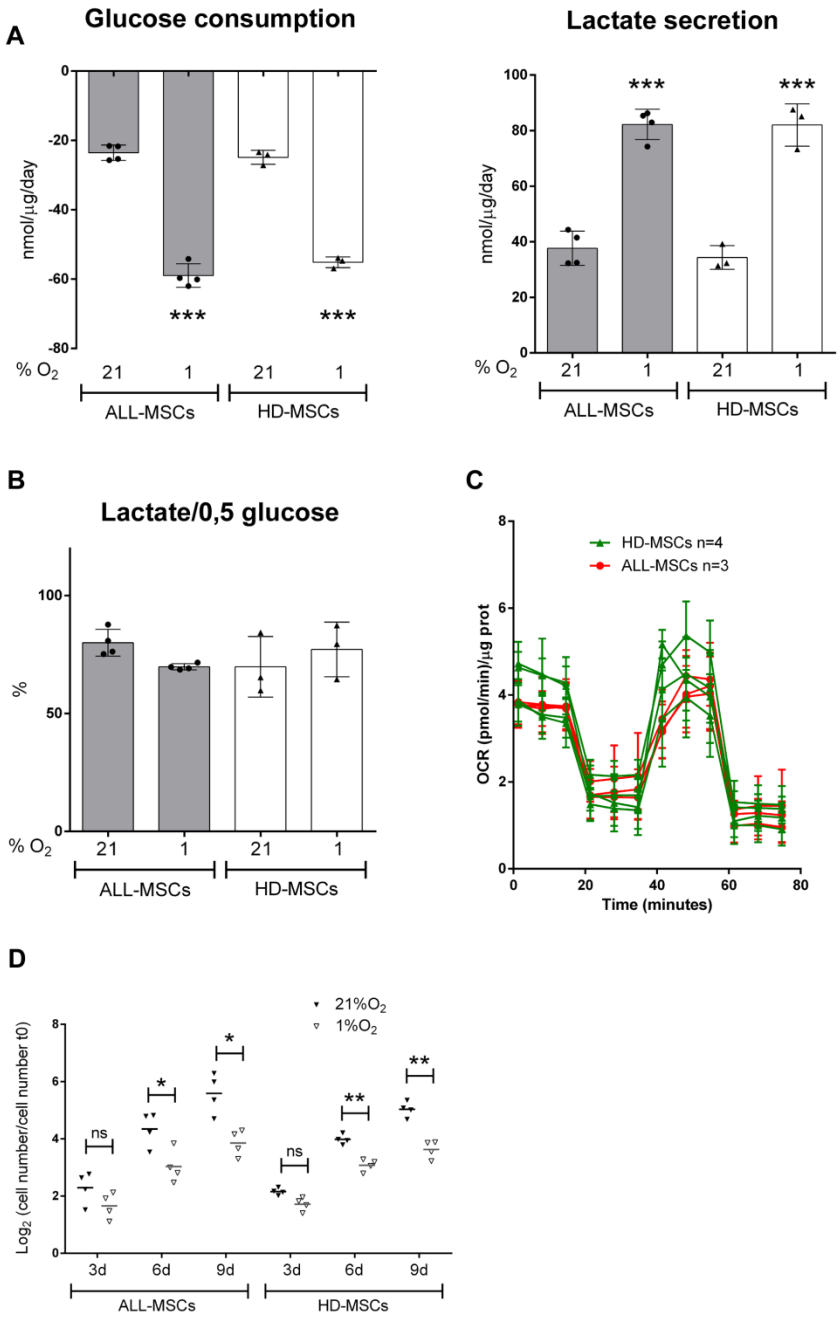

Figure 11. Glucose metabolism in MSCs under aerobic and anaerobic conditions. *ALL-MSCs and HD-MSCs were incubated at 21% or 1% of O_2 in Plasmax™ supplemented with 10% dialyzed FBS Panel A-B. Exchange rates of glucose and lactate measured after 48h. Exchange rates (A) are expressed as nmol/µg protein/day and are calculated according to Eq. 4 (Materials and Methods) or (B) as the percentage of the ratio between the nmol of secreted lactate and nmol of consumed glucose. Data represent means ± SD of MSCs from four different leukemia patients and three different healthy donors, each used in triplicate. *** p< 0.001 cells cultured at 1% O_2 vs. cells cultured at 21% O_2 (two-tail t test for unpaired data). Panel C. Oxygen consumption rate (OCR), was measured after 24h at 21% O_2 using the Agilent Seahorse XF Cell Mito Stress Test Kit (see Materials and Methods). Data are expressed as pmol/min/ µg protein and represent means ± SD of MSCs from three different leukemia patients and four different healthy donors, each with 10 replicates. Panel D. Cell growth was estimated up to 9d of culture from cell counts. Data are expressed as Log_2 of the ratio between cell number at the experimental time and cell number at time 0, and are means ± SD of cells from four ALL patients and four healthy donors, each used in triplicate. * p< 0.05, ** p< 0.01 1% O_2 vs. 21% O_2 at the same experimental time (two-tail t test for paired data).*

4.10.3. MSCs secrete glutamine-derived citrate

To further investigate the metabolic features of MSCs, we quantified the different isotopologues of Krebs cycle intermediates, culturing stromal cells in Plasmax™ in the presence of $^{13}C_5$ glutamine under aerobic (21%O_2) or anaerobic (1%O_2) conditions.

As shown in Figure 12A, in aerobiosis Gln was deamidated into Glu and then deaminated into α-oxoglutarate (α-KG), which entered the Krebs cycle, where more than 45% of each intermediate was labeled and, therefore, derived from the amino acid. Moreover, a large fraction of Asp was labeled with only a small fraction of this used for Asn synthesis. In anaerobiosis, the intracellular levels of Gln, Glu and α-KG were higher, while, on the contrary, the intracellular levels of the other Krebs cycle intermediates were lower. Intracellular Aspartate was also markedly lowered, whereas Asn levels remained stable, even if the fraction derived from labelled Asp was clearly less evident. In summary, under hypoxic conditions the decrease or the increase of most intracellular metabolites proportionally involved all the isotopologues. In contrast, while most fractions of citrate were lower at 1%O_2 than at 21%O_2, the $^{13}C_5$-labeled part, which derived from reductive carboxylation of Gln-derived α-KG, was higher under anaerobic than aerobic conditions. To confirm these data, we calculated the percentage of each citrate isotopologue, demonstrating that $^{13}C_5$-labeled fraction was roughly 3% in aerobiosis but increased to 15% under anaerobic conditions (Figure 12B).

Evaluating the exchange rates, we found that 1.5 nmol/μg prot/day of citrate was secreted under aerobic conditions, more than 45% of which derived from Gln. Citrate secretion was still evident in hypoxia, even if was lower than in normoxia; on the other hand, the $^{13}C_5$-labeled fraction of secreted citrate was still higher in anaerobic than in aerobic conditions (Figure 12C).

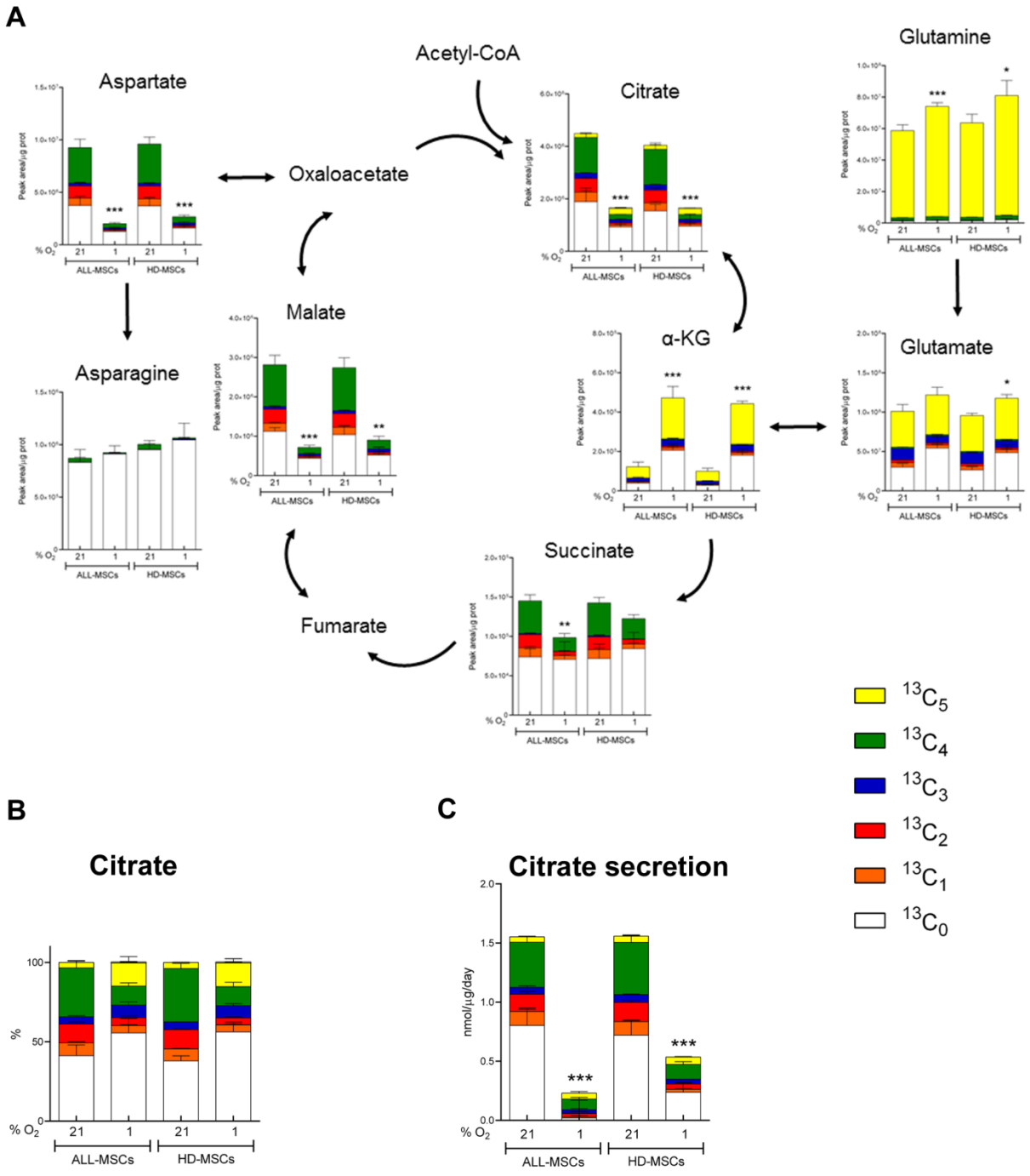

Figure 12. Citrate metabolism in MSCs under aerobic and anaerobic conditions. *Panels A-B-C. ALL-MSCs and HD-MSCs, incubated for 48h at 21% or 1% of O_2 in Plasmax™, supplemented with 10% dialyzed FBS and 0.6 mM $^{13}C_5$-glutamine. Relative isotopologue distribution of the indicated metabolites (A-B) and exchange rates of citrate (B) were measured in LC-MS. Data are expressed as peak areal/µg protein (A), percentage of total citrate (B) and nmol/µg protein/day (C), according to Eq. 4 (Materials and Methods). Data represent means ± SD of MSCs from four different leukemia patients and four different healthy donors, each used in triplicate. * p< 0.05, ** p< 0.01, *** p< 0.001 cells cultured at 1%O_2 vs. cells cultured at 21%O_2 (two-tail t test for unpaired data).*

5. Discussion

In this report we demonstrate that primary mesenchymal stromal cells, derived from the bone marrow (BM) of ALL patients (ALL-MSCs), protect ALL blasts against L-Asparaginase (ASNase) better than MSCs from healthy donors (HD-MSCs). ALL-MSCs differ from HD-MSCs under many aspects [149, 150] such as, for instance, the higher secretion of Activin A [151]. However, only few seem connected to the nutritional stress imposed by ASNase. A recent report indicates that ASNS is more expressed in ALL-MSCs than in HD-MSCs [152], although the change was only detected at mRNA but not at protein level. Consistently, we could not detect changes of ASNS protein in our panels of ALL-MSCs and HD-MSCs.

Actually, although MSCs are considered of pivotal importance for the survival of ALL blasts during chemotherapy, no detailed information is available on the behavior of these cells during the treatment with ASNase. Here we show that the response of ALL-MSCs and HD-MSCs to ASNase is similar. Indeed, upon incubation with the antileukemic drug, both groups, as other cell types undergoing ASNase treatment [30, 153], exhibit a dramatic fall in cell Gln and Asn, which trigger a nutritional stress response, highlighted by eIF2α phosphorylation, the induction of the pro-apoptotic gene *DDIT3*, and proliferative arrest. However, these changes are only transient, since MSCs resume proliferation after few days, demonstrating their capacity to successfully adapt to ASNase. In both cell types the depletion of Asn and Gln, imposed by ASNase, induces ASNS and GS. However, as in other amino acid depleted cell models [91, 110], *ASNS* induction is readily detectable at mRNA level, but ASNS protein does not show consistent changes, confirming the dissociation between mRNA and protein levels already described in MSCs [152]. On the contrary, a marked increase of GS protein expression is consistently seen at late times of ASNase treatment in all the primary ALL-MSC or HD-MSC strains tested. Increased GS expression is associated with a modest induction of the encoding gene *GLUL* but it is more likely attributable to a prolonged half-life of the protein, due to the depletion of intracellular Gln, which is a powerful negative regulator of GS degradation [107]. The similar behavior exhibited by ALL- and HD-MSCs excludes that their different protective activity on ASNase-treated ALL cells is due to a different ability to adapt to the metabolic stress imposed by the antileukemic enzyme.

In all the strains used, either from ALL patients (Figure 2) or healthy donors (Figure 6), the GS inhibitor MSO suppresses MSC adaptation to ASNase and hindered GS expression at protein, but not at mRNA level, while ASNS expression is not affected. The mechanism

underlying the MSO effect on GS expression is unclear, although it should be recalled that MSO is a Gln analogue and, as such, it could promote GS degradation mimicking the natural amino acid [107]. In cells incubated with ASNase (Figures 2-6) or in a Asn-Gln-free medium (Figure 3), intracellular Gln is lower in cells incubated in the presence of MSO than in its absence, while Asn levels are comparable in the two conditions. This result indicates that GS is operative in Gln-depleted cells. Moreover, GS silencing has the same suppressive effect of MSO on the adaptation of MSCs to ASNase, definitely confirming that GS expression and/or activity are crucial factors for the successful adaptation of bone marrow MSCs, either ALL or HD, to ASNase.

MSO also markedly hinders, but does not abolish, the increase in viability observed in ASNase-treated leukemic cells when they are co-cultured with MSCs (Figure 4). The partial inhibition of the protective effect is conceivable since MSCs operate several pro-survival activities for ALL blasts, such as the induction of hERG potassium channel expression on the blast membrane [154], the activation of the Notch [80] or Wnt [155] pathways, down regulation of p21 [156], secretion of cysteine [78], PGE_2 [79] or VEGFA [157]. Consistently, also Iwamoto et al. [68] still observed a significant protection of ALL blasts from ASNase by an immortalized MSC line even after *ASNS* silencing in mesenchymal cells. However, the large effect of the inhibitor on ALL protection demonstrates that GS activity plays a role of substantial importance in the promotion of the survival of ALL cells when they are co-cultured with ALL-MSCs.

The synergistic toxicity between ASNase and MSO on ALL cells is only observed when they are cultured with ALL-MSCs, but not when they are treated with ASNase in monoculture (Figure 5). The simplest explanation of this effect would be that the GS activity in MSCs is needed for ALL cell protection. Nevertheless, although either incubation with MSO or GS silencing abolishes MSC adaptation to ASNase (Figure 2-4), GS silencing in MSCs only marginally hinders their protective activity on ALL cells (Figure 4), which is, instead, heavily affected by MSO under the same conditions. This discrepancy indicates that the interference of MSO on ALL protection by MSCs is only in part due to the inhibition of GS activity in the mesenchymal cells, while most of the effect should be attributed to the suppression of GS activity in ALL cells themselves. This result suggests, therefore, that, during ASNase treatment, a bi-directional, rather than uni-directional flux of nutrients occurs in the ALL niche: MSCs provide Asn to ASNS-negative ALL blasts, but require Gln synthesized by leukemic cells, which are GS-positive [91], to synthesize Asn.

This operational hypothesis is supported by experimental evidence presented here. Indeed, MSCs are able to extrude Asn (Figure 3) not only in Asn- and Gln-free medium, but, more importantly, also in a medium resembling human plasma composition, both in the presence of physiological levels of Asn and in the absence of the amino acid, a condition that mimics the bone marrow situation during ASNase treatment [36, 70].

The existence of a metabolic exchange of Gln and Asn in the ALL niche between MSCs and ALL blasts implies the operation of transporters able to mediate both a net efflux and a net influx of these amino acids. To identify these carriers, given the different competence for ALL protection of ALL- and HD-MSCs, we decided to compare the expression of genes potentially involved in the protective effect in two cell panels obtained from unrelated patients or donors (Figure 7). We found that *SLC38A5*, the gene that encodes for the Asn and Gln transporter SNAT5, is significantly more expressed in MSCs from ALL patients than from healthy donors. Consistently, Asn efflux is significantly faster from ALL-MSCs than from HD-MSCs. The increased expression of SNAT5 in ALL-MSCs has been also confirmed with Western Blot and immunofluorescence. SNAT5, a member of the so called "system N" together with the SNAT3 and the SNAT7 carriers, is a bidirectional transporter, which couples substrate fluxes with a Na^+ symport and a proton antiport and can mediate either the influx or the efflux of Gln and Asn, depending on the prevailing gradient of its substrates [135].

The only obvious difference between MSCs from healthy donors and ALL patients is that the latter have interacted *in vivo* with the leukemic cells. Therefore, to reproduce this situation *in vitro*, we have cultured MSCs from healthy donors with blasts from ALL patients (Figure 8). Importantly, both *SLC38A5* and *ASNS* are significantly induced in MSCs, suggesting that leukemic blasts manipulate amino acid metabolism and transport of stromal cells through changes in gene expression so as to increase MSC capability to exert an effective nutritional support. Conversely, also MSCs are able to influence gene expression in ALL cells. Indeed, *ASNS*, which is a typical marker of nutritional stress induced by Asn deprivation, is markedly down regulated in blasts upon co-culturing with MSCs, indicating that the interaction with stromal cells effectively relieves amino acid depletion in ALL cells. Interestingly, no induction of *SLC38A5* is observed in MSCs from ALL patients upon co-culture with ALL blasts. Intuitively, lack of induction is conceivable since these cells have already interacted *in vivo* with leukemic blasts and, hence, express high levels of SNAT5. Indeed, it should be noted that also in the two panels of MSCs used

for the experiment shown in Figure 8A-8C, ALL-MSCs exhibit a significantly higher *SLC38A5* expression than HD-MSCs (data not shown).

The results reported in this contribution suggest that the different expression of SNAT5 in ALL MSCs mediates a larger efflux of Asn and contributes to their increased ability to support ALL cell viability upon ASNase treatment. However, until now, we have not been able to definitely confirm this hypothesis. In fact, *SLC38A5* silencing in ALL-MSCs does not significantly reduce the protective activity of stromal cells (Appendix 1). The most likely explanation of this negative result is the induction of an another System N transporter, SNAT3, caused by the transfection procedure (Appendix 1, Figure 9). Indeed, paradoxically, the transfection with either *SLC38A5* or scramble siRNA increases amino acid efflux compared to untransfected cells. An alternative approach to demonstrate SNAT5 role in protection would be to increase its expression in HD-MSCs, to verify if this condition leads to an increased protective effect.

This thesis also demonstrates that either ALL blasts or MSCs are able to induce gene expression changes in the other cell type. Actually, the existence of a metabolic relationship between MSCs and ALL cells has been substantiated by other studies, which showed that MSCs drive ALL cells towards glycolysis [158] and mitochondrial uncoupling [159]. However, these reports are mainly focused on changes in central carbon metabolism induced in ALL blasts by stromal cells. Conversely, scarce information is available on the possible influence of ALL cells and, more in general, on the metabolism of bone marrow mesenchymal stromal cells themselves. For this reason, we undertook a preliminary characterization of the metabolic features of ALL-MSCs and HD-MSCs under physiological conditions at 21% or 1% of O_2, thus mimicking as far as possible the bone marrow environment (Appendix 2). All the MSC strains tested, from leukemia patients or healthy donors, exhibit an aerobic glycolytic behavior (Appendix 2, Figure 11). This result seems in contrast with recent data indicating that ALL-derived extracellular vesicles switch MSC glucose metabolism from oxidative phosphorylation to aerobic glycolysis [160]. However, in that contribution HPV-immortalized MSCs, rather than primary cells, were used.

MSCs seem not substantially affected by maintenance in hypoxic conditions and proliferate even at 1%O_2, although the proliferative rate becomes slower with the prolongation of the hypoxic incubation. Actually, it should be recalled that the bone marrow environment is hypoxic.

Interestingly, MSCs secrete citrate (Appendix 2, Figure 12), an uncommon feature in normal cells and typical only of prostatic epithelium and astrocytes [161]. Under hypoxic conditions, citrate secretion is still evident, although lowered, but the amount of citrate synthetized through a reductive carboxylation of Gln-derived α-ketoglutarate increases.

In summary, the preliminary results obtained thus far indicate that MSCs derived from ALL patients and healthy donors are both highly glycolytic and secrete significant amounts of citrate. Further experiments will ascertain if this metabolic behavior is modified by co-culturing MSCs with ALL blasts and, in this case, if ALL- and HD-MSCs will behave similarly.

6. Conclusions and perspectives

In conclusion, this dissertation describes mechanisms involved in the complex interaction occurring in the bone marrow between ASNS-negative Acute Lymphoblastic Leukemia blasts and mesenchymal stromal cells. The results allow to propose a working model of an amino acid trade-off between the two cell populations (Figure 13 upper). Under basal conditions, MSCs are able to synthetize and secrete Asn, and the presence of ALL blasts boost these stromal activities. In particular, leukemic cells induce ASNS and the bi-directional Asn and Gln transporter SNAT5 in MSCs. At the same time, they provide MSCs with neo-synthetized Gln, the obliged substrate of ASNS. Thus, stromal cells have all the tools needed to increase synthesis, secretion and extracellular availability of Asn, which is required for the survival and proliferation of ALL blasts.

An interesting aspect of this model is that, at least for SNAT5, the change in gene expression persists under *in vitro* culture conditions. Therefore, we propose that SNAT5 induction is due to epigenetic mechanisms, an issue left for future investigations. Similarly, how leukemic cells induce these gene changes in MSCs remains an open question. We can speculate that, while a direct contact between the two cells does not seem to be an absolute requirement, cytokines or signaling molecules, either free in solution or enclosed in exosomes or extracellular microvesicles, are an interesting possibility.

The proposed amino acid exchange would assume a peculiar relevance upon the Gln and Asn depletion induced by the anti-leukemic drug L-Asparaginase (Figure 13 lower). Under these conditions, MSCs adapt to ASNase through the up-regulation of Glutamine Synthetase. Thus, GS expression is required to maintain intracellular Gln, since fueling from ALL blasts is likely reduced by ASNase mediated hydrolysis of extracellular Gln. Since the protective effect is detected with ASNase present throughout the experiment, an involvement of targeted exosomes or extracellular microvesicles in the Asn/Gln intercellular fluxes is highly likely.

Another point that should be underlined is that we focused our attention on MSCs; however, quite paradoxically, scarce information is available about amino acid transport and metabolism in ALL blasts. The transporters used to mediate the influx and efflux of Gln and Asn have never been investigated in these cells; moreover, neither ALL blast metabolic behavior during the treatment with ASNase nor its possible modulation by stromal cells have been studied. All these issues should be evaluated under conditions as far as possible reproducing the *in vivo* bone marrow environment, for instance in 3D-cell cultures or through microfluidic Organ-on-a-Chip models.

In light of our results we can conclude that Glutamine Synthetase and the transporter SNAT5 play key, but distinct, roles in the metabolic exchanges occurring in the ALL niche and, therefore, could be proposed as therapeutic targets to counteract ALL resistance to ASNase. Examples of nutritional support of cancer cells exerted by stromal cells through the release of amino acids have been increasingly reported in the last few years, for both haematological [59, 78] and non-haematological tumors [58, 162]. While Asn supply is very important for Asn-auxotrophic ALL cells, Gln is more often involved in nutritional exchanges between other cancers and stromal cells or between clones of cancer cells endowed with different metabolic properties. In these cases, cells with sizable GS expression have been proposed to produce Gln to support neoplastic cells [58, 162], although the transporters involved in these processes have remained thus far elusive. The results presented here point to the Asn-Gln SNAT5 transporter as one of these routes and prompt further studies on SNAT5 expression in stromal and cancer cells of Gln-addicted human tumors.

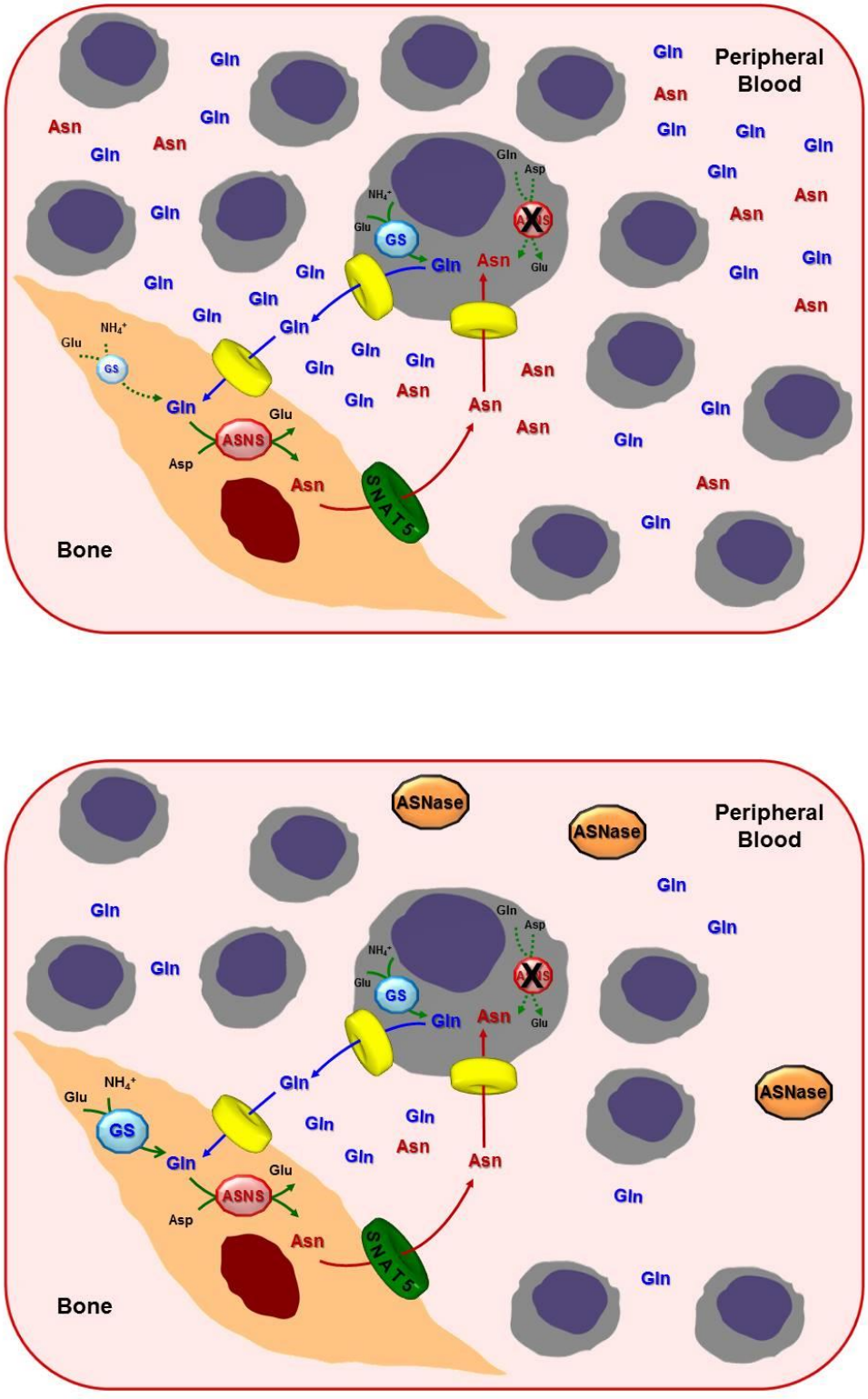

Figure 13. Amino acid trade-off between ALL blasts and Mesenchymal stromal cells(MSCs) in Bone Marrow Niche: a working model. *Under basal conditions (upper panel), Asparagine Synthetase (ASNS)-negative ALL blasts synthetize Glutamine (Gln) that is provided to MSCs for Asparagine (Asn) synthesis. In turn, Asn is extruded through the SNAT5 transporter to make it available for blasts. Upon Asparaginase (ASNase) treatment (lower panel), Asn and a large part of Gln in the bulk phase are hydrolyzed, promoting Glutamine Synthetase (GS) expression in MSCs that contributes to maintain the MSC pool Gln at levels permissive for the synthesis of Asn, which is then extruded towards ALL blasts, allowing their survival. In yellow, thus far unidentified transporters.*

7. References

1. *Paul S, Kantarjian H, Jabbour EJ. Adult Acute Lymphoblastic Leukemia. Mayo Clin Proc. (2016) 91: 1645-1666*

2. *Chiaretti S, Vitale A, Cazzaniga G, Orlando SM, Silvestri D, Fazi P, Valsecchi MG, Elia L, Testi AM, Mancini F, Conter V, te Kronnie G, Ferrara F, Di Raimondo F, Tedeschi A, Fioritoni G, Fabbiano F, Meloni G, Specchia G, Pizzolo G, Mandelli F, Guarini A, Basso G, Biondi A, Foa R. Clinico-biological features of 5202 patients with acute lymphoblastic leukemia enrolled in the Italian AIEOP and GIMEMA protocols and stratified in age cohorts. Haematologica. (2013) 98: 1702-1710*

3. *Terwilliger T ,Abdul-Hay M. Acute lymphoblastic leukemia: a comprehensive review and 2017 update. Blood Cancer J. (2017) 7: e577*

4. *Bennett JM, Catovsky D, Daniel MT, Flandrin G, Galton DA, Gralnick HR, Sultan C. Proposals for the classification of the acute leukaemias. French-American-British (FAB) co-operative group. Br J Haematol. (1976) 33: 451-458*

5. *Arber DA, Orazi A, Hasserjian R, Thiele J, Borowitz MJ, Le Beau MM, Bloomfield CD, Cazzola M, Vardiman JW. The 2016 revision to the World Health Organization classification of myeloid neoplasms and acute leukemia. Blood. (2016) 127: 2391-2405*

6. *Mrozek K, Harper DP, Aplan PD. Cytogenetics and molecular genetics of acute lymphoblastic leukemia. Hematol Oncol Clin North Am. (2009) 23: 991-1010, v*

7. *Bursen A, Schwabe K, Ruster B, Henschler R, Ruthardt M, Dingermann T, Marschalek R. The AF4.MLL fusion protein is capable of inducing ALL in mice without requirement of MLL.AF4. Blood. (2010) 115: 3570-3579*

8. *Godfrey L, Kerry J, Thorne R, Repapi E, Davies JO, Tapia M, Ballabio E, Hughes JR, Geng H, Konopleva M, Milne TA. MLL-AF4 binds directly to a BCL-2 specific enhancer and modulates H3K27 acetylation. Exp Hematol. (2017) 47: 64-75*

9. *Ayton PM ,Cleary ML. Transformation of myeloid progenitors by MLL oncoproteins is dependent on Hoxa7 and Hoxa9. Genes Dev. (2003) 17: 2298-2307*

10. *Wilkinson AC, Ballabio E, Geng H, North P, Tapia M, Kerry J, Biswas D, Roeder RG, Allis CD, Melnick A, de Bruijn MF, Milne TA. RUNX1 is a key target in t(4;11) leukemias that contributes to gene activation through an AF4-MLL complex interaction. Cell Rep. (2013) 3: 116-127*

11. *Figueroa ME, Chen SC, Andersson AK, Phillips LA, Li Y, Sotzen J, Kundu M, Downing JR, Melnick A, Mullighan CG. Integrated genetic and epigenetic analysis of childhood acute lymphoblastic leukemia. J Clin Invest. (2013) 123: 3099-3111*

12. *Vitale A, Guarini A, Chiaretti S, Foa R. The changing scene of adult acute lymphoblastic leukemia. Curr Opin Oncol. (2006) 18: 652-659*

13. *Kato M ,Manabe A. Treatment and biology of pediatric acute lymphoblastic leukemia. Pediatr Int. (2018) 60: 4-12*

14. *Gaynon PS, Trigg ME, Heerema NA, Sensel MG, Sather HN, Hammond GD, Bleyer WA. Children's Cancer Group trials in childhood acute lymphoblastic leukemia: 1983-1995. Leukemia. (2000) 14: 2223-2233*

15. *Pui CH, Campana D, Pei D, Bowman WP, Sandlund JT, Kaste SC, Ribeiro RC, Rubnitz JE, Raimondi SC, Onciu M, Coustan-Smith E, Kun LE, Jeha S, Cheng C, Howard SC, Simmons V, Bayles A, Metzger ML, Boyett JM, Leung W, Handgretinger R, Downing JR, Evans WE, Relling MV. Treating childhood acute lymphoblastic leukemia without cranial irradiation. N Engl J Med. (2009) 360: 2730-2741*

16. *Maude SL, Teachey DT, Porter DL, Grupp SA. CD19-targeted chimeric antigen receptor T-cell therapy for acute lymphoblastic leukemia. Blood. (2015) 125: 4017-4023*

17. *Cario G, Leoni V, Conter V, Attarbaschi A, Zaliova M, Sramkova L, Cazzaniga G, Fazio G, Sutton R, Elitzur S, Izraeli S, Lauten M, Locatelli F, Basso G, Buldini B, Bergmann AK, Lentes J, Steinemann D, Gohring G, Schlegelberger B, Haas OA, Schewe D, Buchmann S, Moericke A, White D, Revesz T, Stanulla M, Mann G, Bodmer N, Arad-Cohen N, Zuna J, Valsecchi MG, Zimmermann M, Schrappe M, Biondi A. Relapses and treatment-related events contributed equally to poor prognosis in children with ABL-class fusion positive B-cell acute lymphoblastic leukemia treated according to AIEOP-BFM protocols. Haematologica. (2019)*

18. *Fielding AK, Richards SM, Chopra R, Lazarus HM, Litzow MR, Buck G, Durrant IJ, Luger SM, Marks DI, Franklin IM, McMillan AK, Tallman MS, Rowe JM, Goldstone AH. Outcome of 609 adults after relapse of acute lymphoblastic leukemia (ALL); an MRC UKALL12/ECOG 2993 study. Blood. (2007) 109: 944-950*

19. *Schraw JM, Junco JJ, Brown AL, Scheurer ME, Rabin KR, Lupo PJ. Metabolomic profiling identifies pathways associated with minimal residual disease in childhood acute lymphoblastic leukaemia. EBioMedicine. (2019)*

20. *Avramis VI ,Tiwari PN. Asparaginase (native ASNase or pegylated ASNase) in the treatment of acute lymphoblastic leukemia. Int J Nanomedicine. (2006) 1: 241-254*

21. *Kidd JG. Regression of transplanted lymphomas induced in vivo by means of normal guinea pig serum. II. Studies on the nature of the active serum constituent: histological mechanism of the regression: tests for effects of guinea pig serum on lymphoma cells in vitro: discussion. J Exp Med. (1953) 98: 583-606*

22. *Kidd JG. Regression of transplanted lymphomas induced in vivo by means of normal guinea pig serum. I. Course of transplanted cancers of various kinds in mice and rats given guinea pig serum, horse serum, or rabbit serum. J Exp Med. (1953) 98: 565-582*

23. *Broome JD. Evidence that the L-asparaginase of guinea pig serum is responsible for its antilymphoma effects. I. Properties of the L-asparaginase of guinea pig serum in relation to those of the antilymphoma substance. J Exp Med. (1963) 118: 99-120*

24. *Broome JD. Evidence that the L-asparaginase of guinea pig serum is responsible for its antilymphoma effects. II. Lymphoma 6C3HED cells cultured in a medium devoid of L-asparagine lose their susceptibility to the effects of guinea pig serum in vivo. J Exp Med. (1963) 118: 121-148*

25. *Narta UK, Kanwar SS, Azmi W. Pharmacological and clinical evaluation of L-asparaginase in the treatment of leukemia. Crit Rev Oncol Hematol. (2007) 61: 208-221*

26. *Pavlova NN, Hui S, Ghergurovich JM, Fan J, Intlekofer AM, White RM, Rabinowitz JD, Thompson CB, Zhang J. As Extracellular Glutamine Levels Decline, Asparagine Becomes an Essential Amino Acid. Cell Metab. (2018) 27: 428-438 e425*

27. *Batool T, Makky EA, Jalal M, Yusoff MM. A Comprehensive Review on L-Asparaginase and Its Applications. Appl Biochem Biotechnol. (2016) 178: 900-923*

28. *Tabe Y, Lorenzi PL, Konopleva M. Amino acid metabolism in hematologic malignancies and the era of targeted therapy. Blood. (2019) 134: 1014-1023*

29. *Panosyan EH, Grigoryan RS, Avramis IA, Seibel NL, Gaynon PS, Siegel SE, Fingert HJ, Avramis VI. Deamination of glutamine is a prerequisite for optimal asparagine deamination by asparaginases in vivo (CCG-1961). Anticancer Res. (2004) 24: 1121-1125*

30. *Tardito S, Chiu M, Uggeri J, Zerbini A, Da Ros F, Dall'Asta V, Missale G, Bussolati O. L-Asparaginase and inhibitors of glutamine synthetase disclose glutamine addiction of beta-catenin-mutated human hepatocellular carcinoma cells. Curr Cancer Drug Targets. (2011) 11: 929-943*

31. *Chan WK, Lorenzi PL, Anishkin A, Purwaha P, Rogers DM, Sukharev S, Rempe SB, Weinstein JN. The glutaminase activity of L-asparaginase is not required for anticancer activity against ASNS-negative cells. Blood. (2014) 123: 3596-3606*

32. *Chan WK, Horvath TD, Tan L, Link T, Harutyunyan KG, Pontikos MA, Anishkin A, Du D, Martin LA, Yin E, Rempe SB, Sukharev S, Konopleva M, Weinstein JN, Lorenzi PL. Glutaminase Activity of L-Asparaginase Contributes to Durable Preclinical Activity against Acute Lymphoblastic Leukemia. Mol Cancer Ther. (2019) 18: 1587-1592*

33. *Timmerman LA, Holton T, Yuneva M, Louie RJ, Padro M, Daemen A, Hu M, Chan DA, Ethier SP, van 't Veer LJ, Polyak K, McCormick F, Gray JW. Glutamine sensitivity analysis identifies the xCT antiporter as a common triple-negative breast tumor therapeutic target. Cancer Cell. (2013) 24: 450-465*

34. *Salzer W, Bostrom B, Messinger Y, Perissinotti AJ, Marini B. Asparaginase activity levels and monitoring in patients with acute lymphoblastic leukemia. Leuk Lymphoma. (2018) 59: 1797-1806*

35. *Covini D, Tardito S, Bussolati O, Chiarelli LR, Pasquetto MV, Digilio R, Valentini G, Scotti C. Expanding targets for a metabolic therapy of cancer: L-asparaginase. Recent Pat Anticancer Drug Discov. (2012) 7: 4-13*

36. *Tong WH, Pieters R, Hop WC, Lanvers-Kaminsky C, Boos J, van der Sluis IM. No evidence of increased asparagine levels in the bone marrow of patients with acute lymphoblastic leukemia during asparaginase therapy. Pediatr Blood Cancer. (2013) 60: 258-261*

37. *Hijiya N ,van der Sluis IM. Asparaginase-associated toxicity in children with acute lymphoblastic leukemia. Leuk Lymphoma. (2016) 57: 748-757*

38. *Thomson B, Park JR, Felgenhauer J, Meshinchi S, Holcenberg J, Geyer JR, Avramis V, Douglas JG, Loken MR, Hawkins DS. Toxicity and efficacy of intensive chemotherapy for children with acute lymphoblastic leukemia (ALL) after first bone marrow or extramedullary relapse. Pediatr Blood Cancer. (2004) 43: 571-579*

39. *Zalewska-Szewczyk B, Andrzejewski W, Mlynarski W, Jedrychowska-Danska K, Witas H, Bodalski J. The anti-asparagines antibodies correlate with L-asparagines activity and may affect clinical outcome of childhood acute lymphoblastic leukemia. Leuk Lymphoma. (2007) 48: 931-936*

40. *Ettinger LJ, Ettinger AG, Avramis VI, Gaynon PS. Acute lymphoblastic leukaemia: a guide to asparaginase and pegaspargase therapy. BioDrugs. (1997) 7: 30-39*

41. *Ortega JA, Nesbit ME, Jr., Donaldson MH, Hittle RE, Weiner J, Karon M, Hammond D. L-Asparaginase, vincristine, and prednisone for induction of first remission in acute lymphocytic leukemia. Cancer Res. (1977) 37: 535-540*

42. *Amylon MD, Shuster J, Pullen J, Berard C, Link MP, Wharam M, Katz J, Yu A, Laver J, Ravindranath Y, Kurtzberg J, Desai S, Camitta B, Murphy SB. Intensive high-dose asparaginase consolidation improves survival for pediatric patients with T cell acute lymphoblastic leukemia and advanced stage lymphoblastic lymphoma: a Pediatric Oncology Group study. Leukemia. (1999) 13: 335-342*

43. *Pession A, Valsecchi MG, Masera G, Kamps WA, Magyarosy E, Rizzari C, van Wering ER, Lo Nigro L, van der Does A, Locatelli F, Basso G, Arico M. Long-term results of a randomized trial on extended use of high dose L-asparaginase for standard risk childhood acute lymphoblastic leukemia. J Clin Oncol. (2005) 23: 7161-7167*

44. *Balasubramanian MN, Butterworth EA, Kilberg MS. Asparagine synthetase: regulation by cell stress and involvement in tumor biology. Am J Physiol Endocrinol Metab. (2013) 304: E789-799*

45. *Appel IM, den Boer ML, Meijerink JP, Veerman AJ, Reniers NC, Pieters R. Up-regulation of asparagine synthetase expression is not linked to the clinical response L-asparaginase in pediatric acute lymphoblastic leukemia. Blood. (2006) 107: 4244-4249*

46. *Hermanova I, Zaliova M, Trka J, Starkova J. Low expression of asparagine synthetase in lymphoid blasts precludes its role in sensitivity to L-asparaginase. Exp Hematol. (2012) 40: 657-665*

47. *Nakamura A, Nambu T, Ebara S, Hasegawa Y, Toyoshima K, Tsuchiya Y, Tomita D, Fujimoto J, Kurasawa O, Takahara C, Ando A, Nishigaki R, Satomi Y, Hata A, Hara T. Inhibition of GCN2 sensitizes ASNS-low cancer cells to asparaginase by disrupting the amino acid response. Proc Natl Acad Sci U S A. (2018) 115: E7776-E7785*

48. *Pakos-Zebrucka K, Koryga I, Mnich K, Ljujic M, Samali A, Gorman AM. The integrated stress response. EMBO Rep. (2016) 17: 1374-1395*

49. *Aslanian AM ,Kilberg MS. Multiple adaptive mechanisms affect asparagine synthetase substrate availability in asparaginase-resistant MOLT-4 human leukaemia cells. Biochem J. (2001) 358: 59-67*

50. *Chien WW, Le Beux C, Rachinel N, Julien M, Lacroix CE, Allas S, Sahakian P, Cornut-Thibaut A, Lionnard L, Kucharczak J, Aouacheria A, Abribat T, Salles G. Differential mechanisms of asparaginase resistance in B-type acute lymphoblastic leukemia and malignant natural killer cell lines. Sci Rep. (2015) 5: 8068*

51. *Kang SM, Rosales JL, Meier-Stephenson V, Kim S, Lee KY, Narendran A. Genome-wide loss-of-function genetic screening identifies opioid receptor mu1 as a key regulator of L-asparaginase resistance in pediatric acute lymphoblastic leukemia. Oncogene. (2017) 36: 5910-5913*

52. *Yeldag G, Rice A, Del Rio Hernandez A. Chemoresistance and the Self-Maintaining Tumor Microenvironment. Cancers (Basel). (2018) 10:*

53. *Senthebane DA, Rowe A, Thomford NE, Shipanga H, Munro D, Mazeedi M, Almazyadi HAM, Kallmeyer K, Dandara C, Pepper MS, Parker MI, Dzobo K. The Role of Tumor Microenvironment in Chemoresistance: To Survive, Keep Your Enemies Closer. Int J Mol Sci. (2017) 18:*

54. *Lyssiotis CA ,Kimmelman AC. Metabolic Interactions in the Tumor Microenvironment. Trends Cell Biol. (2017) 27: 863-875*

55. *Danhier P, Banski P, Payen VL, Grasso D, Ippolito L, Sonveaux P, Porporato PE. Cancer metabolism in space and time: Beyond the Warburg effect. Biochim Biophys Acta Bioenerg. (2017) 1858: 556-572*

56. *Rattigan YI, Patel BB, Ackerstaff E, Sukenick G, Koutcher JA, Glod JW, Banerjee D. Lactate is a mediator of metabolic cooperation between stromal carcinoma associated fibroblasts and glycolytic tumor cells in the tumor microenvironment. Exp Cell Res. (2012) 318: 326-335*

57. *Yang L, Achreja A, Yeung TL, Mangala LS, Jiang D, Han C, Baddour J, Marini JC, Ni J, Nakahara R, Wahlig S, Chiba L, Kim SH, Morse J, Pradeep S, Nagaraja AS, Haemmerle M, Kyunghee N, Derichsweiler M, Plackemeier T, Mercado-Uribe I, Lopez-Berestein G, Moss T, Ram PT, Liu J, Lu X, Mok SC, Sood AK, Nagrath D. Targeting Stromal Glutamine Synthetase in Tumors Disrupts Tumor Microenvironment-Regulated Cancer Cell Growth. Cell Metab. (2016) 24: 685-700*

58. *Tardito S, Oudin A, Ahmed SU, Fack F, Keunen O, Zheng L, Miletic H, Sakariassen PO, Weinstock A, Wagner A, Lindsay SL, Hock AK, Barnett SC, Ruppin E, Morkve SH, Lund-Johansen M, Chalmers AJ, Bjerkvig R, Niclou SP, Gottlieb E. Glutamine synthetase activity fuels nucleotide biosynthesis and supports growth of glutamine-restricted glioblastoma. Nat Cell Biol. (2015) 17: 1556-1568*

59. *Zhang W, Trachootham D, Liu J, Chen G, Pelicano H, Garcia-Prieto C, Lu W, Burger JA, Croce CM, Plunkett W, Keating MJ, Huang P. Stromal control of cystine metabolism promotes cancer cell survival in chronic lymphocytic leukaemia. Nat Cell Biol. (2012) 14: 276-286*

60. *Kwong-Lam F ,Chi-Fung CG. Vincristine could partly suppress stromal support to T-ALL blasts during pegylated arginase I treatment. Exp Hematol Oncol. (2013) 2: 11*

61. *Pando A, Reagan JL, Quesenberry P, Fast LD. Extracellular vesicles in leukemia. Leuk Res. (2018) 64: 52-60*

62. *Colmone A, Amorim M, Pontier AL, Wang S, Jablonski E, Sipkins DA. Leukemic cells create bone marrow niches that disrupt the behavior of normal hematopoietic progenitor cells. Science. (2008) 322: 1861-1865*

63. *Vilchis-Ordonez A, Contreras-Quiroz A, Vadillo E, Dorantes-Acosta E, Reyes-Lopez A, Quintela-Nunez del Prado HM, Venegas-Vazquez J, Mayani H, Ortiz-Navarrete V, Lopez-Martinez B, Pelayo R. Bone Marrow Cells in Acute Lymphoblastic Leukemia Create a Proinflammatory Microenvironment Influencing Normal Hematopoietic Differentiation Fates. Biomed Res Int. (2015) 2015: 386165*

64. *Ma Z, Zhao X, Deng M, Huang Z, Wang J, Wu Y, Cui D, Liu Y, Liu R, Ouyang G. Bone Marrow Mesenchymal Stromal Cell-Derived Periostin Promotes B-ALL Progression by Modulating CCL2 in Leukemia Cells. Cell Rep. (2019) 26: 1533-1543 e1534*

65. *van den Berk LC, van der Veer A, Willemse ME, Theeuwes MJ, Luijendijk MW, Tong WH, van der Sluis IM, Pieters R, den Boer ML. Disturbed CXCR4/CXCL12 axis in paediatric precursor B-cell acute lymphoblastic leukaemia. Br J Haematol. (2014) 166: 240-249*

66. *Allavena P, Germano G, Belgiovine C, D'Incalci M, Mantovani A. Trabectedin: A drug from the sea that strikes tumor-associated macrophages. Oncoimmunology. (2013) 2: e24614*

67. *van der Meer LT, Terry SY, van Ingen Schenau DS, Andree KC, Franssen GM, Roeleveld DM, Metselaar JM, Reinheckel T, Hoogerbrugge PM, Boerman OC, van Leeuwen FN. In Vivo Imaging of Antileukemic Drug Asparaginase Reveals a Rapid Macrophage-Mediated Clearance from the Bone Marrow. J Nucl Med. (2017) 58: 214-220*

68. *Iwamoto S, Mihara K, Downing JR, Pui CH, Campana D. Mesenchymal cells regulate the response of acute lymphoblastic leukemia cells to asparaginase. J Clin Invest. (2007) 117: 1049-1057*

69. *Steiner M, Hochreiter D, Kasper DC, Kornmuller R, Pichler H, Haas OA, Potschger U, Hutter C, Dworzak MN, Mann G, Attarbaschi A. Asparagine and aspartic acid concentrations in bone marrow versus peripheral blood during Berlin-Frankfurt-Munster-based induction therapy for childhood acute lymphoblastic leukemia. Leuk Lymphoma. (2012) 53: 1682-1687*

70. *Chiu M, Franchi-Gazzola R, Bussolati O, D'Amico G, Dell'Acqua F, Rizzari C. Asparagine levels in the bone marrow of patients with acute lymphoblastic leukemia during asparaginase therapy. Pediatr Blood Cancer. (2013) 60: 1915*

71. *Fung KL, Liang RH, Chan GC. Vincristine but not imatinib could suppress mesenchymal niche's support to lymphoid leukemic cells. Leuk Lymphoma. (2010) 51: 515-522*

72. *Ehsanipour EA, Sheng X, Behan JW, Wang X, Butturini A, Avramis VI, Mittelman SD. Adipocytes cause leukemia cell resistance to L-asparaginase via release of glutamine. Cancer Res. (2013) 73: 2998-3006*

73. *Friedenstein AJ, Gorskaja JF, Kulagina NN. Fibroblast precursors in normal and irradiated mouse hematopoietic organs. Exp Hematol. (1976) 4: 267-274*

74. *Dominici M, Le Blanc K, Mueller I, Slaper-Cortenbach I, Marini F, Krause D, Deans R, Keating A, Prockop D, Horwitz E. Minimal criteria for defining multipotent mesenchymal stromal cells. The International Society for Cellular Therapy position statement. Cytotherapy. (2006) 8: 315-317*

75. *Fernandez Vallone VB, Romaniuk MA, Choi H, Labovsky V, Otaegui J, Chasseing NA. Mesenchymal stem cells and their use in therapy: what has been achieved? Differentiation. (2013) 85: 1-10*

76. *Kim N ,Cho SG. Clinical applications of mesenchymal stem cells. Korean J Intern Med. (2013) 28: 387-402*

77. *Melzer C, Yang Y, Hass R. Interaction of MSC with tumor cells. Cell Commun Signal. (2016) 14: 20*

78. *Boutter J, Huang Y, Marovca B, Vonderheit A, Grotzer MA, Eckert C, Cario G, Wollscheid B, Horvath P, Bornhauser BC, Bourquin JP. Image-based RNA interference screening reveals an individual dependence of acute lymphoblastic leukemia on stromal cysteine support. Oncotarget. (2014) 5: 11501-11512*

79. *Naderi EH, Skah S, Ugland H, Myklebost O, Sandnes DL, Torgersen ML, Josefsen D, Ruud E, Naderi S, Blomhoff HK. Bone marrow stroma-derived PGE2 protects BCP-ALL cells from DNA damage-induced p53 accumulation and cell death. Mol Cancer. (2015) 14: 14*

80. *Nwabo Kamdje AH, Mosna F, Bifari F, Lisi V, Bassi G, Malpeli G, Ricciardi M, Perbellini O, Scupoli MT, Pizzolo G, Krampera M. Notch-3 and Notch-4 signaling rescue from apoptosis human B-ALL cells in contact with human bone marrow-derived mesenchymal stromal cells. Blood. (2011) 118: 380-389*

81. *Tiziani S, Kang Y, Harjanto R, Axelrod J, Piermarocchi C, Roberts W, Paternostro G. Metabolomics of the tumor microenvironment in pediatric acute lymphoblastic leukemia. PLoS One. (2013) 8: e82859*

82. *Altman BJ, Stine ZE, Dang CV. From Krebs to clinic: glutamine metabolism to cancer therapy. Nat Rev Cancer. (2016) 16: 619-634*

83. *Windmueller HG ,Spaeth AE. Uptake and metabolism of plasma glutamine by the small intestine. J Biol Chem. (1974) 249: 5070-5079*

84. *Zhang J, Pavlova NN, Thompson CB. Cancer cell metabolism: the essential role of the nonessential amino acid, glutamine. EMBO J. (2017) 36: 1302-1315*

85. *Wise DR ,Thompson CB. Glutamine addiction: a new therapeutic target in cancer. Trends Biochem Sci. (2010) 35: 427-433*

86. *Wellen KE, Lu C, Mancuso A, Lemons JM, Ryczko M, Dennis JW, Rabinowitz JD, Coller HA, Thompson CB. The hexosamine biosynthetic pathway couples growth factor-induced glutamine uptake to glucose metabolism. Genes Dev. (2010) 24: 2784-2799*

87. *Domercq M, Sanchez-Gomez MV, Sherwin C, Etxebarria E, Fern R, Matute C. System xc- and glutamate transporter inhibition mediates microglial toxicity to oligodendrocytes. J Immunol. (2007) 178: 6549-6556*

88. *Nicklin P, Bergman P, Zhang B, Triantafellow E, Wang H, Nyfeler B, Yang H, Hild M, Kung C, Wilson C, Myer VE, MacKeigan JP, Porter JA, Wang YK, Cantley LC, Finan PM, Murphy LO. Bidirectional transport of amino acids regulates mTOR and autophagy. Cell. (2009) 136: 521-534*

89. *Jewell JL, Kim YC, Russell RC, Yu FX, Park HW, Plouffe SW, Tagliabracci VS, Guan KL. Metabolism. Differential regulation of mTORC1 by leucine and glutamine. Science. (2015) 347: 194-198*

90. *Chiu M, Tardito S, Barilli A, Bianchi MG, Dall'Asta V, Bussolati O. Glutamine stimulates mTORC1 independent of the cell content of essential amino acids. Amino Acids. (2012) 43: 2561-2567*

91. *Bolzoni M, Chiu M, Accardi F, Vescovini R, Airoldi I, Storti P, Todoerti K, Agnelli L, Missale G, Andreoli R, Bianchi MG, Allegri M, Barilli A, Nicolini F, Cavalli A, Costa F, Marchica V, Toscani D, Mancini C, Martella E, Dall'Asta V, Donofrio G, Aversa F, Bussolati O, Giuliani N. Dependence on glutamine uptake and glutamine addiction characterize myeloma cells: a new attractive target. Blood. (2016) 128: 667-679*

92. *Chiu M, Tardito S, Pillozzi S, Arcangeli A, Armento A, Uggeri J, Missale G, Bianchi MG, Barilli A, Dall'Asta V, Campanini N, Silini EM, Fuchs J, Armeanu-Ebinger S, Bussolati O. Glutamine depletion by crisantaspase hinders the growth of human hepatocellular carcinoma xenografts. Br J Cancer. (2014) 111: 1159-1167*

93. *Willems L, Jacque N, Jacquel A, Neveux N, Maciel TT, Lambert M, Schmitt A, Poulain L, Green AS, Uzunov M, Kosmider O, Radford-Weiss I, Moura IC, Auberger P, Ifrah N, Bardet V, Chapuis N, Lacombe C, Mayeux P, Tamburini J, Bouscary D. Inhibiting glutamine uptake represents an attractive new strategy for treating acute myeloid leukemia. Blood. (2013) 122: 3521-3532*

94. *Hensley CT, Wasti AT, DeBerardinis RJ. Glutamine and cancer: cell biology, physiology, and clinical opportunities. J Clin Invest. (2013) 123: 3678-3684*

95. *Schop D, Janssen FW, Borgart E, de Bruijn JD, van Dijkhuizen-Radersma R. Expansion of mesenchymal stem cells using a microcarrier-based cultivation system: growth and metabolism. J Tissue Eng Regen Med. (2008) 2: 126-135*

96. *Higuera GA, Schop D, Spitters TW, van Dijkhuizen-Radersma R, Bracke M, de Bruijn JD, Martens D, Karperien M, van Boxtel A, van Blitterswijk CA. Patterns of amino acid metabolism by proliferating human mesenchymal stem cells. Tissue Eng Part A. (2012) 18: 654-664*

97. *Danielyan L, Schafer R, Schulz A, Ladewig T, Lourhmati A, Buadze M, Schmitt AL, Verleysdonk S, Kabisch D, Koeppen K, Siegel G, Proksch B, Kluba T, Eckert A, Kohle C, Schoneberg T, Northoff H, Schwab M, Gleiter CH. Survival, neuron-like differentiation and functionality of mesenchymal stem cells in neurotoxic environment: the critical role of erythropoietin. Cell Death Differ. (2009) 16: 1599-1614*

98. *Capasso S, Alessio N, Squillaro T, Di Bernardo G, Melone MA, Cipollaro M, Peluso G, Galderisi U. Changes in autophagy, proteasome activity and metabolism to determine a specific signature for acute and chronic senescent mesenchymal stromal cells. Oncotarget. (2015) 6: 39457-39468*

99. *Zhou T, Yang Y, Chen Q, Xie L. Glutamine Metabolism Is Essential for Stemness of Bone Marrow Mesenchymal Stem Cells and Bone Homeostasis. Stem Cells Int. (2019) 2019: 8928934*

100. *Huang T, Liu R, Fu X, Yao D, Yang M, Liu Q, Lu WW, Wu C, Guan M. Aging Reduces an ERRalpha-Directed Mitochondrial Glutaminase Expression Suppressing Glutamine Anaplerosis and Osteogenic Differentiation of Mesenchymal Stem Cells. Stem Cells. (2017) 35: 411-424*

101. *Huang YF, Wang Y, Watford M. Glutamine directly downregulates glutamine synthetase protein levels in mouse C2C12 skeletal muscle myotubes. J Nutr. (2007) 137: 1357-1362*

102. *Gebhardt R ,Mecke D. Heterogeneous distribution of glutamine synthetase among rat liver parenchymal cells in situ and in primary culture. EMBO J. (1983) 2: 567-570*

103. *Kanamori K. In vivo N-15 MRS study of glutamate metabolism in the rat brain. Anal Biochem. (2017) 529: 179-192*

104. *Austinat M, Dunsch R, Wittekind C, Tannapfel A, Gebhardt R, Gaunitz F. Correlation between beta-catenin mutations and expression of Wnt-signaling target genes in hepatocellular carcinoma. Mol Cancer. (2008) 7: 21*

105. *Bott AJ, Peng IC, Fan Y, Faubert B, Zhao L, Li J, Neidler S, Sun Y, Jaber N, Krokowski D, Lu W, Pan JA, Powers S, Rabinowitz J, Hatzoglou M, Murphy DJ, Jones R, Wu S, Girnun G, Zong WX. Oncogenic Myc Induces Expression of Glutamine Synthetase through Promoter Demethylation. Cell Metab. (2015) 22: 1068-1077*

106. *Wise DR, DeBerardinis RJ, Mancuso A, Sayed N, Zhang XY, Pfeiffer HK, Nissim I, Daikhin E, Yudkoff M, McMahon SB, Thompson CB. Myc regulates a transcriptional program that stimulates mitochondrial glutaminolysis and leads to glutamine addiction. Proc Natl Acad Sci U S A. (2008) 105: 18782-18787*

107. *Nguyen TV, Lee JE, Sweredoski MJ, Yang SJ, Jeon SJ, Harrison JS, Yim JH, Lee SG, Handa H, Kuhlman B, Jeong JS, Reitsma JM, Park CS, Hess S, Deshaies RJ. Glutamine*

Triggers Acetylation-Dependent Degradation of Glutamine Synthetase via the Thalidomide Receptor Cereblon. Mol Cell. (2016) 61: 809-820

108. *Castegna A ,Menga A. Glutamine Synthetase: Localization Dictates Outcome. Genes (Basel). (2018) 9:*

109. *Chiu M, Taurino G, Bianchi MG, Ottaviani L, Andreoli R, Ciociola T, Lagrasta CAM, Tardito S, Bussolati O. Oligodendroglioma Cells Lack Glutamine Synthetase and Are Auxotrophic for Glutamine, but Do not Depend on Glutamine Anaplerosis for Growth. Int J Mol Sci. (2018) 19:*

110. *Lomelino CL, Andring JT, McKenna R, Kilberg MS. Asparagine synthetase: Function, structure, and role in disease. J Biol Chem. (2017) 292: 19952-19958*

111. *Heng HH, Shi XM, Scherer SW, Andrulis IL, Tsui LC. Refined localization of the asparagine synthetase gene (ASNS) to chromosome 7, region q21.3, and characterization of the somatic cell hybrid line 4AF/106/KO15. Cytogenet Cell Genet. (1994) 66: 135-138*

112. *Kilberg MS, Balasubramanian M, Fu L, Shan J. The transcription factor network associated with the amino acid response in mammalian cells. Adv Nutr. (2012) 3: 295-306*

113. *Kilberg MS, Shan J, Su N. ATF4-dependent transcription mediates signaling of amino acid limitation. Trends Endocrinol Metab. (2009) 20: 436-443*

114. *Dubbers A, Wurthwein G, Muller HJ, Schulze-Westhoff P, Winkelhorst M, Kurzknabe E, Lanvers C, Pieters R, Kaspers GJ, Creutzig U, Ritter J, Boos J. Asparagine synthetase activity in paediatric acute leukaemias: AML-M5 subtype shows lowest activity. Br J Haematol. (2000) 109: 427-429*

115. *Dufour E, Gay F, Aguera K, Scoazec JY, Horand F, Lorenzi PL, Godfrin Y. Pancreatic tumor sensitivity to plasma L-asparagine starvation. Pancreas. (2012) 41: 940-948*

116. *Pacher M, Seewald MJ, Mikula M, Oehler S, Mogg M, Vinatzer U, Eger A, Schweifer N, Varecka R, Sommergruber W, Mikulits W, Schreiber M. Impact of constitutive IGF1/IGF2 stimulation on the transcriptional program of human breast cancer cells. Carcinogenesis. (2007) 28: 49-59*

117. *Yang H, He X, Zheng Y, Feng W, Xia X, Yu X, Lin Z. Down-regulation of asparagine synthetase induces cell cycle arrest and inhibits cell proliferation of breast cancer. Chem Biol Drug Des. (2014) 84: 578-584*

118. *Knott SRV, Wagenblast E, Khan S, Kim SY, Soto M, Wagner M, Turgeon MO, Fish L, Erard N, Gable AL, Maceli AR, Dickopf S, Papachristou EK, D'Santos CS, Carey LA, Wilkinson JE, Harrell JC, Perou CM, Goodarzi H, Poulogiannis G, Hannon GJ. Asparagine bioavailability governs metastasis in a model of breast cancer. Nature. (2018) 554: 378-381*

119. *Patrikainen L, Porvari K, Kurkela R, Hirvikoski P, Soini Y, Vihko P. Expression profiling of PC-3 cell line variants and comparison of MIC-1 transcript levels in benign and malignant prostate. Eur J Clin Invest. (2007) 37: 126-133*

120. *Toda K, Kawada K, Iwamoto M, Inamoto S, Sasazuki T, Shirasawa S, Hasegawa S, Sakai Y. Metabolic Alterations Caused by KRAS Mutations in Colorectal Cancer Contribute to Cell Adaptation to Glutamine Depletion by Upregulation of Asparagine Synthetase. Neoplasia. (2016) 18: 654-665*

121. *Sullivan LB, Gui DY, Vander Heiden MG. Altered metabolite levels in cancer: implications for tumour biology and cancer therapy. Nat Rev Cancer. (2016) 16: 680-693*

122. *Krall AS, Xu S, Graeber TG, Braas D, Christofk HR. Asparagine promotes cancer cell proliferation through use as an amino acid exchange factor. Nat Commun. (2016) 7: 11457*

123. *Richards NG ,Kilberg MS. Asparagine synthetase chemotherapy. Annu Rev Biochem. (2006) 75: 629-654*

124. *Koroniak L, Ciustea M, Gutierrez JA, Richards NG. Synthesis and characterization of an N-acylsulfonamide inhibitor of human asparagine synthetase. Org Lett. (2003) 5: 2033-2036*

125. *Gutierrez JA, Pan YX, Koroniak L, Hiratake J, Kilberg MS, Richards NG. An inhibitor of human asparagine synthetase suppresses proliferation of an L-asparaginase-resistant leukemia cell line. Chem Biol. (2006) 13: 1339-1347*

126. *Ikeuchi H, Ahn YM, Otokawa T, Watanabe B, Hegazy L, Hiratake J, Richards NG. A sulfoximine-based inhibitor of human asparagine synthetase kills L-asparaginase-resistant leukemia cells. Bioorg Med Chem. (2012) 20: 5915-5927*

127. *Bhutia YD ,Ganapathy V. Glutamine transporters in mammalian cells and their functions in physiology and cancer. Biochim Biophys Acta. (2016) 1863: 2531-2539*

128. *Liu Y, Zhao T, Li Z, Wang L, Yuan S, Sun L. The role of ASCT2 in cancer: A review. Eur J Pharmacol. (2018) 837: 81-87*

129. *Broer A, Rahimi F, Broer S. Deletion of Amino Acid Transporter ASCT2 (SLC1A5) Reveals an Essential Role for Transporters SNAT1 (SLC38A1) and SNAT2 (SLC38A2) to Sustain Glutaminolysis in Cancer Cells. J Biol Chem. (2016) 291: 13194-13205*

130. *Chiu M, Sabino C, Taurino G, Bianchi MG, Andreoli R, Giuliani N, Bussolati O. GPNA inhibits the sodium-independent transport system L for neutral amino acids. Amino Acids. (2017) 49: 1365-1372*

131. *Corti A, Dominici S, Piaggi S, Belcastro E, Chiu M, Taurino G, Pacini S, Bussolati O, Pompella A. gamma-Glutamyltransferase enzyme activity of cancer cells modulates L-gamma-glutamyl-p-nitroanilide (GPNA) cytotoxicity. Sci Rep. (2019) 9: 891*

132. *Hafliger P ,Charles RP. The L-Type Amino Acid Transporter LAT1-An Emerging Target in Cancer. Int J Mol Sci. (2019) 20:*

133. *Oda K, Hosoda N, Endo H, Saito K, Tsujihara K, Yamamura M, Sakata T, Anzai N, Wempe MF, Kanai Y, Endou H. L-type amino acid transporter 1 inhibitors inhibit tumor cell growth. Cancer Sci. (2010) 101: 173-179*

134. *Mackenzie B ,Erickson JD. Sodium-coupled neutral amino acid (System N/A) transporters of the SLC38 gene family. Pflugers Arch. (2004) 447: 784-795*

135. *Broer S. The SLC38 family of sodium-amino acid co-transporters. Pflugers Arch. (2014) 466: 155-172*

136. *Hagglund MGA, Hellsten SV, Bagchi S, Philippot G, Lofqvist E, Nilsson VCO, Almkvist I, Karlsson E, Sreedharan S, Tafreshiha A, Fredriksson R. Transport of L-glutamine, L-alanine, L-arginine and L-histidine by the neuron-specific Slc38a8 (SNAT8) in CNS. J Mol Biol. (2015) 427: 1495-1512*

137. *Broer A, Albers A, Setiawan I, Edwards RH, Chaudhry FA, Lang F, Wagner CA, Broer S. Regulation of the glutamine transporter SN1 by extracellular pH and intracellular sodium ions. J Physiol. (2002) 539: 3-14*

138. *Baird FE, Beattie KJ, Hyde AR, Ganapathy V, Rennie MJ, Taylor PM. Bidirectional substrate fluxes through the system N (SNAT5) glutamine transporter may determine net glutamine flux in rat liver. J Physiol. (2004) 559: 367-381*

139. *Deitmer JW, Broer A, Broer S. Glutamine efflux from astrocytes is mediated by multiple pathways. J Neurochem. (2003) 87: 127-135*

140. *Nakanishi T, Sugawara M, Huang W, Martindale RG, Leibach FH, Ganapathy ME, Prasad PD, Ganapathy V. Structure, function, and tissue expression pattern of human SN2, a subtype of the amino acid transport system N. Biochem Biophys Res Commun. (2001) 281: 1343-1348*

141. *Kim J, Okamoto H, Huang Z, Anguiano G, Chen S, Liu Q, Cavino K, Xin Y, Na E, Hamid R, Lee J, Zambrowicz B, Unger R, Murphy AJ, Xu Y, Yancopoulos GD, Li WH, Gromada J. Amino Acid Transporter Slc38a5 Controls Glucagon Receptor Inhibition-Induced Pancreatic alpha Cell Hyperplasia in Mice. Cell Metab. (2017) 25: 1348-1361 e1348*

142. *Hagglund MG, Sreedharan S, Nilsson VC, Shaik JH, Almkvist IM, Backlin S, Wrange O, Fredriksson R. Identification of SLC38A7 (SNAT7) protein as a glutamine transporter expressed in neurons. J Biol Chem. (2011) 286: 20500-20511*

143. *Andre V, Longoni D, Bresolin S, Cappuzzello C, Dander E, Galbiati M, Bugarin C, Di Meglio A, Nicolis E, Maserati E, Serafini M, Warren AJ, Te Kronnie G, Cazzaniga G, Sainati L, Cipolli M, Biondi A, D'Amico G. Mesenchymal stem cells from Shwachman-Diamond syndrome patients display normal functions and do not contribute to hematological defects. Blood Cancer J. (2012) 2: e94*

144. *Mihara K, Imai C, Coustan-Smith E, Dome JS, Dominici M, Vanin E, Campana D. Development and functional characterization of human bone marrow mesenchymal cells immortalized by enforced expression of telomerase. Br J Haematol. (2003) 120: 846-849*

145. *Ackermann T ,Tardito S. Cell Culture Medium Formulation and Its Implications in Cancer Metabolism. Trends Cancer. (2019) 5: 329-332*

146. *Vande Voorde J, Ackermann T, Pfetzer N, Sumpton D, Mackay G, Kalna G, Nixon C, Blyth K, Gottlieb E, Tardito S. Improving the metabolic fidelity of cancer models with a physiological cell culture medium. Sci Adv. (2019) 5: eaau7314*

147. *O'Brien J, Wilson I, Orton T, Pognan F. Investigation of the Alamar Blue (resazurin) fluorescent dye for the assessment of mammalian cell cytotoxicity. Eur J Biochem. (2000) 267: 5421-5426*

148. *Bustin SA. Absolute quantification of mRNA using real-time reverse transcription polymerase chain reaction assays. J Mol Endocrinol. (2000) 25: 169-193*

149. *Ge J, Hu Y, Gui Y, Hou R, Yang M, Zeng Q, Xia R. Chemotherapy-induced alteration of SDF-1/CXCR4 expression in bone marrow-derived mesenchymal stem cells from adolescents and young adults with acute lymphoblastic leukemia. J Pediatr Hematol Oncol. (2014) 36: 617-623*

150. *Balandran JC, Purizaca J, Enciso J, Dozal D, Sandoval A, Jimenez-Hernandez E, Aleman-Lazarini L, Perez-Koldenkova V, Quintela-Nunez Del Prado H, Rios de Los Rios J, Mayani H, Ortiz-Navarrete V, Guzman ML, Pelayo R. Pro-inflammatory-Related Loss of CXCL12 Niche Promotes Acute Lymphoblastic Leukemic Progression at the Expense of Normal Lymphopoiesis. Front Immunol. (2016) 7: 666*

151. *Portale F, Cricri G, Bresolin S, Lupi M, Gaspari S, Silvestri D, Russo B, Marino N, Ubezio P, Pagni F, Vergani P, Kronnie GT, Valsecchi MG, Locatelli F, Rizzari C, Biondi A, Dander E, D'Amico G. ActivinA: a new leukemia-promoting factor conferring migratory advantage to B-cell precursor-acute lymphoblastic leukemic cells. Haematologica. (2019) 104: 533-545*

152. *Dimitriou H, Choulaki C, Perdikogianni C, Stiakaki E, Kalmanti M. Expression levels of ASNS in mesenchymal stromal cells in childhood acute lymphoblastic leukemia. Int J Hematol. (2014) 99: 305-310*

153. *Reinert RB, Oberle LM, Wek SA, Bunpo P, Wang XP, Mileva I, Goodwin LO, Aldrich CJ, Durden DL, McNurlan MA, Wek RC, Anthony TG. Role of glutamine depletion in directing tissue-specific nutrient stress responses to L-asparaginase. J Biol Chem. (2006) 281: 31222-31233*

154. *Pillozzi S, Masselli M, De Lorenzo E, Accordi B, Cilia E, Crociani O, Amedei A, Veltroni M, D'Amico M, Basso G, Becchetti A, Campana D, Arcangeli A. Chemotherapy resistance in acute lymphoblastic leukemia requires hERG1 channels and is overcome by hERG1 blockers. Blood. (2011) 117: 902-914*

155. *Yang Y, Mallampati S, Sun B, Zhang J, Kim SB, Lee JS, Gong Y, Cai Z, Sun X. Wnt pathway contributes to the protection by bone marrow stromal cells of acute lymphoblastic leukemia cells and is a potential therapeutic target. Cancer Lett. (2013) 333: 9-17*

156. *Zhang Y, Hu K, Hu Y, Liu L, Wang B, Huang H. Bone marrow mesenchymal stromal cells affect the cell cycle arrest effect of genotoxic agents on acute lymphocytic leukemia cells via p21 down-regulation. Ann Hematol. (2014) 93: 1499-1508*

157. *Zhu N, Wang H, Wei J, Wang B, Shan W, Lai X, Zhao Y, Yu J, Huang H. NR2F2 regulates bone marrow-derived mesenchymal stem cell-promoted proliferation of Reh cells. Mol Med Rep. (2016) 14: 1351-1356*

158. *Moses BS, Slone WL, Thomas P, Evans R, Piktel D, Angel PM, Walsh CM, Cantrell PS, Rellick SL, Martin KH, Simpkins JW, Gibson LF. Bone marrow microenvironment modulation of acute lymphoblastic leukemia phenotype. Exp Hematol. (2016) 44: 50-59 e51-52*

159. *Samudio I, Fiegl M, McQueen T, Clise-Dwyer K, Andreeff M. The warburg effect in leukemia-stroma cocultures is mediated by mitochondrial uncoupling associated with uncoupling protein 2 activation. Cancer Res. (2008) 68: 5198-5205*

160. *Johnson SM, Dempsey C, Chadwick A, Harrison S, Liu J, Di Y, McGinn OJ, Fiorillo M, Sotgia F, Lisanti MP, Parihar M, Krishnan S, Saha V. Metabolic reprogramming of bone marrow stromal cells by leukemic extracellular vesicles in acute lymphoblastic leukemia. Blood. (2016) 128: 453-456*

161. *Mycielska ME, Patel A, Rizaner N, Mazurek MP, Keun H, Ganapathy V, Djamgoz MB. Citrate transport and metabolism in mammalian cells: prostate epithelial cells and prostate cancer. Bioessays. (2009) 31: 10-20*

162. *Kung HN, Marks JR, Chi JT. Glutamine synthetase is a genetic determinant of cell type-specific glutamine independence in breast epithelia. PLoS Genet. (2011) 7: e1002229*